62 7 1934 628

~~CONFIDENTIAL~~

NASA TM X-110

CASE FILE COPY

~~GROUP (3)~~

~~DOWNGRADED AT 12 YEAR INTERVALS; NOT AUTOMATICALLY DECLASSIFIED~~

NASA TM X-110

TECHNICAL MEMORANDUM X-110

AN INVESTIGATION OF THE STATIC AND DYNAMIC AERODYNAMIC CHARACTERISTICS OF A SERIES OF BLUNT-NOSED CYLINDER-FLARE MODELS AT MACH NUMBERS FROM 0.65 TO 2.20

By David E. Reese, Jr., and William R. Wehrend, Jr.

Ames Research Center
Moffett Field, Calif.

CLASSIFICATION CHANGE

TO - UNCLASSIFIED [redacted]

By authority of T.D. No. 73-307

Changed by [illegible] Date 4/19/73

CLASSIFICATION CHANGE

TO - UNCLASSIFIED ~~CONFIDENTIAL~~

By authority of ~~T.D. No.~~ NASA CCN 223-375

Changed by _____ Date _____

[redacted]

NATIONAL AERONAUTICS AND SPACE ADMINISTRATION

WASHINGTON January 1960

~~CONFIDENTIAL~~

[redacted]

NATIONAL AERONAUTICS AND SPACE ADMINISTRATION

TECHNICAL MEMORANDUM X-110

AN INVESTIGATION OF THE STATIC AND DYNAMIC AERODYNAMIC CHARACTERISTICS OF A SERIES OF BLUNT-NOSED CYLINDER-FLARE MODELS AT MACH NUMBERS FROM 0.65 TO 2.20*

By David E. Reese, Jr., and William R. Wehrend, Jr.

SUMMARY

The results of an investigation of the static and dynamic aerodynamic characteristics of a series of blunt-nosed cylinder-flare models are presented herein. Models with variations of nose bluntness, flare base area, flare angle, and cylindrical body length have been tested. Normal-force, pitching-moment, axial-force, and damping-in-pitch data were obtained over a Mach number range from 0.65 to 2.20 at angles of attack up to 18°.

The results of this investigation showed that at angles of attack near zero all models experienced two basic flow conditions; a flow separated symmetrically from the nose at subsonic speeds and an attached flow at supersonic speeds. The separated flow led to nonlinear variations in normal-force, pitching-moment, and damping-in-pitch coefficients with angle of attack. The damping in pitch associated with this flow was unstable at angles of attack near zero and stable at higher angles. In contrast, the values of normal-force and pitching-moment coefficients obtained when the flow was attached showed linear variations with angle of attack although the values were usually smaller than those at subsonic speeds. The damping associated with the attached flow was stable and relatively constant through the angle range.

At Mach numbers from 1.0 to 1.3, all models of this investigation exhibited a large, abrupt stable shift in the pitching moment with increasing angle of attack that was related to two different flow conditions on the model. At small angles of attack, the flow was attached and the pitching moment was small. At large angles of attack, the flow was separated asymmetrically and the pitching moment was more stable.

*Title, Unclassified

[redacted]

However, as angle of attack decreased from the large values the separated flow persisted to an angle of attack less than that for the onset of separation. Thus there was a range of angles for which two values of pitching moment were possible depending on whether the angle of attack was increasing toward that for separation or decreasing toward that for attachment resulting in a pitching-moment loop. This loop can introduce relatively large amounts of energy into the free-flight pitching motion of the vehicle.

INTRODUCTION

Among the problems the designer of ballistic re-entry bodies must face, the most critical are often aerodynamic heating and dynamic stability. Frequently design requirements necessary to alleviate one of these problems will aggravate the other. To understand this interrelationship it is necessary to look at the quantities involved in the dynamic stability of a body in a re-entry trajectory. In references 1 and 2 it is shown that the dynamic stability of the re-entry vehicle is dependent on the magnitude of the term $[C_D - C_{L_\alpha} + (C_{m_q} + C_{m_{\dot{\alpha}}})(d/\sigma)^2]$; if this term is larger than a given positive number which is a function of the flight path, the oscillation amplitude will increase. It can be seen that the high drag coefficient, C_D, that is desirable to minimize heat transfer has an undesirable effect on the dynamic stability. Some of the shapes first suggested for re-entry bodies also had negative values of lift-curve slope, C_{L_α}, because of their short length so that both the lift and the drag terms were destabilizing. Dynamic stability then depended on the presence of stable damping in pitch of sufficient magnitude to overcome the destabilizing tendency of the other two terms. Under these conditions dynamic stability was frequently marginal or unsatisfactory.

One way to overcome this tendency of high drag shapes to have dynamic stability problems is to choose a shape that will have a positive value of C_{L_α}. One simple shape that meets the requirements of high drag and positive C_{L_α} consists of a cylinder with blunted nose in combination with a conical flare for static stability. If rather blunt noses are considered for these bodies, theoretical calculations of the aerodynamic parameters are difficult, particularly in the transonic speed range. As a result experimental data from wind-tunnel tests and rocket and range firings must be provided to predict the stability of these shapes. Some information on blunt-nosed cylinder-flare combinations is available in references 3 through 7. The present investigation was undertaken to provide both static and dynamic stability data at transonic and supersonic Mach numbers on the effects of limited variations in nose contour, flare base area, flare angle, and cylindrical body length.

SYMBOLS

C_A	total axial-force coefficient, $\frac{\text{axial force}}{\frac{1}{2}\rho V^2 S}$
C_{A_o}	total axial-force coefficient at $\alpha = 0^o$
C_m	pitching-moment coefficient, $\frac{\text{pitching moment}}{\frac{1}{2}\rho V^2 Sd}$
C_{m_α}	variation of pitching-moment coefficient with angle of attack, $\frac{\partial C_m}{\partial \alpha}$, per radian
$C_{m_q} + C_{m_{\dot{\alpha}}}$	damping-in-pitch coefficient, $\frac{\partial C_m}{\partial\left(\frac{qd}{V}\right)} + \frac{\partial C_m}{\partial\left(\frac{\dot{\alpha}d}{V}\right)}$, per radian
C_N	normal-force coefficient, $\frac{\text{normal force}}{\frac{1}{2}\rho V^2 S}$
C_{N_α}	variation of normal-force coefficient with angle of attack, $\frac{\partial C_N}{\partial \alpha}$, per radian
C_{p_b}	base pressure coefficient, $\frac{p_b - p}{\frac{1}{2}\rho V^2}$
d	cylindrical body diameter, ft
k	reduced frequency, $\frac{\omega d}{V}$
l	over-all body length, ft
l_n	nose length, ft
L	cylindrical body length, ft
M	free-stream Mach number
p	free-stream static pressure, psf
p_b	static base pressure, psf
q	pitching velocity, radians/sec
r	cylindrical body radius, ft

R	free-stream Reynolds number, based on cylindrical body diameter
S	body cross-section area, sq ft
V	free-stream velocity, ft/sec
α	angle of attack, deg
α_s	stream angle correction, deg
α_{att}	angle of attack at which flow attaches, deg
α_{sep}	angle of attack at which flow separates, deg
$\dot{\alpha}$	plunging velocity, radians/sec
δ	oscillation amplitude, deg
ρ	free-stream density, slugs/ft^3
ω	frequency of oscillation, radians/sec
σ	radius at gyration of body, ft

APPARATUS

Wind Tunnel and Associated Test Equipment

The tests were conducted in the Ames 6- by 6-foot supersonic wind tunnel. This wind tunnel is a closed-return variable-density tunnel capable of operation over a Mach number range from 0.65 to 2.20 and pressures up to one atmosphere absolute. The tunnel has a perforated ceiling and floor which permit testing at transonic Mach numbers.

The static forces and moments on the models were measured by means of a sting-mounted strain-gage balance. Dynamic moments were measured by means of a forced-oscillation dynamic balance similar to the one described in reference 8.

Models

Six groups of models were tested in this investigation. Sketches of these models are shown in figure 1. With the exception of groups 5

and 6, each group consisted of a family of models in which one geometric parameter was changed from model to model. Table I lists the various parameters investigated and their values for each model.

The models have been assigned three-digit numbers for identification purposes. The first digit identifies the nose shape, the second digit, the body, and the third digit, the flare. Figure 2 shows sketches of the various noses, bodies, and flares with detailed dimensions. All parts had circular cross sections with the exception of flare 6. This flare consisted of a cone (identical to that of flare 5) from which sections had been removed. The sharp corners resulting from the removal of these sections were rounded to simulate a flare that would be suitable from an aerodynamic heating standpoint.

A photograph of model 511 mounted on the model support for static tests is shown in figure 3. Figure 4 shows the same model mounted for damping-in-pitch tests.

TESTS AND PROCEDURES

Test Variables

Static-force tests.- Normal-force, pitching-moment, and axial-force coefficients were determined at Mach numbers from 0.65 to 2.20 and at angles of attack from -4° to $+18^{\circ}$. The variation of Reynolds number with Mach number is shown in figure 5. All models were tested at these Reynolds numbers unless otherwise noted.

Damping-in-pitch tests.- The quantities determined during the damping-in-pitch tests were static stability, C_{m_α}, and damping-in-pitch parameter, $C_{m_q} + C_{m_{\dot{\alpha}}}$. The Mach number and Reynolds number ranges for the damping tests were the same as those mentioned above. The maximum angles of attack varied with Mach number for a given model and were different for different models as a result of support-system limitations. These limitations arise from the fact that the dynamic balance is mounted on the sting support by a set of crossed flexures which provide a mechanical spring for the system as well as a rotational axis. As the angle of attack of the sting is varied, the aerodynamic restoring moment deflects the model relative to the sting. The construction of the balance is such that the deflection of the balance relative to the sting is restricted to about $\pm 3\text{-}1/2^{\circ}$. Since the aerodynamic restoring moment varies with both Mach number and model, this $3\text{-}1/2^{\circ}$ limit was reached at different angles of attack for different models and Mach numbers.

Dynamic-stability data were obtained at both $\pm 1^{\circ}$ and $\pm 2^{\circ}$ oscillation amplitudes. Data were obtained initially at an oscillation amplitude of

A-229

$\pm 2^{\circ}$ for all Mach numbers. As the test progressed, it was discovered that for subsonic Mach numbers the variation of damping with angle of attack was very nonlinear at angles near zero. Since the $\pm 2^{\circ}$ oscillation amplitude tended to average the effects of these nonlinearities, data were also obtained at an oscillation amplitude of $\pm 1^{\circ}$ for these conditions.

Early in the investigation some consideration was given to the use of boundary-layer trip wires to simulate Reynolds numbers higher than those of the present investigation. Tests were made on one model with a trip wire located just aft of the junction of the nose and body. These tests showed that the trip wire had little effect on the results except for a strong destabilizing effect on the damping at subsonic speeds. However, inspection of shadowgraph pictures taken during the tests disclosed that at subsonic speeds the trip wire was completely submerged in a region of separated flow near the nose. It was felt that this condition was not representative of flow at higher Reynolds numbers. Because of the effect of the trip wire on the damping at subsonic speeds and the lack of effect on the other characteristics, the remainder of the investigation was made without trip wire.

Reduction of Data

Because the models tested are representative of shapes being considered for re-entry stages of ballistic missiles, it was felt that total-drag values would be of more interest than forebody drag. The axial-force coefficients therefore include the effects of base pressure. The question must be raised, then, as to the applicability of these values to vehicles in free flight since the presence of a sting in wind-tunnel tests will influence the base pressure and hence the axial force. Comparison is made in figure 6 of some of the data from this investigation with some unpublished data from free-flight tests of a geometrically similar model by the Pilotless Aircraft Research Division of the Langley Research Center. Figure 6(a) shows the variation of base-pressure coefficient with Mach number while figure 6(b) shows the variation of C_{A_o} with Mach number. It can be seen that the relatively small differences between flight and wind-tunnel base-pressure coefficients are not important when incorporated into the drag coefficient for the models of this investigation.

Table II shows the distance from the center of moments to the line of tangency of the nose and body in terms of body diameters and to the nose in terms of body length for the static and dynamic data for each model. For all models except those of group 2 and the damping-in-pitch tests of models 311 and 411, data were obtained for the center of moments located one body diameter from the line of tangency. In the case of the latter two models, the flatter nose shapes did not permit these

models to be located on the dynamic balance such that the oscillation axis would be one body diameter from the line of tangency. As a result, the oscillation axis and hence the center of moments for the dynamic test of these models was farther aft than that for the static tests.

Corrections to Data

Stream variation.- Surveys of the stream characteristics of the Ames 6- by 6-foot wind tunnel have shown that there is no appreciable stream curvature within the test section. In addition, the variation of the free-stream static pressure in the axial direction is less than ±1 percent of the dynamic pressure and has a negligible effect on the axial forces.

The stream surveys also showed that there was a stream angle in the test section that was less than 0.3° for all Mach numbers except $M = 2.20$ where it was 0.6°. Corrections for stream angle were incorporated in the computation of the static-force data. These corrections were omitted in the calculation of the dynamic data. However, they were sufficiently small that the interpretation of the results was not affected.

Tunnel-wall interference.- The effects of tunnel-wall interference on the static-force data were determined by testing three geometrically similar models of different size. These results are discussed in detail in the appendix. In summary, the tests showed that wind-tunnel wall effects increased the values of C_{m_α} and C_{N_α} for increasing model size at Mach numbers from about 0.8 to 0.9. In addition, a shock-wave reflection from the wind-tunnel ceiling, present only at $M = 1.1$, affected the results obtained at angles of attack greater than 6° or 7°. However, it is felt that these effects do not substantially change the trends of the data with variations in geometry and therefore do not affect the conclusions of the investigation. For this reason no corrections were made for wind-tunnel wall interference effects.

The effects of tunnel-wall interference on the dynamic data are difficult to assess. Reference 9 shows the effects of wind-tunnel resonance on a two-dimensional model in a solid-wall wind tunnel. However, there is a question as to whether a similar condition will exist for a three-dimensional model in a wind tunnel with perforated walls. Since no specific information is available on this point, no corrections were made to the data.

Model support interference.- Model support interference on the aerodynamic derivatives was considered to be limited to the effect on base pressure and axial force. An investigation of the effect of sting geometry on the base pressure for model 511 is reported in reference 10 and

shows that these effects are relatively small except near $M = 1.0$. In addition, the comparison made in figure 6 shows relatively small differences between wind tunnel and flight values of C_{p_b} and C_{A_o}. As the result of these considerations, no corrections were made for support effects.

One other support interference effect should be considered. When the oscillation frequency of the model in dynamic stability tests is near the resonant frequency of the model support system, the resulting motion of the model support can be sufficient to produce an appreciable translational motion of the model. This motion will be coupled to the angular motion of the model by both mass and aerodynamic forces and will, therefore, introduce errors in the dynamic derivatives being measured. When the damping-in-pitch tests were begun, it was discovered that the values of C_{m_α} measured were not in agreement with those obtained from the static-stability data. Since the model frequency was near that of the model support it was felt that model support vibration might be responsible for the differences. Stiffeners were added to the sting in order to raise the natural frequency of the model support system and to reduce the deflection at the model. These stiffeners can be seen in figure 4. They consisted of two plates 4 inches wide by 1/2 inch thick, tapered and beveled as shown and welded to the sting in the plane of the pitching motion. When the initial dynamic tests were repeated, it was found that the values of C_{m_α} were now in much better agreement with the static data. Although it was not possible to make a direct comparison of this type for the damping-in-pitch coefficients, it was presumed that the addition of stiffeners to the sting also reduced any effects of model support vibration on the damping.

Precision of Data

The precision of the data was determined by an analysis of repeat points taken on various models during the investigation. The root mean square scatter for the coefficients was as follows:

C_N	±0.007
C_A	±0.015
C_m	±0.006
$C_{m_q} + C_{m_{\dot{\alpha}}}$ (Subsonic)	±2.5
$C_{m_q} + C_{m_{\dot{\alpha}}}$ (Supersonic)	±1.0

The difference in accuracy in the damping coefficients obtained at subsonic and supersonic speeds was the result of increased buffeting due to flow separation over the model at subsonic speeds.

RESULTS AND DISCUSSION

The data obtained on the models considered in this investigation are given in tables III and IV. The data in table III are those obtained from static-force tests while those in table IV were obtained from damping-in-pitch tests. In addition to $C_{m_q} + C_{m_{\dot{\alpha}}}$, table IV also presents the reduced frequencies, k, of the damping tests. Inasmuch as C_{m_α} can be obtained from the static-force data it was not felt necessary to present the values of C_{m_α} determined in the damping tests. The results of the investigation will be discussed with the use of summary plots of pertinent aerodynamic parameters as a function of Mach number. The detailed data are plotted only where it was necessary to demonstrate specific points.

The following discussion is divided into three sections; the first on the static characteristics at angles of attack near zero, second, the static stability at angle of attack, and the third, the damping-in-pitch characteristics.

Static Stability at $\alpha = 0^\circ$

It was pointed out in the Introduction that the dynamic stability of the re-entry vehicle is dependent on the values of C_D, C_{L_α}, and $C_{m_q} + C_{m_{\dot{\alpha}}}$. It is, of course, necessary that the vehicle be statically stable. In fact, in the initial portion of the re-entry trajectory the rapid increase in atmospheric density has a powerful constraining effect on the oscillation amplitude for statically stable vehicles. Since the vehicles considered in this investigation would fly nonlifting trajectories, it is important that the values of C_{m_α}, C_{N_α}, and C_A be examined for $\alpha = 0^\circ$.

Flow characteristics at $\alpha = 0^\circ$.- Observations of the flow revealed that all the models of this investigation experienced a flow separated symmetrically from the nose at subsonic speeds and an attached flow over most of the model at supersonic speeds. Shadowgraph pictures of the flow around model 515 at various Mach numbers are given in figure 7 and illustrate the two types of flow mentioned. For the models with nose shapes 1, 2, 5, and 6, transition from separated to attached flow or the reverse

always took place at a Mach number between 0.90 and 1.00. This was not true for the models having noses 3 or 4, however, For these models the point at which the flow became attached as Mach number was increased was between 1.1 and 1.2, while the value at which the flow separated as Mach number was decreased was about 1.00. Thus for Mach numbers from about 1.0 to 1.2, the flow could be either attached or separated.

One detail concerned with the separated flow that is not apparent from the shadowgraph pictures was discovered in a test of one model that had tufts on the cylindrical body. In this test it was found that at $M = 0.65$ the tufts near the nose showed a reverse flow over the surface of the model while the tufts farther back on the body showed flow in the free-stream direction. Thus, although figure 7(a) shows highly turbulent flow over the entire body and flare suggestive of separated flow, the tuft study indicated a region of separated flow near the nose and transition to flow akin to attached flow farther back on the body. The tuft study also showed that as Mach number was increased in the subsonic speed range, the tufts over more and more of the forward portion of the body indicated reverse flow.

As would be expected the static forces are strongly influenced by the condition of the flow over the body. Figure 8 gives values of C_{N_α}, C_{m_α}, and C_A at $\alpha = 0^\circ$ for each group of models. It can be seen that the values of C_{N_α} and C_{m_α} associated with the separated flow are considerably larger than those for attached flow. It is possible that the increase in C_{N_α} and C_{m_α} with increasing subsonic Mach number is due in part to the larger area of separated flow present at the higher speeds.

Effect of nose shape.- Figure 8(a) shows the effect of nose eccentricity on the static aerodynamic characteristics. It is seen that for the pitching-moment and normal-force characteristics the effects of nose shape are limited primarily to Mach numbers where the flow separates from the nose. It should be noted that in the low subsonic speed range ($M = 0.65$), the flow over model 111 was not separated but remained attached. As a result, the values of C_{m_α} and C_{N_α} are considerably lower than for the other models on which separation occurred.

This figure and figure 8(b) also show the results of the two flow conditions possible for the models with noses 3 and 4 in the Mach number range from 1.0 to 1.1. Here the curves for a given model overlap in this region showing the possibility of two different sets of aerodynamic forces and moments depending on the direction this region is approached. The dotted lines attaching the two branches of the curves are drawn to indicate the approximate limits of this region. These lines indicate that at some Mach number between the ends of the lines, the flow (and hence the aerodynamic characteristics) changed abruptly from one type to

the other. Although force data were not obtained for these models at $M = 1.2$, visual observation indicated that flow attachment was always accomplished between $M = 1.1$ and 1.2 as Mach number was increased.

Effect of flare base area.- The effect of flare base area can be seen in figure 8(b). Here, in contrast to the effect of nose shape, increasing flare base area increases C_{m_α}, C_{N_α}, and C_{A_o} through the entire Mach number range.

Effect of flare angle.- Figure 8(c) shows that the static characteristics were not appreciably affected by the change in flare angle from 16.5° to 11.7°.

Effect of body length.- The small change in body length investigated produced little effect on the static characteristics, as can be seen in figure 8(d).

Effect of flare relief.- Figure 8(e) shows the characteristics of models 515 and 516 which were identical in shape except for the removal of sections of the flare on model 516. Despite the removal of about 20 percent of the base area of the flare the static stability, C_{m_α}, was not appreciably changed with flare relief. The flat sides of the flare for model 516 produced a somewhat larger value of lift for that model at supersonic speeds. However, this increase in normal force was accompanied by a forward shift in the center of pressure that left the static stability unchanged. As would be expected flare relief lowered the drag of the model through the entire Mach number range.

Other models.- The static characteristics of the models in group 6 are shown in figure 8(f). The results for model 511 have been repeated here for comparison purposes since the models in this group are variations of model 511. The particular choice of models was based on data obtained on other models at angle of attack. The reasons for these choices will be discussed more fully in the next section. It can be seen that the primary effects of the variations in the models was to change the values of C_{N_α} and C_{m_α} in the subsonic speed range. The nose shape of model 641 tended to delay the separation of the flow in the region of the nose. At $M = 0.65$ the flow was attached for this model. For model 5-8 the flow was separated from the nose at all subsonic Mach numbers tested but apparently the effect of this separated flow over the conical body on the static characteristics was smaller than that over the cylindrical body. The curved flare of model 517 produced somewhat higher values of C_{N_α} and C_{m_α} up to Mach numbers near 1.6 despite the fact that the length and base area of the flare were identical to that of model 511.

Static Stability at Angle of Attack

Flow characteristics at angle of attack.- The static force tests of the models of this investigation also revealed a strongly nonlinear variation of pitching moment with angle of attack that was the result of an abrupt separation of the flow over the model as angle of attack was increased. This phenomenon was observed on all models tested and occurred roughly between Mach numbers from 1.0 to 1.3. When separation took place, the flow assumed one of two forms. For most models and Mach numbers the separated region was confined to the leeward side of the body. However, for models having noses 3 and 4 at Mach numbers of 1.0 and 1.1 the flow separated around the entire body. Figure 9 illustrates the pitching-moment variation and flow characteristics typical of the first type of flow. As angle of attack was increased from a low value, a point was reached where the flow, which was normally attached over the model, separated from the nose on the leeward side of the body, causing an abrupt increase in pitching moment. As the angle of attack was reduced from this point, the flow reattached at a lower angle of attack giving rise to the loop in the pitching-moment curve shown in figure 9. A similar plot for the second type of flow is given in figure 10. In this case as the angle of attack was increased to the point where separation occurred, the flow separated around the entire nose. When the angle of attack was lowered, reattachment did not take place. Instead, the flow remained separated from the nose and was typical of the subsonic flow characteristics shown in figure 7(a).

Figure 9 also shows the transitional nature of the flow typical of Mach numbers from 1.0 to 1.3 at angles of attack sufficient to separate the flow. In this case the separated flow off the leeward side of the body looks very much like the separated flow present at subsonic speeds while the attached flow on the windward side is characteristic of the higher supersonic speeds. This can also be seen to some extent in the pitching-moment characteristics in this Mach number range.

In order to show in more detail the type of pitching-moment data obtained on the models at transonic speeds, the variations of C_m with α for two models are given in figure 11. The data presented in figure 11(a) are typical of models that have flow separation characteristics of the first type. The data shown in figure 11(b) are typical of models having the second type of flow separation. It is important to note that for this second type of flow at Mach numbers from 1.0 to 1.1, once separation has occurred, the flow remained separated for the models tested. Thus the vertical lines in figure 11(b) indicating the abrupt shift in pitching moment associated with separation at these Mach numbers are broken to indicate that this shift will take place only the first time the angle for separation is exceeded. It should also be noted that the data were obtained in steps of decreasing Mach number. Thus since the flow separated

completely around the nose at $M = 1.1$, it was necessary to raise the Mach number until the flow reattached and then to lower it to $M = 1.0$ to obtain data at that Mach number with flow attached.

The data in figure 11 show that, in general, as Mach number is increased, the angles of attack for flow separation and attachment increase. As is pointed out in the appendix, a reflected shock wave caused the flow to separate prematurely at $M = 1.1$. Thus the data given in figure 11 for $M = 1.1$ indicate an angle of attack for separation that is too low. Separation was not observed on any of the models at $M = 1.6$ or above within the angle-of-attack range of this investigation.

A229

Effect of a pitching-moment loop on vehicle dynamics.- The effect of a loop in the pitching-moment curve, such as those shown in figures 9 and 10, on the dynamic stability of a free-flight vehicle is to introduce energy into the system. This can be shown by reference to sketch (a). The potential energy acquired as the result of a deflection α can be expressed as

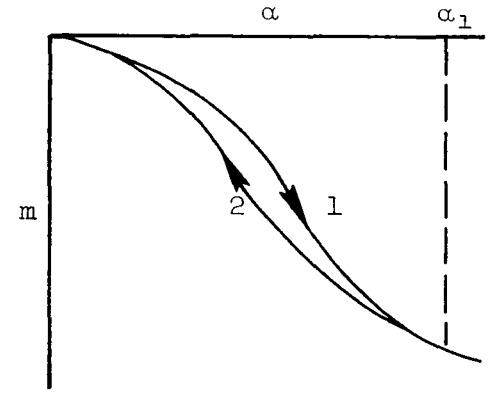

Sketch (a)

$$E = \int_0^{\alpha} m d\alpha$$

where m is the pitching moment. The net energy over the half cycle that extends to an angle of attack, α_1, beyond the loop is then

$$E = \int_0^{\alpha_1} m_1 d\alpha - \int_0^{\alpha_1} m_2 d\alpha$$

where m_1 and m_2 are the moments for branches 1 and 2 of the moment curve. This expression simply states that potential energy is acquired over the first quarter cycle and released over the second quarter. However, if the moment m_2 is more stable than m_1, then a surplus of energy has been released during the traverse around the loop. The amount of energy released is proportional to the area of the loop.

If, in addition to the loop in the static pitching-moment curve, the damping in pitch of the vehicle is stable, the oscillation amplitude of the vehicle will increase until the surplus energy produced by the

loop is balanced by the energy absorbed by the stable pitch damping. The result is a limit-cycle oscillation. The amplitude of the limit cycle is governed, of course, by the relative amounts of energy produced by the loop and absorbed by pitch damping. Unpublished results of a free-flight test of a model similar to 511 in the Ames supersonic free flight wind tunnel show that oscillation amplitudes of from 25° to 30° were achieved even in the limited number of cycles permitted by the range test.

It is evident that the pitching-moment characteristics of the type shown in figure 11(b) at $M = 1.0$ and 1.1 are preferable to those shown in figure 11(a) at $M = 1.0$ to 1.3. In the latter case a deflection greater than the angle of attack for separation in the Mach number range from 1.0 to 1.1 would result in a large amplitude limit-cycle oscillation since the loop is traversed each half cycle in this Mach number range. In the former case the loop would be traversed only over the first half cycle of the oscillation whose amplitude was sufficiently large to separate the flow. For all subsequent cycles, the pitching-moment characteristics would be typical of subsonic flow and the loop would not be present.

Several comments relative to the effect of the pitching-moment loop on the performance of a re-entry body are pertinent here. All models tested in this investigation have relatively large values of drag coefficient. Unless the weight of the vehicle is kept to a rather high value, the terminal velocity for most re-entry trajectories will be in the subsonic speed range. If the vehicle has adequate static and dynamic stability at supersonic speeds, any initial angular misalinement relative to the flight path upon re-entry will have been reduced to a relatively small value before transonic speeds are reached. If the model is not disturbed as it decelerates through the transonic Mach numbers, the pitching-moment loops will not affect the motion of the vehicle since the angle of attack is not likely to exceed the angle for flow separation. However, if the trajectory is such that the transonic portion occurs in the lower altitude range, it is possible for the vehicle to be deflected by atmospheric disturbances. If the angle of attack due to these disturbances exceeds the angle for flow separation, the amplitude of motion will grow rapidly to the limit-cycle value. This oscillatory motion, in itself, is not necessarily detrimental to the accuracy of the vehicle since it will be symmetrical about $\alpha = 0^{\circ}$. However, it is possible that it could have a detrimental effect on the mission of the vehicle through other means. As was mentioned previously, the amplitude of oscillations caused by the pitching-moment loop may be relatively large. If, in addition, the frequency is sufficiently high, the transverse accelerations resulting from this motion may be sufficient to have a detrimental effect on instrumentation or personnel carried in the vehicle. Furthermore, if pressures measured on the surface of the vehicle were to be used in controlling some of the instrumentation carried, large

amplitude deflections would probably change these pressures significantly and adversely affect the performance of the vehicle in this manner.

It can be seen from the above discussion that the effect of the pitching-moment loop is not necessarily detrimental to the performance of the vehicle. If, however, large amplitude oscillatory motion does adversely affect the performance, several points can be made as to modifications necessary to minimize or eliminate these adverse effects. The most obvious change would, of course, be the choice of a configuration that does not have flow-separation problems. However, if design requirements other than aerodynamic stability dictate the use of blunt-nosed cylinder-flare configurations, this may be difficult to achieve. Another choice would be to select a shape that promotes separation around the entire body at as high a Mach number as possible, thereby restricting the Mach number range for which loops will occur at low angles of attack. A third possible choice would be a shape for which the angle of attack for flow separation was as large as possible for all Mach numbers. Under these circumstances, the possibility of encountering an atmospheric disturbance sufficient to deflect the vehicle to these angles of attack would be reduced. The following discussion, therefore, is intended to show the effects of variations in model geometry on the angles of attack for separation and attachment and will serve to point out those models within the range tested which have the more desirable characteristics just mentioned.

A229

Effect of nose shape.- In order to present the effects of variations in model geometry on the pitching-moment loops, summary plots showing the angles of attack for separation and reattachment of the flow as a function of Mach number are given in figure 12. Detailed information of the size of the loops can be obtained from the tabulated data.

It should be noted again at this point that because of wind-tunnel wall effects, the data at $M = 1.1$ are suspect. These data are included in the figures because it is felt that they still give an indication of trends although the magnitudes may be incorrect by as much as 5° to 7°. It should also be noted that the angles of attack given in figure 12 were obtained from data that were taken in 1° increments. This fact alone introduces an uncertainty of $\pm 0.5^{\circ}$ in the results. In addition repeat points for several models have shown that the angles were repeatable only to $\pm 1^{\circ}$. Thus the values plotted in figure 12 are probably not accurate to better than $\pm 1^{\circ}$. It is felt, however, that the trends with changes in various parameters are still correct. It will also be noticed that the points for a given model are connected with straight lines. These lines are included only to make the comparison of the data for the various models easier and should not be taken as an indication of values for Mach numbers between those for which data were obtained.

Figure 12(a) presents the angles for separation and reattachment for the four models having different nose shapes. It is immediately

obvious that the rounder nose shapes delayed separation to a higher angle of attack than did the flatter shapes. For model 111 separation did not occur at $M = 1.3$ up to the maximum angle of attack of this investigation, 18°. The dotted line connecting the angles for separation between $M = 1.0$ and 1.1 for model 411 is to indicate that flow separation will occur at the lower Mach number only if it has not occurred at the higher one. This is also true for comparable points shown in figure 12(b). The point denoting flow separation at $M = 1.0$ for model 311 is missing because of an oversight. Data were not obtained with flow attached at $M = 1.0$ for this model.

Figure 12(a) also shows again that the flatter nose shapes promote complete separation. As the nose shape became flatter, the angle for reattachment decreased until for models 311 and 411 and Mach numbers of 1.0 and 1.1, no angle of attack could be found for which reattachment would take place; that is, the flow remained separated even at $\alpha = 0^{\circ}$.

Effect of flare base area.- The data given in figure 12(b) show that increasing base area reduced the angle of attack for which separation occurred. In this case, the nose shape for the three models was such that complete separation occurred around the nose at Mach numbers of 1.1 and 1.0. While the primary cause of separation for all models investigated herein was nose bluntness, the disturbance created by the flare had an important effect on the angle at which separation occurred. Evidence of the flare disturbance was given by the presence of a shock wave approximately normal to the body surface located between the nose and flare. This shock wave can be seen in figures 7(b), 7(c), 9, and 10. Examination of the shadowgraph pictures taken during the investigation has shown a direct correspondence between the location of this shock wave at $\alpha = 0^{\circ}$ and the angle for flow separation; the nearer this disturbance is to the nose, the lower the angle of attack for separation. For instance, for the three models shown in figure 12(b), the shock-wave position moved nearer the nose as flare base area was increased for Mach numbers of 1.0 and 1.1. However, at $M = 1.3$ the shock location was nearly the same for the three models.

Effect of flare angle.- Figure 12(c) shows that a reduction in flare angle from 16.5° to 11.7° resulted in a significant increase in separation angle of attack at $M = 1.0$ and 1.1.

Effect of body length.- In figure 12(d) it can be seen that a relatively small increase in body length resulted in an appreciable increase in the angle of attack for separation at Mach numbers of 1.0 and 1.1. At $M = 1.3$ the increase in body length had no appreciable effect on the angle for separation. At this Mach number the disturbance from the flare was apparently sufficiently far removed from the nose that it had no effect on the separation angle of attack. This conclusion is further borne out by the fact that all the models with nose 5 and a cylindrical body had approximately the same angle for separation at $M = 1.3$.

Effect of flare relief.- The effect of flare relief on the angles of attack for separation and attachment is shown in figure 12(e). It is seen that the removal of approximately 20 percent of the base area in the manner shown increased the angle for separation appreciably for Mach numbers of 1.0 and 1.1. Although the pitching-moment loop was not precisely defined at $M = 1.3$ for model 516, the data available indicated that, for that Mach number, separation took place between 12° and 15°. Thus flare relief probably has little effect at that Mach number since, as noted previously, the disturbance from the flare occurred sufficiently downstream to be ineffective.

Other models.- The configurations for the models in group 6 were selected on the basis of results obtained during the investigation. The nose shape for model 641 was the result of an attempt to find a nose that would have a relatively high drag, and yet minimize the separation effects. Previous results had shown that increasing the radius of curvature near the junction of the nose and body increased the angle for separation. Thus nose 6 was made up of a flat face to give the necessary drag and an elliptical fairing to the body with the major axis of the ellipse parallel to the body center line to give a relatively large radius of curvature at the shoulder. The curved flare of model 517 was tested in an attempt to find a flare with the same length and base area as flare 1 but with an increased effectiveness as a stabilizing device and a higher angle of attack for separation. An arbitrary choice of constant pressure gradient over the flare was made. Newtonian impact theory was used to calculate the contour of the flare to satisfy this condition. The model with a conical body, 5-8, was tested to investigate the effects on the separation angles of attack of removing the disturbance created by the cylinder-flare junction. The results for model 511 are also presented in this figure for comparison purposes.

A229

It can be seen that the change in nose shape did increase the angle for separation a small amount at $M = 1.0$ and 1.1. However, it decreased it about the same amount at $M = 1.3$. The curved flare had very little effect on the angles for separation and attachment. It did improve the static stability to some extent, as was pointed out in the discussion of figure 8(f). Model 5-8 showed a large increase in both separation and attachment angles of attack. For this model, since the flare began at the nose, the disturbance created by the junction of the cylinder and flare was not present. The absence of this disturbance undoubtedly accounts for the larger angles of attack required for separation.

Damping in Pitch

Effects of flow changes on damping.- Figure 13 shows a plot of $C_{m_q} + C_{m_{\dot{\alpha}}}$ versus α for model 511 at several Mach numbers. This figure

is included to show the typical variation of pitch damping with angle of attack. As with the static data, there was a large difference between the results obtained at subsonic speeds and those obtained at supersonic speeds. Again this behavior can be associated with the flow characteristics. The large unstable damping values at subsonic speeds and $\alpha = 0^{\circ}$ are associated with the flow that is separated symmetrically from the nose. Figure 14 shows a plot of damping coefficient versus angle of attack typical of subsonic speeds, and the associated flow pictures for this speed range. It can be seen that the large unstable damping coefficients at $\alpha = 0^{\circ}$ are linked with the fully separated flow while the stable values at the higher angles of attack are associated with the flow that is attached on one side of the model.

Interpretation of results.- The nonlinear variation of the damping with angle of attack raises the question of how to interpret the results. These damping data, as previously stated in the section on tests and procedures, were obtained for small amplitude oscillations about various angles of attack. Such a technique represents an experimental linearization at each angle of attack and would be expected, therefore, to be more valid for small amplitudes of oscillation than for large amplitudes. Again, from figure 13, it can be seen that at subsonic speeds the damping varies so rapidly with angle of attack that the averaging effect of a 2° oscillation amplitude produced markedly different values from those obtained with a 1° oscillation amplitude. It is clear from these data that the 1° oscillation amplitude data are more representative of the correct damping function. Neglecting possible time dependence on the damping function, the nonlinear differential equation describing the single degree of freedom oscillations of a system having the damping and restoring moment characteristics as presented in figure 13 at subsonic Mach numbers is of the form

$$\ddot{\alpha} + f_1(\alpha)\dot{\alpha} + f_2(\alpha) = 0$$

where $f_1(\alpha)$ and $f_2(\alpha)$ are the damping and restoring functions respectively. Such a nonlinear equation would be expected to have a limit cycle oscillation for the type of damping moments being considered since an energy exchange occurs by virtue of the unstable damping at angles of attack near zero and the stable damping at higher angles. In this case, however, the energy introduced by the unstable damping in pitch is considerably lower than that introduced by the pitching-moment loop. As a result, the limit-cycle amplitude should be considerably smaller. This estimate has been confirmed by tests in the Ames supersonic free flight wind tunnel. A model geometrically similar to model 511 was fired at Mach numbers below 1.0. The unpublished results of this test show that the motion, which was essentially planar, grew in amplitude over the first few cycles to about $\pm 8^{\circ}$. It then decreased slowly during the

remainder of the flight. This motion was compatible with the damping measurements made in this investigation which show larger values of unstable damping at $M = 0.90$ than at $M = 0.65$. Thus the results of this free-flight test tend to confirm the interpretation of the present data in terms of its application to large oscillation amplitudes in planar motion.

Effect of nose shape.- In order to show the effects of the geometric variations on the damping in pitch, the data are plotted in figure 15 as a function of Mach number for three angles of attack. The $\pm 1^{\circ}$ oscillation-amplitude data are indicated by the filled symbols and are plotted whenever the flow was separated around the entire nose.

As was mentioned earlier, the maximum angle of attack for which damping-in-pitch data were obtained varied with Mach number as a result of the variation of aerodynamic restoring moment acting on the model. The pitching-moment loop also played a part in determining the maximum angle of attack for which dynamic data could be obtained. If the model was deflected to a point where the asymmetric flow separation occurred, the energy introduced by the loop resulted in an uncontrollable oscillation limited only by the mechanical stops. It was not possible to obtain damping data under these conditions.

The models shown in figure 15(a) are somewhat different from those presented in previous figures showing the effects of nose shape. One reason for the difference is that damping data were not obtained for model 211. In addition, damping data were obtained for models 311 and 411 about a different moment center than that for model 111. In order to present data for a group of models having the same location of moment center relative to the line of tangency of nose and body, it was decided to omit the data for model 111 from this plot. The damping-in-pitch results for this model are presented in tabular form in table IV. Since model 511 was tested at two centers of rotation, the data for the center of rotation corresponding to that used for models 311 and 411 is used here.

It can be seen that nose shape affects the damping only at Mach numbers where the flow is separated symmetrically from the nose. In this region the flatter nose shapes have much more unstable values of damping at $\alpha = 0^{\circ}$. Since the data obtained at the higher angles of attack are sparse it is difficult to tell what the effects of nose shape are at these angles of attack.

It is interesting to note that nose shapes 3 and 4 were those that promoted separation around the entire nose at Mach numbers as high as 1.1. Thus the Mach number range for which the pitching moment loops at low angles of attack could be encountered was reduced. However, it can be seen in figure 15(a) that when symmetrical separation does take place,

the unstable damping in pitch for these nose shapes will tend to produce larger limit-cycle amplitudes at subsonic speeds than those for the models with more rounded noses.

Effect of flare base area.- Figure 15(b) shows that an increase in flare base area increases the magnitude of the damping in pitch throughout the Mach number range independent of the sign of the damping. It was not possible to obtain dynamic data for model 323 with the flow attached at Mach numbers of 1.0 and 1.1. Figure 8(b) shows that it was possible to have both flow conditions at these Mach numbers for static conditions. However, the angle of attack necessary to cause separation was sufficiently low for model 323 that the flow would not remain attached when the model was oscillating.

Effect of flare angle.- The data plotted in figure 15(c) show that the lower angle and greater length of flare 4 made the damping, in general, more stable.

Effect of body length.- At supersonic speeds the effect of increasing the length of the cylindrical body clearly increased the stable damping (fig. 15(d)). At subsonic speeds the effect was mixed.

Effect of flare relief.- Figure 15(e) shows that there is a definite advantage to providing flare relief in terms of the damping at subsonic speeds. In fact, model 516 was the only model tested in this investigation that had stable damping through virtually the entire Mach number range. For this model, it is believed that the additional moments resulting from the exposure of flat surfaces to the viscous cross flow add to the damping.

Other models.- Of the models in group 6 damping data were not obtained for model 517. The results for the other two models in the group along with those of model 511 for comparison purposes are presented in figure 15(f). It can be seen that the effect of nose 4 on the damping at supersonic speeds was small. The relatively large stable shift in the damping at subsonic speeds for this model is, in part, the result of the 2° oscillation amplitude. However, comparison of the tabulated data for models 641 and 511 at 2° oscillation amplitude shows that at the lower subsonic Mach numbers the damping for model 641 was more stable than that for model 511. The conical model (5-8) showed more stable damping than model 511 at $\alpha = 0^{\circ}$ throughout the speed range except at $M = 2.20$.

Reynolds Number Effects

During the course of the present investigation and of several subsequent investigations, an effort was made to determine the effects of Reynolds number on the characteristics of blunt-nosed cylinder-flare

models. Model 511 was tested statically at Reynolds numbers from approximately 0.25×10^6 to 1.0×10^6 in the 6- by 6-foot wind tunnel and from about 1.0×10^6 to 7.0×10^6 in the 11- by 11-foot wind tunnel. The results of these tests indicated certain trends with Reynolds number that will be discussed below. Subsequent to these tests of model 511, some additional data were obtained showing the effect of Reynolds number on the characteristics of models with nose shapes somewhat different from nose 5. These data show Reynolds number effects that differ to some extent from those found on model 511. Work is continuing in an effort to clarify the situation. The results of the investigation of Reynolds number effects on model 511 in the 6- by 6-foot wind tunnel are presented in figure 16. The reader is cautioned against applying these results to other blunt shapes.

A229

The values of C_{m_α} given in figure 16(a) indicate higher static stability with decreasing Reynolds number throughout the Mach number range, although the effect was most pronounced at subsonic speeds. The reason for the increase in the magnitude of C_{m_α} with decreasing Reynolds number is not fully understood. It is possible that, at subsonic speeds where the flow was separated from the nose, Reynolds number had an effect on the location of the reattachment point of the flow on the body and through this action exhibited a larger effect on the pitching moment than at supersonic speeds. The unpublished results of the investigation of model 511 in the 11- by 11-foot wind tunnel show that the effect of Reynolds number on the static stability continued to Reynolds numbers as high as 7.0×10^6. A reduction in Reynolds number had a definite effect on the angles for separation and attachment as shown in figure 16(b). However, the results of the 11-foot investigation indicated that the angles for separation and attachment obtained at Reynolds numbers of 1.0×10^6 were, in general, the same as those obtained at $R = 7.0\times10^6$ and were in agreement with the results of the present investigation obtained at $R = 1.0\times10^6$. The damping in pitch showed little effect of Reynolds number for the two values tested (fig. 16(c)).

CONCLUSIONS

An investigation of the static and dynamic aerodynamic characteristics of a series of blunt-nosed cylinder-flare models at Mach numbers from 0.65 to 2.20 has led to the following conclusions:

1. The static force data for the models investigated had two distinct characteristics at subsonic speeds, the variations of normal-force and pitching-moment coefficients with angle of attack were nonlinear as a result of flow separation from the nose of the models; in contrast, these variations at supersonic speeds and low angles of attack were linear, although smaller than those at subsonic speeds, as the result of attached flow over the model.

2. The static stability was increased through the Mach number range by increasing flare base area and flare angle and at subsonic speeds by increasing nose bluntness. Increasing cylindrical body length had little effect on the static characteristics.

3. At Mach numbers from 1.0 to 1.3, all models of this investigation exhibited a large, abrupt stable shift in the pitching moment with increasing angle of attack that was related to two different flow conditions on the model. At small angles of attack, the flow was attached and the pitching moment was small. At large angles of attack, the flow was separated asymmetrically and the pitching moment was more stable. However, with decreasing angle of attack the separated flow persisted to an angle of attack less than that for the onset of separation. Thus there was a range of angles for which two values of pitching moment were possible depending on whether the angle of attack was increasing toward that for separation or decreasing toward that for attachment resulting in a pitching-moment loop. This loop can introduce relatively large amounts of energy into the free-flight pitching motion of the vehicle.

4. The angle of attack at which flow separation took place was decreased by increasing flare base area and flare angle and by decreasing Mach number, cylindrical body length, and radius of curvature of the nose at the junction of the nose and body. When the nose radius of curvature was made sufficiently small, the flow separated so that reattachment was not possible by changing angle of attack.

5. The damping in pitch of all models was stable and relatively constant for changes in angle of attack at supersonic Mach numbers where the flow was attached to the body. At subsonic Mach numbers where the flow is separated symmetrically from the nose, the damping was unstable for angles of attack near zero and stable at the higher angles.

6. Increasing nose bluntness increased the unstable damping at angles of attack near zero at subsonic speeds. Increasing the flare base area increased the magnitude of the damping throughout the Mach number range independent of the sign of the damping. The damping was made more stable through the speed range by a decrease in flare angle and at supersonic speeds by an increase in cylindrical body length.

Ames Research Center
National Aeronautics and Space Administration
Moffett Field, Calif., Aug. 5, 1959

APPENDIX

WIND-TUNNEL WALL EFFECTS

A considerable effort has been made in assessing the effects of wind-tunnel walls on models that consist of sharp-nosed bodies of relatively high fineness ratio with and without wings and tails. Since the aerodynamics of blunt shapes such as those investigated here have become important only in recent times, information about wall effects for these shapes is scarce. For this reason tests were made to indicate what wall effects, if any, might exist for the models of this investigation.

One direct method of determining the effects of wind-tunnel walls on the aerodynamic characteristics of a model is to test two geometrically similar models of different size in the same wind tunnel. Another method is to test the same model in two different wind tunnels of different size. Both methods were used in this investigation. A 2.0- and a 0.6-scale model of model 511 were tested in the Ames 6- by 6-foot supersonic wind tunnel. In addition, model 511 was also tested in the Ames 11-foot transonic wind tunnel over a Mach number range from 0.65 to 1.30. The blockage ratios for the various models based on flare base area and expressed as a percentage of the tunnel cross-sectional area were as follows:

Scale of model	Percent blockage in 6- by 6-foot tunnel	Percent blockage in 11- by 11-foot tunnel
2.0	1.19	----
1.0	.30	0.09
.6	.11	----

The Reynolds numbers for all models except the 0.6-scale model were those shown in figure 5. The Reynolds numbers for the 0.6-scale model were 0.6 times those shown in figure 5. Plots of the static characteristics and the angles for separation and reattachment for these models are given in figure 17.

In figure 17(a) it is seen that the values of C_{m_α}, C_{N_α}, and C_{A_o} obtained for model 511 in the two wind tunnels agree very closely except at Mach numbers of 0.80 and 0.90. The reason for this disagreement is not known. However, a contributing factor may be the fact that only the floor and ceiling of the 6- by 6-foot wind tunnel are perforated. The side walls are solid. In addition, the porosity of the floor and ceiling of the 6- by 6-foot wind tunnel is 3 percent of the area of the surface while that for the 11-foot wind tunnel is 6 percent.

The values of C_{m_α} and C_{N_α} for all models agree well in the supersonic speed range except for the 2.0-scale model at $M = 1.20$. Shadowgraph pictures of the flow around this model at this Mach number show the presence of a shock wave that is apparently a reflection of the bow wave from the ceiling of the wind tunnel. This shock wave had a pronounced effect on the static forces and also the separation angle of attack. This same model shows a sizable deviation in drag coefficient in the low supersonic speed range. The deviation is due to a difference in base pressure for the 2.0-scale model.

At subsonic speeds both the 2.0- and 0.6-scale models exhibited higher values of C_{m_α} and C_{N_α} than did model 511 in the 11-foot wind tunnel. In the case of the 0.6-scale model, this increase can be attributed in part to the reduced Reynolds number for this model.

In figure 17(b) it is seen that the separation angles of attack for model 511 in the 6- by 6-foot wind tunnel differ significantly from those obtained in the 11-foot wind tunnel only at $M = 1.10$ while those for the 2.0-scale model differ only at $M = 1.20$. (The maximum angle of attack for the 11-foot wind tunnel tests was 14.7° so that the angle of attack for flow separation was not reached at $M = 1.30$.) The reduction in separation angle for the 2.0-scale model was the result of the reflected disturbance mentioned above. Inspection of the shadowgraph pictures taken of model 511 in the 6- by 6-foot wind tunnel has shown the presence of a similar though weaker disturbance at $M = 1.10$ for this model. There is no evidence that the disturbance affected the static characteristics of this model but the similarity in the reduction of separation angle for this model at $M = 1.10$ and the 2.0-scale model at $M = 1.20$ indicates that the reflected disturbance is probably the cause of this reduction. Inspection of the shadowgraph pictures for all models showed that this disturbance was present for most models of this investigation but only at $M = 1.10$.

The generally lower angles of attack for separation found on the 0.6-scale model are attributable to the lower Reynolds number for this model.

The foregoing discussion shows that the wind-tunnel wall effects for the present investigation appear to be concentrated in a reflected disturbance present only at $M = 1.10$ and in a modification to the lift and pitching-moment data at $M = 0.80$ and 0.90. However, it is felt that the presence of the wall effect has not substantially changed the trends of the data with variations in model geometry. Thus the conclusions of the investigation are not affected by the tunnel wall effects.

REFERENCES

1. Allen, H. Julian: Motion of a Ballistic Missile Angularly Misaligned With the Flight Path Upon Entering the Atmosphere and Its Effect Upon Aerodynamic Heating, Aerodynamic Loads, and Miss Distance. NACA TN 4048, 1957.

2. Sommer, Simon C., and Tobak, Murray: Study of the Oscillatory Motion of Manned Vehicles Entering the Earth's Atmosphere. NASA MEMO 3-2-59A, 1959.

3. Fisher, Lewis R., Keith, Arvid L., Jr., and DiCamillo, Joseph R.: Aerodynamic Characteristics of Some Families of Blunt Bodies at Transonic Speeds. NASA MEMO 10-28-58L, 1958.

4. Tom, William S.: Aerodynamic Characteristics of the ML-404-20 Polaris Re-entry Models; Preliminary Results. Tech. Note 5034-32, U. S. Naval Ord. Test Station (China Lake, Calif.), Nov. 14, 1957.

5. Coltrane, Lucille C.: Stability Investigation of a Blunt Cone and a Blunt Cylinder With a Square Base at Mach Numbers From 0.64 to 2.14. NACA RM L58G24, 1958.

6. Knechtel, Earl D., Wakefield, Roy M., and Treon, Stuart L.: Transonic Static Aerodynamic Characteristics of a Low-Fineness-Ratio Body of Revolution Having a Blunt Ellipsoidal Nose and Flared Afterbodies of Various Angles and Base Areas. NASA TM X-113, 1959.

7. Fletcher, Herman S., and Wolhart, Walter D.: Damping in Pitch and Static Stability of a Group of Blunt-Nose and Cone-Cylinder-Flare Models at a Mach Number of 6.83. NASA MEMO 5-6-59L, 1959.

8. Beam, Benjamin H.: A Wind-Tunnel Test Technique for Measuring the Dynamic Rotary Stability Derivatives at Subsonic and Supersonic Speeds. NACA Rep. 1258, 1956.

9. Runyan, Harry L., Wooston, Donald S., and Rainey, A. Gerald: Theoretical and Experimental Investigation of the Effect of Tunnel Walls on the Forces on an Oscillating Airfoil in Two-Dimensional Subsonic Compressible Flow. NACA Rep. 1262, 1956.

10. Reese, David E., Jr., and Wehrend, William R., Jr.: Effects of Sting-Support Interference on the Base Pressures of a Model Having a Blunt-Nosed Cylinder Body and a Conical Flare at Mach Numbers From 0.65 to 2.20. NASA TM X-161, 1959.

TABLE I.- MODEL GEOMETRY

Group	Model number	Nose eccentricity, l_n/r	Base area ratio, $\frac{A_{base}}{A_{cyl}}$	Flare angle, deg	Length of cylinder, L	Over-all length, l
1. Nose shape	111	0.80	2.13	16.5	2.12 d	3.29 d
	211	.50	2.13	16.5	2.12 d	3.14 d
	311	.29	2.13	16.5	2.12 d	3.04 d
	411	.20	2.13	16.5	2.12 d	2.99 d
2. Flare base area	321	.29	2.13	16.5	2.20 d	3.12 d
	322	.29	2.64	16.5	2.20 d	3.39 d
	323	.29	3.15	16.5	2.20 d	3.77 d
3. Flare angle	511	.50	2.13	16.5	2.12 d	3.14 d
	514	.50	2.13	11.7	2.12 d	3.47 d
4. Cyl. body length	511	.50	2.13	16.5	2.12 d	3.14 d
	531	.50	2.13	16.5	2.45 d	3.47 d
5. Flare relief	515	.50	2.62	12.7	2.12 d	3.74 d
	516	.50	2.20	12.7	2.12 d	3.74 d
6. Other models	641	--	2.13	16.5	2.11 d	3.17 d
	517	.50	2.13	--	2.12 d	3.14 d
	5-8	.50	2.13	4.1	--	3.47 d

TABLE II.- LOCATION OF CENTER OF MOMENTS

Group	Model	Distance from line of tangency to center of moments		Distance from nose to center of moments	
		Static	Dynamic	Static	Dynamic
1. Nose shape	111	1.00 d	1.00 d	0.423 l	0.423 l
	211	1.00 d	---	.396 l	---
	311	1.00 d	1.21 d	.377 l	.447 l
	411	1.00 d	1.21 d	.362 l	.439 l
2. Flare base area	321	1.07 d	1.07 d	.391 l	.391 l
	322	1.07 d	1.07 d	.359 l	.359 l
	323	1.07 d	1.07 d	.332 l	.332 l
3. Flare angle	511	1.00 d	1.00 & 1.21 d	.396 l	.396 & .465 l
	514	1.00 d	1.00 d	.358 l	.358 l
4. Cyl. body length	511	1.00 d	1.00 d	.396 l	.396 l
	531	1.00 d	1.00 d	.358 l	.358 l
5. Flare relief	515	1.00 d	1.00 d	.335 l	.335 l
	516	1.00 d	1.00 d	.335 l	.335 l
6. Other models	641	1.00 d	1.00 d	.402 l	.402 l
	517	1.00 d	---	.400 l	---
	5-8	1.00 d	1.00 d	.358 l	.358 l

[redacted]

TABLE III.- STATIC STABILITY DATA

(a) Model 111 - Center of moments at 0.423l

α	C_N	C_A	C_m
M = 0.65			
-03.0	-0.220	0.843	0.070
-00.0	-0.011	0.836	0.016
02.9	0.202	0.858	-0.064
06.0	0.399	0.884	-0.110
11.9	0.770	0.932	-0.198
18.0	1.174	0.972	-0.301
M = 0.90			
-02.8	-0.340	1.213	0.397
00.1	0.036	1.179	-0.054
03.1	0.383	1.254	-0.432
06.2	0.605	1.283	-0.540
12.2	1.001	1.348	-0.601
18.2	1.488	1.329	-0.738
M = 1.00			
00.2	0.023	1.718	0.013
-00.2	-0.027	1.727	0.012
-00.7	-0.056	1.747	0.015
-01.7	-0.121	1.738	0.020
-02.7	-0.189	1.703	0.029
-03.8	-0.261	1.768	0.032
00.8	0.063	1.767	-0.009
01.3	0.102	1.712	-0.015
02.2	0.166	1.737	-0.020
03.2	0.233	1.755	-0.033
04.2	0.295	1.757	-0.030
06.3	0.425	1.791	-0.019
09.2	0.628	1.796	-0.008
12.3	1.174	1.857	-0.812
15.2	1.402	1.823	-0.881
18.2	1.651	1.781	-0.946
07.2	0.484	1.761	-0.018
08.2	0.560	1.788	-0.012
09.3	0.948	1.861	-0.729
10.2	1.022	1.844	-0.766
09.3	0.964	1.874	-0.761
08.3	0.902	1.827	-0.750
07.2	0.832	1.835	-0.724
06.2	0.767	1.786	-0.718
05.2	0.359	1.761	-0.027
04.2	0.306	1.757	-0.033

α	C_N	C_A	C_m
M = 1.10			
00.2	0.019	1.908	-0.004
-00.2	-0.036	1.896	0.001
-00.7	-0.104	1.793	0.063
-01.8	-0.134	1.888	0.019
-02.8	-0.233	1.831	0.071
-03.6	-0.295	1.770	0.083
00.8	0.038	1.881	0.003
01.3	0.073	1.743	0.013
02.2	0.152	1.900	-0.035
03.2	0.192	1.839	-0.020
04.2	0.264	1.864	-0.038
06.2	0.393	1.748	-0.007
09.3	0.591	1.876	-0.026
12.3	1.081	1.750	-0.683
15.3	1.355	1.800	-0.943
18.2	1.600	1.772	-1.054
10.2	0.657	1.862	-0.014
11.3	1.004	1.772	-0.666
12.3	1.105	1.813	-0.811
11.3	1.041	1.870	-0.809
10.2	0.930	1.774	-0.676
09.2	0.883	1.798	-0.719
08.2	0.846	1.834	-0.750
07.3	0.747	1.762	-0.643
06.2	0.717	1.821	-0.713
05.2	0.320	1.771	-0.004
04.2	0.269	1.885	-0.042

α	C_N	C_A	C_m
M = 1.30			
00.1	-0.000	1.966	-0.000
-00.9	-0.072	1.963	0.010
-02.9	-0.209	1.960	0.024
01.1	0.079	1.964	-0.017
03.1	0.225	1.962	-0.036
06.1	0.422	1.963	-0.028
09.1	0.641	1.949	-0.034
12.1	0.896	1.935	-0.065
15.2	1.191	1.917	-0.124
18.2	1.531	1.911	-0.209
M = 2.20			
-02.3	-0.112	1.569	0.029
00.7	0.055	1.567	-0.012
03.6	0.226	1.569	-0.044
06.7	0.417	1.556	-0.104
12.7	0.882	1.557	-0.324
18.7	1.468	1.568	-0.717

[redacted]

TABLE III.- STATIC STABILITY DATA - Continued
(b) Model 211 - Center of moments at 0.396l

α	C_N	C_A	C_m
M = 0.65			
-00.1	-0.045	1.090	0.006
-00.6	-0.103	1.093	0.072
-01.0	-0.158	1.094	0.125
-02.0	-0.263	1.095	0.217
-03.1	-0.362	1.106	0.296
-04.0	-0.440	1.118	0.352
00.4	0.043	1.095	-0.062
00.9	0.098	1.104	-0.137
01.8	0.193	1.110	-0.224
02.8	0.282	1.123	-0.292
03.9	0.356	1.134	-0.334
05.9	0.485	1.156	-0.374
08.8	0.654	1.159	-0.391
11.9	0.830	1.158	-0.416
14.9	1.006	1.156	-0.438
17.9	1.210	1.148	-0.487
M = 0.80			
-00.1	-0.042	1.224	0.024
-00.5	-0.105	1.225	0.113
-01.0	-0.179	1.235	0.211
-02.0	-0.295	1.258	0.350
-03.0	-0.403	1.281	0.447
-04.1	-0.488	1.295	0.501
00.4	0.066	1.230	-0.094
01.0	0.150	1.237	-0.217
01.9	0.261	1.260	-0.335
02.9	0.351	1.276	-0.398
03.9	0.434	1.297	-0.467
05.9	0.593	1.320	-0.550
08.9	0.771	1.335	-0.601
11.8	0.944	1.334	-0.624
15.0	1.154	1.329	-0.660
17.9	1.374	1.310	-0.717
M = 0.90			
00.1	0.017	1.154	-0.076
-00.3	-0.083	1.162	0.114
-00.9	-0.192	1.191	0.308
-01.9	-0.343	1.285	0.523
-02.9	-0.452	1.363	0.623
-03.8	-0.535	1.426	0.670
00.6	0.119	1.185	-0.258
01.1	0.203	1.233	-0.393
02.2	0.352	1.330	-0.545
03.1	0.445	1.394	-0.620
04.1	0.519	1.418	-0.662
06.1	0.665	1.447	-0.732
09.1	0.878	1.480	-0.819
12.1	1.098	1.503	-0.890
15.1	1.321	1.483	-0.949
18.1	1.568	1.440	-1.034

α	C_N	C_A	C_m
M = 1.00			
00.2	0.020	1.823	-0.009
-00.3	-0.031	1.869	0.007
-00.7	-0.058	1.826	0.019
-01.7	-0.134	1.837	0.042
-02.7	-0.206	1.864	0.067
-03.7	-0.269	1.875	0.085
00.8	0.058	1.882	-0.023
01.3	0.099	1.882	-0.032
02.2	0.158	1.861	-0.051
03.2	0.228	1.914	-0.071
04.2	0.295	1.906	-0.093
06.3	0.798	1.930	-0.888
09.2	0.993	1.941	-0.950
12.2	1.217	1.989	-1.026
15.3	1.449	1.969	-1.091
18.3	1.673	1.903	-1.140
05.2	0.362	1.939	-0.105
06.2	0.441	1.961	-0.132
07.3	0.873	1.944	-0.923
08.3	0.939	1.966	-0.945
07.2	0.873	1.997	-0.916
06.2	0.787	1.796	-0.883
05.2	0.712	1.913	-0.843
04.2	0.627	1.903	-0.783
03.2	0.542	1.878	-0.715
02.2	0.164	1.892	-0.058
01.2	0.101	1.833	-0.036
M = 1.10			
00.3	0.010	2.017	-0.010
-00.2	-0.066	1.966	0.039
-00.7	-0.081	2.009	0.024
-02.7	-0.212	2.032	0.074
-03.7	-0.319	1.993	0.152
00.8	0.031	1.991	-0.014
01.3	0.057	1.899	-0.005
02.2	0.140	2.005	-0.064
03.2	0.190	1.981	-0.078
04.2	0.275	2.028	-0.114
06.3	0.728	1.841	-0.813
09.3	0.947	1.952	-0.944
12.3	1.147	1.976	-1.018
15.3	1.350	1.846	-1.075
18.2	1.583	1.904	-1.155
05.3	0.340	1.891	-0.097
06.3	0.410	1.999	-0.167
07.3	0.811	1.893	-0.901
08.3	0.880	1.905	-0.935
07.2	0.808	1.866	-0.888
06.3	0.737	1.861	-0.870
05.2	0.662	1.862	-0.825
04.2	0.582	1.881	-0.769
03.2	0.494	1.840	-0.689
02.2	0.134	1.998	-0.058
01.2	0.059	1.867	-0.005

α	C_N	C_A	C_m
M = 1.30			
00.0	0.018	2.099	-0.016
-00.9	-0.056	2.099	0.005
-02.8	-0.194	2.094	0.041
01.1	0.083	2.100	-0.027
03.1	0.222	2.096	-0.067
06.2	0.435	2.097	-0.105
09.2	0.647	2.092	-0.135
12.1	0.894	2.077	-0.189
15.2	1.194	2.053	-0.284
18.2	1.592	1.959	-0.902
15.1	1.187	2.051	-0.278
16.2	1.364	1.995	-0.794
17.1	1.474	1.977	-0.863
16.1	1.361	1.993	-0.798
15.1	1.273	2.001	-0.757
14.1	1.181	2.019	-0.716
13.1	1.080	2.033	-0.654
12.1	0.984	2.047	-0.560
11.1	0.808	2.084	-0.171
10.1	0.732	2.088	-0.150
M = 1.60			
-00.0	-0.035	1.966	0.034
-01.1	-0.103	1.966	0.049
-02.9	-0.216	1.958	0.064
01.0	0.045	1.970	0.017
02.9	0.168	1.953	-0.009
06.0	0.360	1.933	-0.041
09.0	0.575	1.917	-0.119
12.0	0.839	1.904	-0.246
15.0	1.144	1.907	-0.433
17.9	1.480	1.907	-0.659
M = 1.90			
00.1	0.007	1.830	0.014
-00.8	-0.066	1.826	0.025
-02.9	-0.188	1.816	0.058
01.1	0.070	1.833	-0.012
03.1	0.193	1.824	-0.051
06.0	0.379	1.809	-0.109
09.0	0.590	1.788	-0.207
12.0	0.843	1.777	-0.352
15.0	1.121	1.774	-0.542
18.1	1.442	1.768	-0.787
M = 2.20			
00.7	0.021	1.715	0.011
-00.3	-0.063	1.712	0.033
-02.2	-0.162	1.717	0.059
01.7	0.068	1.713	-0.002
03.7	0.191	1.712	-0.054
06.6	0.365	1.686	-0.125
09.7	0.560	1.667	-0.239
12.6	0.820	1.668	-0.404
15.7	1.094	1.668	-0.621
18.6	1.373	1.668	-0.842

CONFIDENTIAL

TABLE III.- STATIC STABILITY DATA - Continued
(c) Model 311 - Center of moments at 0.377l

α	C_N	C_A	C_m
M = 0.65			
-04.0	-0.497	1.356	0.555
-03.0	-0.417	1.331	0.495
-02.0	-0.315	1.289	0.391
-01.0	-0.183	1.259	0.218
-00.5	-0.103	1.250	0.104
-00.1	-0.027	1.242	-0.011
00.5	0.060	1.252	-0.132
00.9	0.133	1.263	-0.242
01.9	0.285	1.296	-0.395
02.9	0.385	1.321	-0.485
03.9	0.455	1.340	-0.537
05.9	0.583	1.362	-0.594
08.9	0.742	1.383	-0.617
12.0	0.908	1.382	-0.628
14.9	1.070	1.376	-0.643
17.9	1.272	1.375	-0.685
M = 0.80			
-04.0	-0.572	1.527	0.776
-03.0	-0.485	1.468	0.733
-02.0	-0.364	1.379	0.603
-01.1	-0.211	1.277	0.367
-00.5	-0.084	1.242	0.136
-00.0	-0.001	1.225	-0.038
00.4	0.120	1.246	-0.264
00.9	0.195	1.286	-0.399
01.9	0.360	1.394	-0.654
02.9	0.480	1.473	-0.757
03.9	0.572	1.533	-0.795
05.9	0.707	1.577	-0.825
09.0	0.883	1.604	-0.862
12.0	1.080	1.622	-0.902
14.9	1.286	1.616	-0.952
18.0	1.533	1.574	-1.045
M = 0.90			
-03.8	-0.575	1.557	0.884
-02.8	-0.474	1.433	0.806
-01.9	-0.338	1.308	0.613
-00.8	-0.136	1.176	0.281
-00.3	-0.032	1.152	0.079
00.0	0.061	1.152	-0.121
00.7	0.162	1.198	-0.349
01.1	0.242	1.248	-0.499
02.1	0.400	1.394	-0.751
03.1	0.525	1.509	-0.863
04.1	0.618	1.589	-0.911
06.1	0.757	1.673	-0.955
09.1	0.996	1.735	-1.067
12.2	1.224	1.753	-1.154
15.1	1.484	1.736	-1.295
18.1	1.726	1.694	-1.387

α	C_N	C_A	C_m
M = 1.00			
-03.7	-0.540	2.031	0.687
-02.7	-0.416	1.977	0.575
-01.7	-0.290	1.869	0.455
-00.7	-0.114	1.756	0.188
-00.1	-0.011	1.739	0.007
00.2	0.081	1.746	-0.161
00.8	0.208	1.809	-0.377
01.2	0.280	1.864	-0.455
02.3	0.411	1.995	-0.578
03.2	0.529	2.047	-0.682
04.3	0.637	2.100	-0.787
06.2	0.821	2.159	-0.953
09.3	1.057	2.217	-1.099
12.3	1.285	2.226	-1.205
15.3	1.514	2.190	-1.298
18.3	1.766	2.145	-1.394
M = 1.10			
-03.6	-0.307	2.208	0.195
-02.6	-0.226	2.182	0.137
-01.7	-0.136	2.189	0.065
-00.7	-0.071	2.176	0.024
-00.1	-0.034	2.156	0.006
00.3	-0.004	2.156	-0.005
00.8	0.050	2.158	-0.031
01.3	0.083	2.139	-0.050
02.3	0.171	2.171	-0.107
03.2	0.229	2.150	-0.141
04.2	0.306	2.152	-0.200
06.3	0.761	2.113	-0.906
09.3	0.980	2.122	-1.065
12.4	1.205	2.138	-1.193
15.2	1.435	2.106	-1.315
18.4	1.674	2.070	-1.414
00.1	-0.002	2.195	0.008
01.2	0.096	2.246	-0.060
02.3	0.156	2.145	-0.093
03.2	0.224	2.174	-0.137
04.3	0.305	2.250	-0.176
05.3	0.643	1.968	-0.779
06.2	0.714	1.998	-0.858
05.3	0.645	2.101	-0.812
04.2	0.551	2.062	-0.726
03.2	0.441	1.957	-0.641
02.2	0.352	1.867	-0.596
01.2	0.167	1.634	-0.299
00.2	-0.020	1.617	0.040

α	C_N	C_A	C_m
M = 1.30			
-02.8	-0.193	2.227	0.070
-00.8	-0.058	2.228	0.018
00.1	0.025	2.225	-0.016
01.1	0.099	2.225	-0.046
03.1	0.236	2.227	-0.099
06.1	0.436	2.230	-0.152
09.1	0.649	2.237	-0.196
12.2	0.905	2.235	-0.257
15.2	1.325	2.182	-0.997
18.2	1.636	2.148	-1.139
12.2	0.900	2.239	-0.254
13.2	1.171	2.200	-0.938
14.3	1.252	2.190	-0.971
13.1	1.163	2.202	-0.927
12.2	1.080	2.213	-0.878
11.1	0.986	2.225	-0.795
10.1	0.891	2.233	-0.698
09.1	0.805	2.234	-0.630
08.2	0.573	2.243	-0.174
07.1	0.503	2.244	-0.165
M = 1.60			
-02.9	-0.212	2.079	0.084
-01.0	-0.091	2.087	0.049
-00.0	-0.031	2.089	0.027
01.0	0.054	2.090	0.004
03.0	0.176	2.082	-0.036
06.0	0.356	2.070	-0.080
09.0	0.571	2.075	-0.173
12.1	0.841	2.073	-0.320
15.0	1.140	2.082	-0.513
18.0	1.504	2.095	-0.804
M = 1.90			
-02.8	-0.168	1.961	0.067
-00.9	-0.059	1.966	0.028
00.1	0.033	1.971	-0.013
01.2	0.103	1.968	-0.046
03.1	0.207	1.969	-0.080
06.0	0.393	1.967	-0.162
09.1	0.602	1.962	-0.266
12.2	0.855	1.965	-0.438
15.1	1.130	1.961	-0.637
18.1	1.452	1.958	-0.905
M = 2.20			
-02.3	-0.146	1.865	0.066
-00.2	-0.043	1.871	0.023
00.6	0.052	1.863	-0.022
01.7	0.111	1.871	-0.057
03.6	0.214	1.866	-0.100
06.7	0.389	1.867	-0.184
09.7	0.574	1.850	-0.304
12.7	0.809	1.853	-0.478
15.8	1.088	1.862	-0.700
18.7	1.374	1.863	-0.942

CONFIDENTIAL

TABLE III.- STATIC STABILITY DATA - Continued
(d) Model 411 - Center of moments at 0.362l

α	C_N	C_A	C_m
M = 0.65			
-03.0	-0.418	1.375	0.602
-00.0	-0.007	1.246	0.020
02.9	0.418	1.375	-0.594
05.9	0.629	1.429	-0.698
11.9	0.920	1.451	-0.710
17.9	1.299	1.423	-0.760
M = 0.90			
-02.8	-0.450	1.340	0.857
00.1	0.045	1.060	-0.086
03.1	0.519	1.411	-0.906
06.2	0.768	1.617	-1.016
12.1	1.202	1.696	-1.181
18.2	1.687	1.628	-1.389
00.1	0.036	1.084	-0.069
01.1	0.196	1.156	-0.426
02.1	0.353	1.274	-0.703
03.1	0.488	1.419	-0.880
04.2	0.596	1.539	-0.927
05.2	0.678	1.609	-0.964
06.1	0.749	1.650	-0.991
05.2	0.679	1.592	-0.967
04.2	0.599	1.516	-0.937
03.2	0.506	1.414	-0.882
02.1	0.354	1.272	-0.705
01.1	0.191	1.150	-0.423
00.1	0.006	1.083	-0.051
M = 1.00			
00.2	0.049	2.082	-0.033
-00.2	0.006	1.949	-0.011
-01.8	-0.135	1.931	0.072
-02.7	-0.209	1.898	0.113
00.7	0.076	1.901	-0.045
01.3	0.118	1.970	-0.071
02.2	0.188	1.988	-0.109
03.2	0.262	2.009	-0.142
04.3	0.329	2.013	-0.172
06.3	0.832	1.970	-0.973
09.2	1.092	2.056	-1.161
12.2	1.332	2.108	-1.301
15.3	1.563	2.059	-1.396
18.2	1.795	2.029	-1.476
00.2	0.070	1.568	-0.126
-00.3	-0.057	1.545	0.116
-00.7	-0.163	1.508	0.316
-01.8	-0.346	1.654	0.592
-02.7	-0.464	1.764	0.706
-03.8	-0.588	1.963	0.784
00.7	0.180	1.653	-0.355
01.2	0.267	1.544	-0.496
02.3	0.442	1.815	-0.702
03.3	0.532	1.781	-0.753
04.3	0.642	1.968	-0.819
06.3	0.840	2.020	-0.988

α	C_N	C_A	C_m
M = 1.10			
00.2	0.037	2.306	-0.037
-00.2	-0.057	2.177	0.048
-00.7	-0.052	2.224	0.018
-01.7	-0.123	2.235	0.056
-02.7	-0.260	2.172	0.191
00.8	0.068	2.234	-0.054
01.2	0.071	2.087	-0.034
02.2	0.177	2.237	-0.114
03.2	0.224	2.099	-0.128
04.2	0.311	2.248	-0.157
06.3	0.790	2.142	-0.918
09.4	1.022	2.192	-1.071
12.3	1.260	2.144	-1.284
15.3	1.480	2.161	-1.344
18.3	1.704	2.094	-1.467
00.2	-0.018	1.565	0.016
-00.2	-0.076	1.738	0.132
-00.7	-0.208	1.581	0.365
-01.7	-0.341	1.873	0.560
-02.7	-0.464	1.886	0.614
-03.8	-0.576	1.971	0.727
00.8	0.163	1.751	-0.297
01.3	0.214	1.705	-0.417
02.3	0.391	1.816	-0.663
03.2	0.448	1.846	-0.605
04.2	0.590	2.068	-0.751
06.3	0.772	2.067	-0.934
09.3	1.024	2.130	-1.128
12.3	1.257	2.177	-1.248

α	C_N	C_A	C_m
M = 1.30			
00.0	0.008	2.379	-0.022
-00.9	-0.062	2.365	0.012
-02.9	-0.203	2.366	0.071
01.1	0.078	2.369	-0.036
03.1	0.232	2.365	-0.101
06.1	0.421	2.373	-0.136
09.2	0.647	2.367	-0.183
12.1	1.107	2.228	-0.949
15.2	1.336	2.213	-1.030
18.2	1.660	2.184	-1.194
11.1	0.815	2.364	-0.231
12.2	1.117	2.234	-0.969
13.1	1.187	2.232	-0.991
12.1	1.115	2.239	-0.969
11.1	1.039	2.244	-0.933
10.1	0.963	2.247	-0.884
09.1	0.880	2.248	-0.815
08.0	0.777	2.253	-0.714
07.1	0.708	2.248	-0.664
06.1	0.437	2.383	-0.145
05.0	0.364	2.377	-0.135
M = 2.20			
-02.2	-0.121	1.945	0.075
00.7	0.044	1.950	-0.007
03.7	0.205	1.942	-0.083
06.7	0.381	1.942	-0.179
12.7	0.806	1.936	-0.486
18.7	1.366	1.951	-0.962

[redacted]

TABLE III.- STATIC STABILITY DATA - Continued
(e) Model 321 - Center of moments at 0.391l

α	C_N	C_A	C_m
M = 0.65			
-00.0	-0.003	1.216	0.014
-00.6	-0.098	1.227	0.146
-01.1	-0.177	1.244	0.243
-02.1	-0.296	1.274	0.383
-03.0	-0.396	1.298	0.473
-04.0	-0.471	1.315	0.517
00.4	0.068	1.225	-0.107
00.9	0.148	1.239	-0.206
01.9	0.280	1.269	-0.359
02.9	0.375	1.289	-0.433
03.9	0.453	1.310	-0.483
05.9	0.583	1.327	-0.533
08.9	0.743	1.343	-0.563
11.9	0.904	1.343	-0.577
14.9	1.078	1.335	-0.584
17.7	1.264	1.324	-0.612
M = 0.80			
00.0	0.030	1.212	-0.048
-00.5	-0.083	1.222	0.161
-01.0	-0.183	1.249	0.329
-02.1	-0.333	1.343	0.543
-03.1	-0.444	1.390	0.640
-04.1	-0.529	1.434	0.691
00.4	0.100	1.227	-0.185
00.9	0.192	1.256	-0.340
01.9	0.343	1.337	-0.543
02.9	0.450	1.398	-0.632
03.9	0.529	1.430	-0.669
06.0	0.683	1.490	-0.731
09.0	0.857	1.496	-0.766
11.9	1.035	1.513	-0.790
15.0	1.233	1.493	-0.813
17.9	1.466	1.470	-0.891
M = 0.90			
00.1	0.027	1.082	-0.089
-00.4	-0.097	1.088	0.169
-00.8	-0.176	1.120	0.342
-01.9	-0.342	1.243	0.635
-02.9	-0.480	1.382	0.784
-03.9	-0.556	1.468	0.796
00.5	0.122	1.115	-0.269
01.1	0.209	1.171	-0.427
02.1	0.359	1.292	-0.651
03.1	0.486	1.411	-0.768
04.1	0.584	1.491	-0.825
06.1	0.748	1.571	-0.904
09.1	0.950	1.615	-0.968
12.1	1.152	1.624	-1.033
15.1	1.400	1.612	-1.116
18.1	1.639	1.557	-1.207
M = 1.00			
00.2	0.040	1.930	-0.027
-00.3	0.002	1.988	-0.021
-00.7	-0.047	1.993	0.009
-01.7	-0.119	1.964	0.038
00.8	0.085	2.016	-0.053
01.2	0.114	1.942	-0.060
02.2	0.186	2.015	-0.094
03.3	0.263	1.977	-0.127
04.3	0.352	2.061	-0.188
06.3	0.805	2.027	-0.881
09.3	1.026	2.064	-1.005
12.2	1.249	2.095	-1.103
15.3	1.490	2.075	-1.190
18.2	1.727	2.011	-1.269
00.2	0.072	1.629	-0.144
-00.2	-0.041	1.626	0.052
-00.7	-0.141	1.612	0.232
-01.7	-0.298	1.739	0.437
-02.8	-0.425	1.842	0.536
-03.7	-0.536	1.945	0.653
00.8	0.171	1.636	-0.316
01.2	0.258	1.722	-0.424
02.2	0.382	1.801	-0.523
03.2	0.507	1.916	-0.632
04.2	0.612	1.907	-0.733
05.2	0.713	1.969	-0.824
M = 1.10			
00.3	-0.010	2.046	0.014
-00.7	-0.105	2.015	0.072
-01.7	-0.120	2.145	0.026
00.8	0.056	2.125	-0.045
01.2	0.094	2.128	-0.062
02.2	0.160	2.125	-0.094
03.2	0.231	2.128	-0.133
04.3	0.318	2.145	-0.200
06.3	0.743	2.007	-0.860
09.3	0.966	2.076	-0.999
12.3	1.170	2.062	-1.092
15.3	1.418	2.025	-1.233
18.3	1.651	1.980	-1.322
-00.2	-0.113	1.618	0.192
-00.7	-0.191	1.729	0.324
-01.7	-0.325	1.837	0.472
-02.7	-0.446	1.913	0.560
-03.7	-0.532	1.987	0.652
00.8	0.097	1.565	-0.195
02.3	0.322	1.835	-0.454
03.2	0.438	1.936	-0.580
04.3	0.562	1.967	-0.707
05.2	0.658	2.017	-0.789
M = 1.30			
00.2	0.033	2.295	-0.025
-00.4	-0.013	2.297	-0.014
-00.9	-0.052	2.294	-0.001
-01.9	-0.120	2.298	0.018
-02.8	-0.188	2.298	0.041
-03.8	-0.260	2.302	0.059
00.6	0.064	2.294	-0.035
01.1	0.103	2.292	-0.052
03.1	0.234	2.299	-0.083
06.1	0.434	2.297	-0.118
09.2	0.651	2.286	-0.142
12.1	0.901	2.279	-0.184
15.1	1.299	2.199	-0.846
18.3	1.660	2.159	-1.008
12.1	0.901	2.279	-0.184
13.1	0.995	2.275	-0.206
14.2	1.217	2.213	-0.814
15.2	1.302	2.200	-0.846
14.1	1.213	2.213	-0.811
13.0	1.134	2.221	-0.794
12.1	1.061	2.230	-0.764
11.1	0.968	2.244	-0.687
10.2	0.853	2.264	-0.526
09.1	0.651	2.296	-0.138
08.1	0.574	2.299	-0.133
M = 1.60			
00.0	-0.007	2.096	0.021
-01.0	-0.079	2.094	0.041
-03.0	-0.208	2.087	0.064
01.0	0.045	2.097	0.012
02.9	0.170	2.083	-0.011
06.0	0.365	2.060	-0.059
09.0	0.584	2.041	-0.135
12.0	0.851	2.037	-0.266
15.0	1.170	2.037	-0.457
17.9	1.519	2.045	-0.724
M = 1.90			
00.1	0.043	1.964	-0.024
-00.9	-0.030	1.959	0.007
-02.9	-0.155	1.959	0.047
01.1	0.093	1.967	-0.040
03.1	0.213	1.959	-0.075
06.1	0.389	1.941	-0.131
09.1	0.611	1.924	-0.242
12.1	0.855	1.917	-0.387
15.1	1.148	1.918	-0.585
18.0	1.469	1.910	-0.840
M = 2.20			
00.7	0.056	1.872	-0.020
00.1	0.028	1.875	-0.010
-00.3	-0.000	1.873	-0.000
-01.3	-0.071	1.874	0.032
-02.3	-0.129	1.874	0.059
01.6	0.103	1.872	-0.041
03.6	0.222	1.858	-0.088
06.7	0.404	1.837	-0.167
09.7	0.596	1.823	-0.277
12.7	0.831	1.823	-0.444
15.7	1.114	1.830	-0.664
18.6	1.405	1.825	-0.897

[redacted]

TABLE III.- STATIC STABILITY DATA - Continued
(f) Model 322 - Center of moments at 0.359l

α	C_N	C_A	C_m
M = 0.65			
-00.1	-0.004	1.448	-0.001
-00.5	-0.106	1.454	0.116
-01.0	-0.207	1.466	0.268
-02.1	-0.341	1.502	0.442
-03.1	-0.454	1.532	0.563
-04.0	-0.541	1.551	0.631
00.4	0.038	1.456	-0.106
00.9	0.139	1.470	-0.258
01.8	0.278	1.500	-0.411
02.9	0.407	1.534	-0.544
03.9	0.498	1.557	-0.626
05.9	0.641	1.575	-0.708
08.9	0.848	1.584	-0.808
11.9	1.050	1.572	-0.892
14.9	1.253	1.554	-0.963
17.8	1.482	1.537	-1.065
M = 0.80			
-00.0	0.016	1.483	-0.024
-00.5	-0.102	1.499	0.196
-01.1	-0.204	1.529	0.392
-02.0	-0.382	1.619	0.655
-03.0	-0.502	1.679	0.774
-04.1	-0.595	1.711	0.820
00.4	0.112	1.505	-0.259
01.0	0.212	1.542	-0.440
01.9	0.365	1.622	-0.681
02.9	0.492	1.685	-0.790
03.9	0.584	1.723	-0.847
05.9	0.744	1.749	-0.921
08.9	0.959	1.766	-1.023
11.9	1.178	1.760	-1.127
14.9	1.407	1.730	-1.220
17.9	1.673	1.692	-1.350
M = 0.90			
00.1	0.060	1.388	-0.153
-00.4	-0.086	1.390	0.181
-00.9	-0.203	1.441	0.432
-01.9	-0.399	1.566	0.810
-02.8	-0.537	1.705	1.008
-03.9	-0.639	1.796	1.058
00.6	0.166	1.433	-0.383
01.1	0.268	1.494	-0.594
02.1	0.446	1.627	-0.904
03.0	0.565	1.748	-1.048
04.1	0.664	1.833	-1.093
06.1	0.828	1.863	-1.130
09.1	1.067	1.930	-1.271
12.1	1.317	1.925	-1.406
15.1	1.590	1.867	-1.556
18.1	1.853	1.798	-1.711
M = 1.00			
00.2	0.051	2.351	-0.042
-00.2	0.013	2.365	-0.015
-00.7	-0.054	2.351	0.033
-01.8	-0.149	2.358	0.106
00.7	0.097	2.430	-0.080
01.2	0.135	2.452	-0.108
02.2	0.218	2.457	-0.175
03.2	0.585	2.337	-0.887
04.2	0.699	2.343	-1.002
06.2	0.916	2.411	-1.208
09.3	1.182	2.453	-1.412
12.2	1.438	2.441	-1.586
15.3	1.702	2.425	-1.735
18.3	1.974	2.339	-1.878
00.2	0.093	1.853	-0.212
-00.3	-0.060	1.896	0.099
-00.6	-0.130	2.001	0.272
-01.7	-0.364	1.976	0.694
-02.8	-0.490	2.297	0.771
-03.7	-0.610	2.270	0.890
00.7	0.210	1.985	-0.433
01.2	0.312	2.023	-0.622
02.2	0.456	2.239	-0.804
03.2	0.587	2.309	-0.890
04.2	0.701	2.335	-0.992
M = 1.10			
00.2	0.020	2.641	-0.028
-00.3	-0.028	2.651	-0.005
-00.7	-0.061	2.658	0.017
-01.8	-0.147	2.664	0.089
00.8	0.066	2.645	-0.068
01.2	0.113	2.654	-0.111
02.2	0.209	2.668	-0.182
03.2	0.284	2.611	-0.258
04.3	0.643	2.531	-0.952
06.3	0.853	2.590	-1.164
09.3	1.102	2.626	-1.359
12.3	1.371	2.551	-1.600
15.3	1.631	2.518	-1.749
18.3	1.897	2.401	-1.945
00.2	0.017	2.063	-0.048
-00.2	-0.106	2.070	0.233
-00.8	-0.211	2.136	0.435
-01.7	-0.422	2.138	0.803
-02.7	-0.469	2.474	0.725
-03.8	-0.601	2.509	0.871
00.8	0.178	2.129	-0.376
01.3	0.252	2.032	-0.539
02.2	0.427	2.294	-0.792
03.2	0.518	2.357	-0.859
04.2	0.622	2.435	-0.927
05.2	0.741	2.548	-1.061
M = 1.30			
00.1	0.030	2.704	-0.030
-00.9	-0.076	2.698	0.033
-02.9	-0.227	2.706	0.116
01.1	0.104	2.704	-0.071
03.1	0.258	2.708	-0.157
06.2	0.493	2.715	-0.261
09.1	0.733	2.706	-0.343
12.2	1.014	2.678	-0.454
15.2	1.490	2.576	-1.340
18.1	1.853	2.527	-1.541
12.1	1.012	2.674	-0.451
13.1	1.119	2.661	-0.498
14.2	1.404	2.589	-1.297
15.2	1.499	2.572	-1.346
14.1	1.406	2.584	-1.304
13.1	1.322	2.602	-1.260
12.1	1.232	2.619	-1.206
11.1	1.149	2.632	-1.143
10.1	1.032	2.645	-1.024
09.1	0.915	2.663	-0.854
08.1	0.655	2.705	-0.318
07.2	0.582	2.714	-0.300
M = 1.60			
-00.0	0.003	2.373	0.010
-01.0	-0.082	2.374	0.045
-03.0	-0.215	2.372	0.105
01.0	0.068	2.373	-0.025
03.1	0.226	2.368	-0.103
05.9	0.442	2.363	-0.222
09.0	0.689	2.349	-0.362
12.0	0.983	2.346	-0.563
15.0	1.332	2.347	-0.824
18.0	1.750	2.357	-1.233
M = 1.90			
00.1	0.027	2.201	-0.008
-00.8	-0.056	2.200	0.034
-02.9	-0.206	2.189	0.132
01.1	0.100	2.192	-0.045
03.1	0.234	2.190	-0.134
06.1	0.452	2.188	-0.265
09.1	0.688	2.175	-0.437
12.1	0.969	2.170	-0.663
15.1	1.323	2.174	-0.993
18.1	1.700	2.174	-1.378
M = 2.20			
00.7	0.036	2.069	-0.009
-00.3	-0.027	2.072	0.033
-02.3	-0.168	2.064	0.112
01.7	0.098	2.069	-0.065
03.7	0.228	2.062	-0.147
06.7	0.460	2.052	-0.324
09.7	0.690	2.037	-0.519
12.7	0.981	2.041	-0.793
15.7	1.300	2.053	-1.115
18.6	1.648	2.063	-1.478

[redacted]

TABLE III.- STATIC STABILITY DATA - Continued
(g) Model 323 - Center of moments at 0.332l

α	C_N	C_A	C_m
M = 0.65			
-00.0	-0.045	1.663	0.027
-00.6	-0.162	1.668	0.223
-01.1	-0.244	1.688	0.354
-02.1	-0.383	1.725	0.552
-03.1	-0.496	1.740	0.679
-04.0	-0.593	1.744	0.753
00.4	0.053	1.677	-0.125
00.9	0.139	1.694	-0.280
01.9	0.303	1.724	-0.482
02.9	0.407	1.745	-0.584
03.9	0.515	1.758	-0.693
05.9	0.699	1.777	-0.857
08.9	0.935	1.778	-1.038
11.9	1.166	1.768	-1.195
15.0	1.416	1.733	-1.357
17.9	1.680	1.712	-1.530
M = 0.80			
-00.0	-0.025	1.721	0.011
-00.5	-0.143	1.729	0.257
-01.0	-0.250	1.770	0.494
-02.0	-0.426	1.870	0.799
-02.1	-0.542	1.923	0.885
-03.0	-0.637	1.945	0.953
00.4	0.120	1.751	-0.278
01.0	0.247	1.797	-0.533
01.9	0.392	1.878	-0.765
02.9	0.517	1.933	-0.891
03.8	0.618	1.957	-0.958
05.9	0.804	1.984	-1.101
08.9	1.058	1.986	-1.302
11.9	1.303	1.973	-1.469
14.9	1.580	1.932	-1.651
17.9	1.908	1.895	-1.895
M = 0.90			
00.1	0.048	1.716	-0.150
-00.3	-0.072	1.716	0.155
-00.8	-0.231	1.705	0.510
-01.8	-0.472	1.851	1.017
-02.8	-0.612	1.992	1.243
-03.9	-0.710	2.083	1.298
00.6	0.190	1.708	-0.456
01.1	0.326	1.791	-0.753
02.1	0.509	1.934	-1.107
03.1	0.650	2.043	-1.295
04.1	0.733	2.130	-1.324
06.2	0.907	2.178	-1.404
09.1	1.176	2.210	-1.584
12.1	1.450	2.184	-1.771
15.2	1.737	2.113	-1.970
18.0	2.057	2.038	-2.229
M = 1.00			
00.2	0.046	2.913	-0.042
-00.2	-0.015	2.889	0.014
-00.8	-0.070	2.861	0.067
-01.7	-0.172	2.893	0.179
00.7	0.089	2.860	-0.086
01.2	0.147	2.906	-0.155
02.3	0.541	2.510	-1.074
03.2	0.643	2.742	-1.134
04.3	0.778	2.759	-1.299
06.3	1.019	2.941	-1.527
09.3	1.304	2.989	-1.791
12.2	1.597	2.964	-2.026
15.3	1.890	2.873	-2.256
18.3	2.170	2.794	-2.416
00.2	0.098	2.291	-0.244
-00.2	-0.025	2.157	0.059
-00.8	-0.208	2.220	0.454
-01.7	-0.413	2.392	0.858
-02.7	-0.577	2.613	1.093
-03.8	-0.697	2.754	1.163
00.7	0.246	2.334	-0.563
01.2	0.372	2.384	-0.806
02.2	0.526	2.615	-1.041
03.2	0.653	2.710	-1.147
M = 1.10			
00.3	0.041	2.924	-0.052
-00.2	-0.029	2.938	0.006
-00.7	-0.074	2.932	0.053
-01.7	-0.160	2.927	0.148
00.7	0.067	2.934	-0.086
01.3	0.124	2.936	-0.150
02.2	0.235	2.965	-0.299
03.2	0.601	2.843	-1.156
04.2	0.703	2.925	-1.231
06.3	0.939	3.010	-1.454
09.2	1.219	3.055	-1.700
12.3	1.485	3.016	-1.945
15.3	1.777	2.930	-2.124
18.3	2.044	2.856	-2.312
00.3	0.031	2.542	-0.093
-00.2	-0.107	2.520	0.247
-00.8	-0.237	2.625	0.522
-01.7	-0.486	2.638	1.023
-02.7	-0.550	2.858	1.023
-03.7	-0.706	2.890	1.207
00.8	0.186	2.579	-0.435
01.2	0.308	2.585	-0.700
02.2	0.501	2.732	-1.078
03.2	0.607	2.855	-1.185
04.3	0.732	2.943	-1.265
05.3	0.835	2.999	-1.297
M = 1.30			
00.0	0.022	3.068	-0.015
-00.9	-0.077	3.066	0.059
-02.9	-0.258	3.072	0.203
01.1	0.109	3.074	-0.088
03.0	0.281	3.070	-0.230
06.1	0.562	3.079	-0.434
09.1	0.835	3.071	-0.592
12.2	1.151	3.041	-0.785
15.2	1.684	2.944	-1.806
18.2	2.079	2.913	-2.111
13.1	1.264	3.030	-0.853
14.1	1.581	2.961	-1.740
15.2	1.686	2.944	-1.810
14.1	1.585	2.955	-1.736
13.1	1.487	2.973	-1.669
12.1	1.374	2.988	-1.566
11.1	1.269	3.008	-1.457
10.1	1.164	3.026	-1.334
09.1	1.028	3.047	-1.136
08.1	0.740	3.078	-0.540
07.1	0.650	3.085	-0.487
M = 1.60			
-00.0	-0.029	2.661	0.022
-01.0	-0.105	2.752	0.081
-02.9	-0.260	2.739	0.198
01.0	0.065	2.747	-0.034
02.9	0.240	2.741	-0.175
06.0	0.496	2.640	-0.370
08.9	0.769	2.652	-0.589
12.0	1.117	2.638	-0.899
15.0	1.517	2.644	-1.286
18.0	1.978	2.653	-1.818
M = 1.90			
00.1	-0.007	2.428	0.005
-00.9	-0.085	2.425	0.078
-02.9	-0.248	2.412	0.223
01.1	0.089	2.427	-0.059
03.1	0.250	2.425	-0.199
06.1	0.506	2.426	-0.421
09.1	0.782	2.418	-0.679
12.2	1.124	2.411	-1.036
15.1	1.507	2.422	-1.467
18.1	1.953	2.436	-2.008
M = 2.20			
00.7	0.043	2.256	-0.029
00.1	0.008	2.256	0.001
-00.4	-0.058	2.251	0.049
-02.3	-0.210	2.254	0.193
01.7	0.110	2.257	-0.092
03.7	0.273	2.257	-0.256
06.7	0.522	2.250	-0.507
09.7	0.803	2.237	-0.803
12.7	1.120	2.251	-1.171
15.7	1.503	2.266	-1.640
18.7	1.928	2.274	-2.168

[redacted]

TABLE III.- STATIC STABILITY DATA - Continued
(h) Model 511 - Center of moments at 0.396l

α	C_N	C_A	C_m
M = 0.65			
-00.1	0.034	1.101	0.001
-00.6	-0.095	1.106	0.071
-01.0	-0.160	1.107	0.119
-02.0	-0.248	1.122	0.179
-02.9	-0.344	1.140	0.244
-04.0	-0.420	1.154	0.291
00.4	0.082	1.095	-0.035
00.9	0.140	1.100	-0.080
01.9	0.243	1.099	-0.147
02.9	0.344	1.121	-0.258
03.8	0.421	1.140	-0.330
05.8	0.550	1.157	-0.393
08.8	0.734	1.174	-0.441
11.7	0.906	1.187	-0.471
14.7	1.090	1.186	-0.518
17.6	1.270	1.174	-0.546
M = 0.80			
-00.0	0.000	1.240	0.075
-00.5	-0.069	1.247	0.146
-01.0	-0.164	1.253	0.184
-02.0	-0.264	1.263	0.269
-02.9	-0.360	1.285	0.349
-03.9	-0.439	1.303	0.407
00.4	0.079	1.246	-0.035
00.9	0.163	1.250	-0.137
01.9	0.287	1.264	-0.281
02.9	0.373	1.277	-0.355
03.9	0.468	1.294	-0.427
05.8	0.615	1.321	-0.528
08.7	0.801	1.348	-0.612
11.6	0.988	1.367	-0.670
14.7	1.193	1.359	-0.710
17.7	1.395	1.350	-0.756
M = 0.90			
00.1	0.045	1.225	-0.009
-00.3	-0.047	1.253	0.133
-00.8	-0.125	1.290	0.248
-01.8	-0.235	1.353	0.377
-02.8	-0.375	1.379	0.463
-03.7	-0.477	1.418	0.549
00.6	0.096	1.234	-0.177
01.2	0.176	1.276	-0.301
02.2	0.324	1.354	-0.428
03.0	0.419	1.392	-0.499
04.1	0.525	1.427	-0.587
06.0	0.695	1.479	-0.724
09.1	0.909	1.518	-0.848
11.9	1.110	1.551	-0.917
14.9	1.306	1.515	-0.941
17.9	1.568	1.492	-1.018
M = 1.00			
00.3	0.084	1.900	-0.056
-00.2	0.041	1.848	-0.041
-00.7	-0.019	1.870	-0.042
-01.6	-0.114	1.844	0.005
-02.6	-0.187	1.854	0.041
-03.6	-0.263	1.873	0.067
00.7	0.102	1.868	-0.053
01.3	0.153	1.882	-0.081
02.2	0.218	1.861	-0.099
03.2	0.290	1.856	-0.123
04.2	0.367	1.909	-0.152
06.2	0.514	1.910	-0.228
07.2	0.884	1.980	-0.871
09.1	1.009	2.020	-0.918
12.1	1.227	2.016	-1.012
15.1	1.462	1.980	-1.098
18.0	1.704	1.973	-1.176
05.2	0.430	1.881	-0.169
06.1	0.813	1.964	-0.843
07.1	0.885	1.924	-0.871
06.1	0.814	1.936	-0.838
05.2	0.736	1.954	-0.798
04.2	0.660	1.934	-0.738
03.2	0.286	1.937	-0.124
M = 1.10			
00.3	0.000	1.934	0.012
-00.1	-0.014	2.029	-0.030
-00.6	-0.082	1.943	0.039
-01.6	-0.115	2.028	0.017
-02.6	-0.195	2.020	0.061
-03.6	-0.288	2.006	0.125
00.7	0.047	1.991	-0.035
01.3	0.085	1.992	-0.050
02.3	0.157	1.989	-0.081
03.3	0.226	1.980	-0.110
04.2	0.305	2.016	-0.151
06.2	0.739	1.953	-0.837
09.2	0.911	1.922	-0.875
12.1	1.123	1.960	-1.005
15.1	1.347	1.922	-1.090
18.1	1.608	1.922	-1.237
05.1	0.367	1.984	-0.177
06.2	0.726	1.920	-0.812
07.1	0.769	1.877	-0.783
06.2	0.742	1.999	-0.811
05.1	0.643	1.878	-0.736
04.2	0.573	1.928	-0.708
03.2	0.219	1.958	-0.101
02.3	0.151	1.966	-0.072
M = 1.20			
00.2	0.038	2.101	-0.017
-00.7	-0.044	2.100	0.007
-02.7	-0.190	2.103	0.060
01.2	0.095	2.101	-0.030
03.2	0.244	2.105	-0.085
06.2	0.442	2.121	-0.119
12.0	0.889	2.117	-0.157
15.0	1.321	2.068	-0.919
14.0	1.061	2.104	-0.177
14.9	1.312	2.065	-0.913
16.0	1.392	2.051	-0.934
14.9	1.314	2.067	-0.908
13.9	1.241	2.080	-0.883
13.0	1.166	2.092	-0.866
11.9	1.075	2.104	-0.790
11.0	0.979	2.113	-0.711
10.0	0.900	2.113	-0.655
09.0	0.827	2.112	-0.619
08.1	0.755	2.109	-0.565
07.1	0.510	2.125	-0.127
06.0	0.444	2.122	-0.126
M = 1.30			
00.1	0.022	2.090	-0.025
-00.8	-0.048	2.090	-0.005
-02.8	-0.183	2.083	0.033
01.2	0.094	2.089	-0.037
03.1	0.230	2.087	-0.075
06.0	0.435	2.096	-0.110
12.0	0.892	2.090	-0.187
15.0	1.186	2.079	-0.264
17.9	1.580	2.023	-0.876
14.8	1.168	2.082	-0.253
15.9	1.352	2.042	-0.774
16.8	1.464	2.032	-0.838
15.8	1.337	2.045	-0.776
14.8	1.246	2.056	-0.727
13.8	1.147	2.073	-0.690
12.8	1.063	2.080	-0.625
11.8	0.882	2.097	-0.183
M = 1.60			
-00.0	-0.008	1.931	-0.008
-00.9	-0.056	1.932	-0.011
-02.9	-0.178	1.924	0.013
01.0	0.053	1.931	-0.013
02.9	0.188	1.928	-0.050
05.9	0.376	1.922	-0.086
11.8	0.842	1.922	-0.268
14.8	1.140	1.932	-0.429
17.8	1.483	1.944	-0.664
M = 1.90			
00.1	0.036	1.819	-0.015
-00.8	-0.027	1.818	-0.005
-02.8	-0.158	1.810	0.037
01.1	0.073	1.817	-0.018
03.1	0.208	1.819	-0.065
06.0	0.396	1.812	-0.133
11.9	0.842	1.809	-0.357
14.9	1.123	1.812	-0.547
17.9	1.449	1.818	-0.793
M = 2.20			
00.7	0.055	1.716	-0.021
-00.3	0.008	1.713	-0.004
-02.1	-0.122	1.715	0.029
01.7	0.114	1.710	-0.040
03.7	0.229	1.708	-0.087
06.6	0.402	1.706	-0.169
12.5	0.831	1.696	-0.425
15.5	1.101	1.712	-0.626
18.4	1.386	1.706	-0.850

[redacted]

TABLE III.- STATIC STABILITY DATA - Continued
(i) Model 514 - Center of moments at 0.358l

α	C_N	C_A	C_m
M = 0.65			
-03.0	-0.335	1.031	0.302
-01.0	-0.153	1.023	0.146
-00.0	-0.029	1.012	0.039
01.0	0.070	1.007	-0.070
03.0	0.246	1.024	-0.220
05.9	0.458	1.053	-0.336
11.9	0.834	1.086	-0.454
18.0	1.273	1.120	-0.641
M = 0.90			
-02.9	-0.398	1.298	0.569
-00.8	-0.164	1.171	0.274
00.1	0.017	1.160	-0.031
01.2	0.176	1.221	-0.301
03.2	0.377	1.299	-0.514
06.1	0.613	1.358	-0.685
12.2	1.054	1.397	-0.906
18.2	1.596	1.379	-1.196
M = 1.00			
00.3	0.043	1.633	-0.021
-00.2	-0.005	1.789	-0.018
-00.7	-0.054	1.797	0.011
-01.7	-0.127	1.652	0.039
-02.8	-0.202	1.671	0.059
-03.8	-0.264	1.679	0.076
00.7	0.074	1.680	-0.032
01.3	0.116	1.747	-0.054
02.2	0.175	1.712	-0.068
03.2	0.241	1.705	-0.081
04.2	0.310	1.750	-0.097
06.2	0.454	1.667	-0.133
07.3	0.794	1.871	-0.760
09.2	0.939	1.880	-0.838
12.2	1.180	1.866	-0.972
15.2	1.440	1.840	-1.099
18.4	1.733	1.822	-1.242
05.2	0.387	1.789	-0.120
06.3	0.459	1.712	-0.133
07.3	0.541	1.723	-0.150
08.3	0.875	1.842	-0.809
09.3	0.949	1.962	-0.844
08.3	0.872	1.871	-0.807
07.3	0.797	1.870	-0.763
06.2	0.720	1.824	-0.713
05.2	0.633	1.785	-0.658
04.2	0.550	1.780	-0.597
03.2	0.247	1.697	-0.088
02.2	0.180	1.743	-0.067

α	C_N	C_A	C_m
M = 1.10			
00.2	-0.003	1.884	-0.016
-00.2	-0.024	1.922	-0.020
-00.7	-0.043	1.943	-0.020
-01.8	-0.139	1.889	0.033
-02.7	-0.198	1.913	0.037
-03.7	-0.255	1.917	0.050
00.8	0.038	1.868	-0.013
01.2	0.072	1.876	-0.030
02.2	0.131	1.872	-0.042
03.3	0.219	1.909	-0.093
04.2	0.257	1.834	-0.050
06.3	0.426	1.926	-0.149
09.3	0.599	1.790	-0.044
12.3	1.120	1.932	-0.992
15.3	1.335	1.797	-1.060
18.3	1.645	1.820	-1.331
10.3	0.675	1.870	-0.113
11.3	1.031	1.897	-0.934
12.2	1.089	1.877	-0.962
11.2	1.043	1.906	-0.957
10.3	0.974	1.910	-0.919
09.2	0.896	1.932	-0.873
08.2	0.813	1.947	-0.759
07.2	0.728	1.851	-0.742
06.2	0.679	1.903	-0.734
05.2	0.330	1.880	-0.099
04.2	0.252	1.817	-0.039

α	C_N	C_A	C_m
M = 1.30			
00.1	0.026	1.910	-0.030
-00.9	-0.048	1.904	-0.021
-02.9	-0.178	1.903	-0.011
00.6	0.051	1.909	-0.037
01.0	0.092	1.908	-0.040
03.1	0.219	1.906	-0.059
06.1	0.422	1.911	-0.074
09.2	0.638	1.920	-0.091
12.1	0.896	1.922	-0.138
15.2	1.248	1.905	-0.455
18.2	1.657	1.914	-0.850
14.1	1.098	1.923	-0.203
15.2	1.248	1.912	-0.448
16.3	1.390	1.908	-0.617
15.1	1.249	1.911	-0.459
14.1	1.110	1.914	-0.274
13.1	1.004	1.918	-0.217
12.1	0.888	1.925	-0.131
11.1	0.808	1.924	-0.116
M = 2.20			
-02.2	-0.149	1.703	0.063
-00.2	-0.035	1.709	0.018
00.6	0.040	1.713	-0.003
01.7	0.096	1.715	-0.011
03.7	0.222	1.713	-0.062
06.7	0.416	1.721	-0.158
12.7	0.910	1.739	-0.507
18.7	1.583	1.756	-1.109

[redacted]

TABLE III.- STATIC STABILITY DATA - Continued
(j) Model 531 - Center of moments at 0.358l

α	C_N	C_A	C_m
M = 0.65			
-03.0	-0.281	1.134	0.329
-01.0	-0.120	1.108	0.149
-00.0	0.004	1.095	-0.017
00.9	0.111	1.103	-0.151
02.9	0.292	1.124	-0.338
05.9	0.496	1.148	-0.450
09.0	0.664	1.153	-0.492
11.9	0.831	1.151	-0.528
14.9	1.021	1.153	-0.593
18.0	1.225	1.149	-0.674
M = 0.80			
-03.0	-0.336	1.271	0.429
-01.0	-0.140	1.243	0.211
00.0	0.010	1.231	-0.012
00.9	0.140	1.246	-0.205
02.9	0.345	1.264	-0.437
05.9	0.574	1.317	-0.632
08.9	0.748	1.337	-0.703
12.0	0.934	1.341	-0.754
15.0	1.137	1.333	-0.824
18.0	1.384	1.343	-0.931
M = 0.90			
-02.8	-0.370	1.383	0.571
-00.8	-0.149	1.245	0.289
00.1	0.034	1.217	-0.070
01.1	0.187	1.278	-0.354
03.1	0.398	1.385	-0.593
06.1	0.653	1.460	-0.835
09.2	0.856	1.501	-0.954
12.2	1.054	1.509	-1.020
15.2	1.290	1.505	-1.137
18.2	1.565	1.475	-1.293
M = 1.00			
00.2	0.035	1.756	-0.027
-00.2	0.002	1.738	-0.012
-00.7	-0.054	1.778	0.011
-01.7	-0.116	1.760	0.036
-02.7	-0.184	1.751	0.061
-03.7	-0.251	1.763	0.086
00.8	0.074	1.796	-0.041
00.9	0.101	1.755	-0.052
02.2	0.162	1.775	-0.070
03.2	0.239	1.741	-0.106
04.3	0.304	1.780	-0.119
05.9	0.434	1.789	-0.162
09.2	0.962	1.913	-1.015
12.2	1.160	1.895	-1.115
15.2	1.368	1.872	-1.189
18.3	1.635	1.817	-1.303
06.3	0.429	1.817	-0.141
07.3	0.819	1.866	-0.931
08.2	0.883	1.871	-0.972
07.3	0.828	1.853	-0.953
06.2	0.750	1.846	-0.889
05.3	0.672	1.841	-0.819
04.2	0.595	1.811	-0.763
03.2	0.232	1.749	-0.099
02.2	0.169	1.758	-0.082
M = 1.10			
00.3	0.020	2.037	-0.024
-00.2	-0.016	2.052	-0.023
-00.7	-0.053	2.051	-0.014
-01.7	-0.136	2.043	0.040
-02.6	-0.202	2.026	0.079
-03.8	-0.250	2.070	0.066
00.8	0.067	2.075	-0.050
01.2	0.079	2.034	-0.052
02.2	0.154	2.056	-0.088
03.3	0.209	2.018	-0.097
04.2	0.283	2.070	-0.139
06.3	0.409	2.051	-0.162
09.3	0.597	2.015	-0.152
12.3	1.086	2.001	-1.085
15.3	1.330	1.996	-1.246
18.3	1.576	1.945	-1.375
10.3	0.666	1.986	-0.142
11.3	0.999	1.964	-0.974
12.2	1.086	2.000	-1.081
11.3	1.027	1.996	-1.039
10.2	0.970	2.026	-1.030
09.2	0.903	2.065	-0.970
08.2	0.834	2.025	-0.954
07.2	0.770	2.065	-0.879
06.2	0.705	2.033	-0.862
05.2	0.631	2.061	-0.771
04.2	0.287	2.073	-0.145
03.3	0.234	2.091	-0.124
M = 1.30			
00.1	0.013	2.104	-0.032
-00.8	-0.056	2.104	-0.007
-02.9	-0.190	2.103	0.033
01.0	0.092	2.104	-0.052
03.1	0.227	2.103	-0.099
06.1	0.429	2.116	-0.142
09.1	0.651	2.105	-0.180
12.2	0.910	2.097	-0.219
15.2	1.244	2.060	-0.541
18.2	1.604	2.046	-0.836
14.1	1.096	2.086	-0.261
15.2	1.254	2.062	-0.559
16.2	1.359	2.055	-0.667
15.2	1.248	2.061	-0.560
14.1	1.103	2.076	-0.344
13.1	1.002	2.084	-0.294
12.1	0.911	2.100	-0.215
11.0	0.822	2.098	-0.209
M = 1.60			
-02.9	-0.174	1.958	0.039
-00.9	-0.051	1.964	0.008
00.0	0.007	1.965	-0.008
01.0	0.073	1.968	-0.033
03.0	0.191	1.961	-0.060
06.0	0.380	1.949	-0.115
09.0	0.602	1.952	-0.207
12.0	0.872	1.960	-0.348
15.0	1.207	1.967	-0.581
18.0	1.601	1.962	-0.908
M = 1.90			
-02.8	-0.157	1.839	0.068
-00.8	-0.036	1.842	0.021
00.1	0.020	1.842	-0.004
01.0	0.080	1.842	-0.028
03.1	0.205	1.840	-0.082
06.1	0.396	1.831	-0.165
09.1	0.621	1.834	-0.294
12.1	0.885	1.829	-0.480
15.2	1.204	1.835	-0.736
18.1	1.561	1.831	-1.067
M = 2.20			
-02.2	-0.153	1.743	0.063
-00.2	-0.043	1.745	0.017
00.7	0.028	1.743	-0.012
01.6	0.087	1.737	-0.034
03.6	0.205	1.742	-0.087
06.7	0.394	1.732	-0.191
09.7	0.598	1.730	-0.331
12.7	0.859	1.732	-0.545
15.7	1.162	1.735	-0.821
18.7	1.492	1.733	-1.136

[redacted]

TABLE III.- STATIC STABILITY DATA - Continued
(k) Model 515 - Center of moments at 0.335l

α	C_N	C_A	C_m
M = 0.65			
-00.0	-0.010	1.211	0.026
-00.6	-0.095	1.210	0.109
-01.2	-0.157	1.207	0.190
-02.0	-0.256	1.216	0.292
-03.0	-0.348	1.219	0.373
-04.0	-0.447	1.226	0.467
00.4	0.041	1.210	-0.035
00.9	0.099	1.214	-0.109
01.9	0.202	1.213	-0.217
02.9	0.308	1.226	-0.331
03.9	0.394	1.236	-0.408
05.9	0.562	1.254	-0.540
08.9	0.781	1.263	-0.667
11.9	1.007	1.267	-0.803
14.9	1.251	1.267	-0.957
17.8	1.522	1.261	-1.134
M = 0.80			
00.0	0.009	1.380	0.012
-00.4	-0.064	1.379	0.127
-01.1	-0.160	1.384	0.247
-02.0	-0.274	1.393	0.381
-03.0	-0.384	1.403	0.499
-04.1	-0.479	1.417	0.589
00.4	0.053	1.381	-0.065
00.9	0.138	1.389	-0.183
01.9	0.257	1.402	-0.332
02.9	0.359	1.408	-0.447
04.0	0.462	1.422	-0.556
05.9	0.651	1.444	-0.732
08.9	0.879	1.464	-0.905
11.9	1.123	1.473	-1.058
14.9	1.384	1.463	-1.225
17.9	1.667	1.444	-1.405
M = 0.90			
00.1	0.027	1.431	-0.032
-00.4	-0.067	1.443	0.159
-00.8	-0.171	1.477	0.356
-01.8	-0.301	1.540	0.559
-02.9	-0.415	1.561	0.663
-03.9	-0.526	1.599	0.762
00.6	0.109	1.461	-0.200
01.1	0.205	1.501	-0.377
02.1	0.325	1.554	-0.531
03.1	0.437	1.590	-0.651
04.1	0.527	1.608	-0.746
06.1	0.730	1.641	-0.950
09.1	0.988	1.664	-1.164
12.1	1.248	1.679	-1.338
15.1	1.532	1.640	-1.525
18.1	1.826	1.601	-1.713
M = 1.00			
00.2	0.040	2.171	-0.022
-00.2	-0.004	2.048	0.008
-00.7	-0.055	2.093	0.032
-01.7	-0.123	2.094	0.077
-02.7	-0.221	2.084	0.144
-03.8	-0.307	2.090	0.199
00.8	0.085	2.080	-0.056
01.2	0.122	2.063	-0.083
02.2	0.202	2.068	-0.135
03.2	0.287	2.089	-0.196
04.3	0.363	2.091	-0.236
06.3	0.821	2.107	-1.058
09.2	1.095	2.198	-1.278
12.2	1.337	2.181	-1.443
15.3	1.621	2.139	-1.624
18.2	1.911	2.091	-1.808
05.3	0.451	2.115	-0.292
06.3	0.836	2.184	-1.052
07.3	0.926	2.107	-1.181
06.3	0.833	2.140	-1.072
05.3	0.751	2.138	-0.989
04.2	0.645	2.127	-0.877
03.2	0.536	2.079	-0.776
02.2	0.205	2.090	-0.135
01.2	0.120	2.062	-0.079
M = 1.10			
00.2	0.022	2.398	-0.043
-00.3	-0.036	2.392	-0.007
-00.7	-0.048	2.403	0.003
-01.8	-0.153	2.388	0.077
-02.6	-0.206	2.403	0.103
-03.7	-0.286	2.415	0.151
00.8	0.047	2.377	-0.046
01.2	0.102	2.399	-0.103
02.2	0.183	2.409	-0.162
03.3	0.264	2.404	-0.214
04.2	0.322	2.379	-0.234
06.3	0.515	2.419	-0.369
09.3	1.039	2.387	-1.279
12.3	1.281	2.294	-1.458
15.3	1.561	2.240	-1.670
18.3	1.871	2.168	-1.917
07.3	0.592	2.439	-0.414
08.3	0.953	2.403	-1.191
09.3	1.041	2.307	-1.287
08.3	0.929	2.234	-1.151
07.3	0.877	2.314	-1.153
06.3	0.777	2.241	-1.034
05.2	0.697	2.333	-0.920
04.2	0.594	2.334	-0.860
03.2	0.252	2.384	-0.192
02.2	0.177	2.391	-0.152
M = 1.30			
00.1	0.029	2.240	-0.022
-00.9	-0.056	2.243	0.017
-02.8	-0.205	2.238	0.089
01.1	0.111	2.241	-0.061
03.0	0.254	2.238	-0.138
06.1	0.490	2.247	-0.245
09.1	0.738	2.254	-0.341
12.1	1.026	2.248	-0.461
15.1	1.366	2.235	-0.641
18.2	1.879	2.208	-1.423
14.1	1.248	2.242	-0.572
15.2	1.380	2.237	-0.640
16.2	1.580	2.209	-1.132
17.2	1.727	2.207	-1.270
16.2	1.590	2.203	-1.145
15.2	1.447	2.211	-0.994
14.1	1.285	2.226	-0.750
13.1	1.141	2.235	-0.572
12.1	1.027	2.247	-0.458
11.1	0.930	2.253	-0.415
M = 1.60			
00.0	-0.006	2.043	0.026
-01.0	-0.088	2.039	0.056
-03.0	-0.231	2.038	0.119
01.0	0.061	2.043	-0.011
03.0	0.216	2.043	-0.095
06.0	0.431	2.042	-0.204
08.9	0.675	2.043	-0.343
11.9	0.993	2.041	-0.582
15.0	1.372	2.056	-0.914
18.0	1.824	2.081	-1.386
M = 1.90			
00.0	0.017	1.912	0.009
-00.9	-0.075	1.910	0.054
-02.9	-0.211	1.903	0.140
01.1	0.086	1.910	-0.040
03.1	0.231	1.914	-0.131
06.1	0.458	1.914	-0.276
09.0	0.706	1.900	-0.466
12.1	1.012	1.907	-0.739
15.1	1.381	1.920	-1.114
18.0	1.794	1.921	-1.575
M = 2.20			
00.7	0.040	1.804	-0.007
-00.2	-0.051	1.803	0.035
-01.2	-0.121	1.799	0.089
-02.2	-0.180	1.808	0.130
01.8	0.095	1.809	-0.049
03.7	0.247	1.799	-0.170
06.7	0.463	1.797	-0.346
09.6	0.710	1.790	-0.555
12.7	1.014	1.793	-0.872
15.7	1.390	1.805	-1.279
18.6	1.750	1.770	-1.690

[redacted]

TABLE III.- STATIC STABILITY DATA - Continued
(1) Model 516 - Center of moments at 0.335l

α	C_N	C_A	C_m
M = 0.65			
-00.0	-0.040	1.064	0.056
-00.5	-0.092	1.064	0.114
-01.1	-0.143	1.065	0.171
-02.1	-0.239	1.062	0.256
-03.1	-0.339	1.070	0.343
-04.0	-0.425	1.069	0.414
00.4	0.034	1.064	-0.034
00.9	0.086	1.063	-0.093
01.9	0.184	1.059	-0.187
02.9	0.278	1.049	-0.273
03.9	0.372	1.063	-0.360
05.9	0.553	1.074	-0.517
08.9	0.793	1.079	-0.686
11.9	1.041	1.077	-0.841
14.9	1.289	1.095	-1.010
M = 0.80			
-00.0	0.003	1.234	0.005
-00.5	-0.074	1.233	0.114
-01.1	-0.144	1.239	0.205
-02.0	-0.253	1.238	0.331
-03.0	-0.340	1.240	0.408
-04.1	-0.439	1.240	0.505
00.4	0.059	1.233	-0.058
00.9	0.118	1.234	-0.138
01.9	0.222	1.235	-0.268
02.9	0.324	1.231	-0.376
03.9	0.431	1.245	-0.483
05.9	0.620	1.253	-0.664
09.0	0.896	1.275	-0.913
11.9	1.165	1.281	-1.117
14.9	1.441	1.280	-1.316
17.9	1.742	1.270	-1.524
M = 0.90			
00.1	0.027	1.387	-0.037
00.2	0.045	1.294	-0.092
-00.4	-0.069	1.297	0.132
-00.9	-0.167	1.306	0.317
-01.9	-0.286	1.361	0.481
-03.0	-0.396	1.392	0.607
-03.8	-0.493	1.409	0.702
00.6	0.110	1.312	-0.215
01.1	0.180	1.353	-0.321
02.1	0.288	1.373	-0.460
03.1	0.404	1.399	-0.601
04.1	0.505	1.412	-0.702
06.1	0.710	1.442	-0.909
09.1	1.001	1.447	-1.178
12.2	1.294	1.459	-1.407
15.2	1.613	1.460	-1.654
18.2	1.934	1.418	-1.899
M = 1.00			
00.3	0.045	1.913	-0.037
-00.2	-0.016	1.910	0.007
-00.7	-0.061	1.934	0.040
-01.7	-0.144	1.908	0.095
-02.7	-0.229	1.931	0.152
-03.7	-0.314	1.946	0.208
00.7	0.085	1.973	-0.065
01.2	0.131	1.966	-0.098
02.2	0.219	1.947	-0.159
03.2	0.304	1.994	-0.215
04.3	0.397	1.962	-0.273
06.3	0.571	1.985	-0.381
09.3	0.834	1.928	-0.523
12.3	1.370	1.907	-1.409
15.3	1.708	1.890	-1.707
18.3	2.060	1.866	-1.990
09.3	0.846	1.989	-0.529
10.3	0.941	1.961	-0.582
11.3	1.277	1.914	-1.327
12.3	1.373	1.899	-1.407
11.2	1.277	1.926	-1.334
10.3	1.187	1.889	-1.267
09.3	1.090	1.848	-1.192
08.3	0.995	1.915	-1.112
07.2	0.882	1.831	-1.010
06.3	0.786	1.910	-0.906
05.2	0.678	1.896	-0.796
04.2	0.385	1.873	-0.263
03.2	0.304	1.967	-0.215
M = 1.10			
00.2	0.028	2.043	-0.071
-00.2	-0.012	2.056	-0.041
-00.6	-0.052	2.025	-0.011
-01.8	-0.146	2.049	0.060
-02.8	-0.221	2.044	0.107
-03.8	-0.313	2.033	0.170
00.8	0.079	2.043	-0.096
01.3	0.125	2.058	-0.131
02.3	0.188	2.009	-0.161
03.2	0.258	1.999	-0.200
04.2	0.322	1.956	-0.207
06.3	0.540	2.056	-0.402
09.3	0.758	1.998	-0.475
12.2	1.282	1.931	-1.396
15.3	1.583	1.868	-1.622
18.3	1.940	1.858	-1.973
10.3	0.857	2.012	-0.536
11.3	1.218	1.976	-1.358
12.2	1.280	1.919	-1.392
11.3	1.193	1.927	-1.323
10.3	1.113	1.947	-1.271
09.3	1.029	1.964	-1.207
08.3	0.921	1.905	-1.080
07.2	0.839	1.947	-1.027
06.2	0.680	1.851	-0.767
05.2	0.646	1.957	-0.818
04.2	0.330	1.973	-0.228
03.2	0.258	1.983	-0.192
M = 1.30			
00.1	0.036	2.009	-0.049
-00.9	-0.047	2.011	-0.012
-02.9	-0.212	2.005	0.078
01.1	0.107	2.010	-0.080
03.1	0.261	2.003	-0.163
06.2	0.511	1.986	-0.290
09.1	0.764	1.951	-0.401
12.1	1.045	1.932	-0.506
15.2	1.456	1.932	-0.925
18.2	1.936	1.935	-1.457
M = 1.60			
-00.0	-0.025	1.874	0.045
-01.1	-0.105	1.871	0.090
-03.0	-0.248	1.870	0.163
01.0	0.057	1.871	-0.000
02.9	0.199	1.871	-0.078
06.0	0.438	1.862	-0.213
08.9	0.691	1.839	-0.373
12.0	1.003	1.821	-0.602
15.0	1.354	1.804	-0.883
18.0	1.800	1.804	-1.347
M = 1.90			
00.0	0.013	1.766	-0.008
-00.9	-0.083	1.764	0.063
-01.9	-0.142	1.760	0.098
-02.9	-0.228	1.758	0.162
01.1	0.077	1.766	-0.044
03.1	0.230	1.766	-0.150
06.1	0.465	1.768	-0.314
09.1	0.717	1.752	-0.506
12.1	1.017	1.733	-0.756
15.1	1.346	1.729	-1.042
18.2	1.745	1.692	-1.465
M = 2.20			
00.7	0.036	1.672	-0.014
-00.3	-0.040	1.673	0.029
-02.3	-0.178	1.672	0.134
01.7	0.092	1.669	-0.053
03.8	0.247	1.667	-0.175
06.7	0.461	1.660	-0.345
09.7	0.713	1.646	-0.567
12.7	0.995	1.643	-0.831
15.7	1.319	1.631	-1.154
18.6	1.670	1.613	-1.519

[redacted]

TABLE III.- STATIC STABILITY DATA - Continued
(m) Model 641 - Center of moments at 0.402l

α	C_N	C_A	C_m
M = 0.65			
-04.0	-0.298	0.851	0.044
-03.0	-0.238	0.851	0.044
-02.0	-0.168	0.853	0.020
-01.0	-0.094	0.855	-0.002
-00.5	-0.075	0.851	0.007
-00.0	-0.049	0.851	0.006
00.4	-0.001	0.860	-0.022
00.9	0.045	0.857	-0.014
01.9	0.102	0.857	-0.016
02.9	0.170	0.853	-0.042
03.9	0.234	0.857	-0.054
05.9	0.362	0.870	-0.080
08.9	0.612	0.998	-0.175
12.0	0.843	1.085	-0.265
14.9	1.073	1.146	-0.354
17.9	1.307	1.186	-0.445
M = 0.80			
-04.0	-0.398	1.096	0.255
-02.9	-0.311	1.074	0.210
-02.0	-0.243	1.076	0.177
-01.0	-0.128	1.059	0.085
-00.5	-0.084	1.058	0.047
-00.0	-0.020	1.054	-0.009
00.5	0.050	1.063	-0.052
00.9	0.103	1.061	-0.097
01.9	0.212	1.071	-0.180
02.9	0.296	1.088	-0.227
04.0	0.379	1.109	-0.270
05.9	0.519	1.141	-0.324
08.9	0.724	1.218	-0.398
12.0	0.955	1.268	-0.482
14.9	1.176	1.290	-0.536
18.0	1.421	1.296	-0.591
M = 0.90			
-03.8	-0.467	1.326	0.495
-02.8	-0.388	1.292	0.451
-01.8	-0.277	1.210	0.338
-00.8	-0.147	1.237	0.173
-00.3	-0.062	1.225	0.064
00.1	0.011	1.198	-0.042
00.6	0.099	1.227	-0.169
01.2	0.183	1.243	-0.280
02.1	0.293	1.254	-0.382
03.1	0.385	1.298	-0.444
04.1	0.480	1.323	-0.528
06.1	0.626	1.371	-0.587
09.1	0.831	1.430	-0.640
12.2	1.063	1.433	-0.690
15.1	1.282	1.425	-0.718
18.2	1.560	1.476	-0.775
M = 1.00			
-03.7	-0.250	1.686	0.010
-02.7	-0.177	1.677	0.006
-01.7	-0.117	1.665	0.000
-00.7	-0.052	1.721	-0.003
-00.2	-0.007	1.715	-0.016
00.2	0.018	1.672	-0.013
00.7	0.067	1.716	-0.011
01.2	0.097	1.649	-0.014
02.3	0.164	1.726	-0.012
03.2	0.227	1.644	-0.017
04.3	0.295	1.709	-0.018
06.2	0.414	1.772	-0.001
09.2	0.967	1.811	-0.815
12.3	1.191	1.880	-0.852
15.2	1.404	1.857	-0.877
18.3	1.654	1.899	-0.915
06.2	0.413	1.742	0.002
07.2	0.484	1.750	-0.007
08.3	0.898	1.877	-0.766
09.3	0.957	1.903	-0.785
08.2	0.899	1.910	-0.779
07.2	0.834	1.810	-0.770
06.3	0.762	1.848	-0.736
05.2	0.693	1.786	-0.722
04.2	0.292	1.866	-0.024
03.2	0.228	1.677	-0.016
M = 1.10			
-03.6	-0.284	1.791	0.044
-02.7	-0.177	1.889	-0.004
-01.7	-0.157	1.784	0.036
-00.7	-0.083	1.839	0.016
-00.2	-0.032	1.875	-0.015
00.2	-0.003	1.878	-0.017
00.8	0.034	1.734	0.020
01.3	0.055	1.808	0.010
02.2	0.147	1.895	-0.026
03.3	0.187	1.754	0.013
04.3	0.250	1.841	-0.017
06.3	0.375	1.766	0.022
09.3	0.899	1.894	-0.780
12.4	1.082	1.816	-0.752
15.3	1.345	1.938	-0.928
18.3	1.570	1.864	-0.950
07.3	0.432	1.831	0.025
08.3	0.817	1.804	-0.681
09.3	0.904	1.867	-0.782
08.3	0.849	1.907	-0.785
07.3	0.772	1.817	-0.741
06.2	0.700	1.816	-0.716
05.2	0.322	1.889	-0.039
04.2	0.253	1.751	0.004
M = 1.30			
-02.8	-0.193	1.968	-0.001
-00.8	-0.070	1.968	-0.002
00.1	0.004	1.968	-0.014
01.1	0.078	1.972	-0.010
03.1	0.219	1.970	-0.018
06.1	0.422	1.979	-0.008
09.1	0.633	1.984	0.002
12.2	0.903	1.990	-0.019
15.1	1.250	1.977	-0.415
18.2	1.615	1.977	-0.670
13.2	1.001	1.992	-0.024
14.3	1.148	1.977	-0.319
15.1	1.247	1.975	-0.412
14.2	1.140	1.977	-0.311
13.2	1.011	1.981	-0.109
12.2	0.897	1.876	-0.015
M = 1.60			
-02.9	-0.198	1.830	0.012
-01.0	-0.082	1.827	0.016
-00.0	-0.021	1.830	0.013
01.0	0.057	1.825	0.013
03.0	0.181	1.824	0.012
05.9	0.372	1.810	0.009
09.0	0.593	1.822	-0.025
12.0	0.857	1.827	-0.103
15.0	1.180	1.849	-0.266
18.0	1.552	1.877	-0.504
M = 1.90			
-02.8	-0.158	1.719	0.007
-00.9	-0.037	1.718	-0.017
00.0	0.032	1.720	-0.022
01.1	0.099	1.720	-0.022
03.1	0.218	1.720	-0.035
06.0	0.409	1.717	-0.076
09.1	0.625	1.720	-0.136
12.2	0.887	1.731	-0.250
15.1	1.189	1.742	-0.425
18.1	1.533	1.758	-0.662
M = 2.20			
-02.2	-0.133	1.622	0.019
-00.3	-0.016	1.620	-0.007
00.7	0.035	1.613	-0.013
01.7	0.105	1.616	-0.032
03.7	0.220	1.623	-0.053
06.6	0.404	1.620	-0.107
09.7	0.620	1.623	-0.208
12.7	0.874	1.637	-0.342
15.7	1.152	1.650	-0.531
18.7	1.482	1.665	-0.756

[redacted]

TABLE III.- STATIC STABILITY DATA - Continued
(n) Model 517 - Center of moments at 0.4001

α	C_N	C_A	C_m
M = 0.65			
-00.0	-0.052	1.211	0.040
-00.6	-0.120	1.211	0.126
-01.1	-0.185	1.219	0.197
-02.0	-0.278	1.220	0.273
-03.1	-0.377	1.247	0.368
-04.1	-0.459	1.259	0.423
00.4	0.037	1.216	-0.035
00.9	0.098	1.215	-0.108
01.9	0.209	1.224	-0.208
02.9	0.311	1.240	-0.308
03.9	0.384	1.260	-0.364
05.9	0.508	1.283	-0.412
08.9	0.668	1.285	-0.411
11.9	0.823	1.280	-0.402
14.9	0.987	1.282	-0.414
17.8	1.168	1.266	-0.436
M = 0.80			
-00.0	-0.034	1.325	0.084
-00.6	-0.120	1.333	0.187
-01.0	-0.190	1.339	0.254
-02.0	-0.300	1.360	0.373
-03.0	-0.401	1.387	0.462
-04.1	-0.486	1.404	0.533
00.5	0.059	1.329	-0.059
00.9	0.138	1.339	-0.184
01.9	0.259	1.361	-0.327
02.9	0.355	1.386	-0.417
03.9	0.455	1.413	-0.500
05.9	0.606	1.447	-0.597
08.9	0.767	1.473	-0.642
11.9	0.928	1.478	-0.636
14.9	1.118	1.464	-0.656
17.9	1.344	1.446	-0.727
M = 0.90			
00.1	0.012	1.225	-0.021
-00.3	-0.085	1.230	0.157
-00.9	-0.186	1.277	0.344
-01.9	-0.331	1.400	0.528
-02.8	-0.439	1.485	0.622
-03.9	-0.531	1.520	0.697
00.6	0.101	1.261	-0.211
01.1	0.175	1.331	-0.314
02.1	0.321	1.431	-0.480
03.1	0.423	1.500	-0.592
04.1	0.513	1.529	-0.665
06.2	0.696	1.588	-0.799
09.1	0.878	1.621	-0.872
12.1	1.070	1.658	-0.917
15.1	1.291	1.635	-0.978
18.1	1.507	1.585	-1.013
M = 1.00			
00.2	0.029	1.999	-0.016
-00.2	-0.016	1.969	0.006
-00.7	-0.054	1.978	0.020
-01.7	-0.125	1.991	0.044
-02.8	-0.194	2.023	0.065
-03.8	-0.259	2.011	0.087
00.6	0.060	2.043	-0.027
01.2	0.097	1.986	-0.042
02.2	0.169	2.006	-0.066
03.2	0.236	2.054	-0.088
04.2	0.306	2.069	-0.109
06.3	0.440	2.124	-0.139
09.2	1.002	2.150	-0.997
12.2	1.187	2.154	-1.030
15.3	1.386	2.119	-1.054
18.3	1.595	2.053	-1.080
05.3	0.368	2.029	-0.132
06.2	0.813	2.057	-0.933
07.2	0.883	2.089	-0.968
06.2	0.819	2.086	-0.945
05.2	0.736	2.066	-0.888
04.2	0.659	2.062	-0.833
03.2	0.571	1.977	-0.769
02.2	0.166	2.014	-0.071
01.2	0.103	2.048	-0.049
M = 1.10			
00.3	0.014	2.170	-0.013
-00.1	-0.060	2.109	0.040
-00.6	-0.063	2.174	0.016
-01.7	-0.153	2.149	0.074
-02.7	-0.256	2.129	0.157
-03.7	-0.333	2.108	0.205
00.8	0.058	2.181	-0.037
01.2	0.063	2.117	-0.028
02.2	0.151	2.176	-0.071
03.2	0.212	2.114	-0.110
04.3	0.278	2.145	-0.134
06.3	0.406	2.208	-0.143
09.3	0.950	2.123	-1.008
12.3	1.102	2.050	-1.016
15.3	1.321	2.098	-1.093
18.3	1.530	2.014	-1.158
05.2	0.343	2.183	-0.158
06.3	0.429	2.102	-0.208
07.2	0.832	2.114	-0.948
08.3	0.892	2.120	-0.981
07.3	0.820	2.015	-0.937
06.2	0.760	2.041	-0.934
05.2	0.687	2.080	-0.867
04.2	0.275	2.174	-0.127
03.2	0.210	2.105	-0.111
M = 1.30			
00.1	0.018	2.245	-0.012
-00.9	-0.075	2.321	0.044
-01.8	-0.154	2.320	0.091
-02.9	-0.234	2.325	0.131
01.1	0.088	2.318	-0.053
03.1	0.256	2.324	-0.146
06.2	0.467	2.341	-0.201
09.1	0.674	2.343	-0.206
12.2	0.911	2.324	-0.228
15.2	1.236	2.248	-0.728
18.2	1.568	2.135	-0.891
14.1	1.086	2.232	-0.262
15.2	1.220	2.183	-0.716
16.2	1.341	2.156	-0.786
15.2	1.230	2.179	-0.729
14.1	1.128	2.199	-0.683
13.1	1.045	2.220	-0.655
12.1	0.964	2.231	-0.597
11.1	0.832	2.254	-0.219
10.1	0.751	2.260	-0.215
M = 1.60			
-00.0	-0.018	2.178	0.037
-01.0	-0.095	2.173	0.068
-03.0	-0.227	2.160	0.103
01.0	0.058	2.176	-0.003
02.9	0.181	2.164	-0.039
06.0	0.384	2.140	-0.088
09.0	0.617	2.108	-0.189
12.0	0.882	2.093	-0.317
15.0	1.179	2.085	-0.465
18.0	1.519	2.066	-0.682
M = 1.90			
00.1	0.007	2.006	0.014
-00.8	-0.056	2.000	0.027
-02.9	-0.186	1.993	0.060
01.1	0.061	2.006	-0.008
03.1	0.178	1.997	-0.036
06.2	0.372	1.975	-0.101
09.1	0.589	1.952	-0.193
12.0	0.839	1.937	-0.353
15.1	1.121	1.923	-0.532
18.0	1.449	1.911	-0.786
M = 2.20			
00.7	0.017	1.860	0.018
-00.3	-0.035	1.857	0.031
-02.3	-0.157	1.854	0.067
01.7	0.068	1.861	-0.010
03.7	0.191	1.845	-0.054
06.7	0.361	1.827	-0.128
09.7	0.568	1.808	-0.239
12.6	0.801	1.801	-0.399
15.7	1.106	1.801	-0.635
18.6	1.394	1.799	-0.869

[redacted]

TABLE III.- STATIC STABILITY DATA - Concluded
(o) Model 5-8 - Center of moments at 0.358l

α	C_N	C_A	C_m
M = 0.65			
-04.0	-0.386	0.706	0.085
-03.0	-0.306	0.694	0.084
-02.1	-0.233	0.685	0.074
-01.0	-0.136	0.679	0.048
-00.5	-0.094	0.683	0.034
00.0	-0.041	0.682	0.014
00.4	-0.004	0.683	-0.001
00.9	0.061	0.680	-0.011
01.9	0.155	0.690	-0.038
02.9	0.231	0.698	-0.046
03.8	0.307	0.707	-0.055
05.9	0.449	0.718	-0.045
08.9	0.670	0.736	-0.044
11.9	0.882	0.758	-0.051
14.9	1.102	0.785	-0.071
18.0	1.340	0.811	-0.111
M = 0.80			
-04.0	-0.383	0.807	0.134
-03.0	-0.305	0.796	0.125
-02.0	-0.215	0.787	0.097
-01.0	-0.121	0.774	0.054
-00.6	-0.073	0.779	0.030
00.0	-0.017	0.775	0.002
00.5	0.045	0.773	-0.024
00.9	0.088	0.778	-0.044
02.0	0.181	0.788	-0.081
02.9	0.275	0.796	-0.108
03.9	0.346	0.802	-0.114
05.9	0.504	0.825	-0.131
08.9	0.728	0.853	-0.137
12.0	0.967	0.886	-0.139
14.9	1.207	0.911	-0.154
17.9	1.482	0.925	-0.210
M = 0.90			
-03.8	-0.386	0.878	0.193
-02.8	-0.301	0.847	0.165
-01.9	-0.218	0.837	0.136
-00.8	-0.110	0.822	0.070
-00.3	-0.059	0.824	0.032
00.0	-0.008	0.817	-0.011
00.7	0.081	0.825	-0.066
01.2	0.126	0.818	-0.082
02.1	0.169	0.837	-0.009
03.1	0.310	0.849	-0.168
04.1	0.392	0.879	-0.187
06.1	0.561	0.908	-0.210
09.2	0.798	0.938	-0.222
12.2	1.061	0.978	-0.248
15.1	1.346	1.005	-0.294
18.2	1.648	1.022	-0.365
M = 1.00			
-03.7	-0.291	1.139	-0.065
-02.6	-0.204	1.117	-0.051
-01.7	-0.130	1.132	-0.043
-00.7	-0.051	1.164	-0.025
-00.2	-0.019	1.115	-0.012
00.1	0.029	1.174	-0.008
00.7	0.080	1.163	-0.004
01.2	0.117	1.207	0.007
02.3	0.200	1.140	0.020
03.2	0.277	1.241	0.033
04.3	0.351	1.122	0.054
06.2	0.507	1.158	0.084
09.2	0.760	1.366	0.122
12.3	1.036	1.353	0.176
15.2	1.462	1.420	-0.136
18.3	1.913	1.493	-0.370
12.3	1.033	1.346	0.180
13.4	1.135	1.339	0.192
14.4	1.353	1.378	-0.093
15.3	1.466	1.415	-0.135
16.4	1.602	1.393	-0.202
15.2	1.450	1.348	-0.119
14.4	1.333	1.368	-0.070
13.3	1.223	1.364	-0.054
12.3	1.116	1.252	-0.044
11.3	1.023	1.319	-0.037
10.2	0.921	1.321	-0.032
09.2	0.757	1.274	0.121
08.3	0.676	1.169	0.112
M = 1.10			
-03.7	-0.316	1.209	-0.072
-02.6	-0.209	1.264	-0.097
-01.8	-0.127	1.344	-0.064
-00.6	-0.066	1.240	-0.066
-00.2	-0.039	1.256	-0.046
00.2	-0.005	1.230	-0.036
00.8	0.054	1.261	-0.042
01.4	0.109	1.316	-0.037
02.2	0.184	1.340	-0.016
03.3	0.181	1.122	0.131
04.3	0.321	1.337	0.014
06.3	0.412	1.174	0.150
09.3	0.618	1.199	0.251
12.3	0.966	1.442	0.121
15.4	1.320	1.339	-0.079
18.3	1.749	1.428	-0.365
12.3	0.887	1.201	0.335
13.4	0.999	1.338	0.255
14.4	1.229	1.394	-0.106
15.3	1.327	1.401	-0.130
14.4	1.224	1.412	-0.103
13.4	1.063	1.241	0.086
12.3	1.039	1.423	-0.099
11.3	0.871	1.270	0.074
10.3	0.747	1.295	0.136
09.2	0.678	1.344	0.097
M = 1.30			
-02.8	-0.215	1.369	-0.059
-00.8	-0.064	1.364	-0.038
00.0	0.020	1.364	-0.024
01.1	0.095	1.367	-0.004
03.2	0.264	1.371	0.009
06.1	0.504	1.393	0.018
09.1	0.770	1.434	0.004
12.2	1.108	1.489	-0.076
15.2	1.500	1.545	-0.248
18.2	1.996	1.600	-0.636
16.2	1.661	1.567	-0.338
17.3	1.830	1.584	-0.442
18.3	2.002	1.603	-0.642
17.2	1.824	1.587	-0.490
16.2	1.657	1.567	-0.370
15.2	1.498	1.547	-0.241
14.2	1.362	1.531	-0.170
M = 1.60			
-02.9	-0.264	1.416	0.033
-00.9	-0.108	1.407	0.023
-00.0	-0.034	1.404	0.012
01.0	0.062	1.403	0.010
03.0	0.218	1.406	0.000
06.0	0.460	1.427	-0.037
09.0	0.732	1.465	-0.123
12.1	1.063	1.501	-0.272
15.1	1.443	1.548	-0.512
18.0	1.869	1.587	-0.809
M = 1.90			
-02.8	-0.237	1.428	0.072
-00.9	-0.079	1.426	0.024
00.1	-0.006	1.426	0.005
01.1	0.084	1.424	0.002
03.1	0.237	1.429	-0.041
06.0	0.480	1.446	-0.119
09.1	0.743	1.464	-0.236
12.2	1.045	1.492	-0.391
15.1	1.376	1.511	-0.603
18.2	1.762	1.520	-0.893
M = 2.20			
-02.2	-0.193	1.421	0.071
-00.3	-0.063	1.417	0.027
00.7	0.016	1.415	0.003
01.6	0.112	1.413	-0.019
03.7	0.259	1.416	-0.068
06.6	0.485	1.426	-0.165
09.6	0.715	1.436	-0.276
12.7	0.999	1.452	-0.444
15.7	1.310	1.467	-0.653
18.7	1.655	1.455	-0.901

[redacted]

TABLE IV.- DAMPING IN PITCH DATA

(a) Model 111 - Center of moments at 0.423l

$\delta = \pm 1^{\circ}$

α	$C_{m_q}+C_{m_{\dot{\alpha}}}$	k
M = 0.65		
-00.3	02.21	.0288
-00.7	01.37	.0287
-01.2	00.92	.0283
-02.2	-01.27	.0281
00.1	02.65	.0284
00.5	02.66	.0283
01.5	00.51	.0282
03.4	-03.94	.0278
05.3	-04.70	.0276
08.3	-04.41	.0275
M = 0.80		
-00.3	08.45	.0257
-00.7	10.03	.0256
-01.0	04.54	.0254
-01.8	00.89	.0247
00.0	09.90	.0255
00.4	09.34	.0254
01.2	03.85	.0249
02.9	-04.50	.0238
04.7	-08.50	.0233
07.6	-09.87	.0227

α	$C_{m_q}+C_{m_{\dot{\alpha}}}$	k
M = 0.90		
-00.4	11.96	.0247
-00.6	13.17	.0250
-00.9	08.13	.0244
-01.6	00.60	.0239
00.0	14.79	.0251
00.3	16.18	.0253
00.9	02.92	.0245
02.4	11.15	.0232
03.8	04.15	.0216

$\delta = \pm 2^{\circ}$

α	$C_{m_q}+C_{m_{\dot{\alpha}}}$	k
M = 0.65		
-00.3	00.91	.0288
-00.7	00.91	.0288
-01.2	00.04	.0286
-02.2	-01.87	.0284
00.1	00.70	.0286
00.5	00.47	.0285
01.5	-00.81	.0284
03.4	-03.89	.0281
05.3	-06.12	.0279
08.3	-06.11	.0278
M = 0.80		
-00.3	03.04	.0256
-00.6	03.24	.0254
-01.0	02.52	.0253
-01.8	-01.54	.0250
00.0	05.95	.0256
00.4	04.50	.0255
01.2	02.34	.0250
02.9	-05.59	.0241
04.7	-09.05	.0235
07.6	-10.87	.0230
M = 0.90		
-00.4	06.55	.0248
-00.6	09.50	.0248
-00.9	08.54	.0247
00.0	05.94	.0247
00.3	06.49	.0252
00.9	00.75	.0246
02.4	-02.96	.0231
M = 1.00		
-00.3	-16.52	.0182
-00.8	-16.34	.0183
-01.2	-16.47	.0183
-02.1	-16.05	.0183
00.1	-16.84	.0183
00.5	-16.42	.0183
01.6	-16.08	.0183
03.5	-14.89	.0183
M = 1.10		
-00.3	-14.62	.0169
-00.5	-14.81	.0169
-01.2	-14.05	.0169
-02.3	-12.33	.0169
00.2	-14.44	.0170
00.5	-14.31	.0169
01.4	-12.98	.0169
03.5	-13.08	.0169

α	$C_{m_q}+C_{m_{\dot{\alpha}}}$	k
M = 1.20		
-00.3	-13.71	.0158
-00.8	-12.22	.0158
-01.2	-12.42	.0158
00.2	-12.93	.0158
00.6	-12.88	.0158
01.5	-13.78	.0157
M = 1.30		
-00.3	-10.98	.0149
-00.8	-11.53	.0149
-01.2	-12.19	.0149
-02.2	-13.77	.0148
00.1	-11.04	.0149
00.6	-11.68	.0149
01.5	-13.61	.0147
03.5	-19.04	.0145
05.5	-16.95	.0146
08.4	-14.20	.0148
M = 1.60		
-00.4	-13.21	.0129
-00.9	-13.14	.0129
-01.3	-14.68	.0128
00.0	-12.88	.0129
00.5	-13.17	.0129
05.4	-16.24	.0128
11.1	-12.49	.0135
16.1	-13.10	.0142
13.6	-12.38	.0138
08.3	-13.72	.0131
05.4	-16.18	.0128
02.4	-14.13	.0128
M = 2.20		
-00.2	-14.92	.0109
-00.7	-13.25	.0109
-01.2	-15.54	.0109
-02.1	-14.98	.0109
00.2	-14.97	.0109
00.7	-15.61	.0108
01.6	-13.96	.0108
03.6	-13.91	.0108
05.5	-13.25	.0109
11.0	-11.73	.0112
16.2	-11.21	.0115

[redacted]

TABLE IV.- DAMPING IN PITCH DATA - Continued
(b) Model 311 - Center of moments at 0.447l

$\delta = \pm 1^\circ$

α	$C_{m_q}+C_{m_{\dot{\alpha}}}$	k
M = 0.65		
-00.3	30.21	.0360
-00.7	27.60	.0358
-01.0	24.28	.0354
-01.7	13.82	.0343
-00.0	31.80	.0356
00.3	25.30	.0352
01.1	14.90	.0340
02.7	-06.22	.0314
04.6	-12.38	.0303
07.6	-11.59	.0297
M = 0.70		
-00.3	32.77	.0343
-00.6	29.75	.0339
-00.9	27.08	.0337
00.0	31.66	.0340
00.3	29.80	.0339
M = 0.75		
-00.3	34.90	.0335
-00.6	31.89	.0333
-00.9	32.84	.0331
-00.0	39.63	.0334
00.3	38.02	.0329
M = 0.80		
-00.3	57.99	.0342
-00.6	56.28	.0340
-00.9	52.43	.0335
-00.0	52.66	.0338
00.1	40.40	.0334
00.7	31.41	.0321
01.4	11.02	.0299

α	$C_{m_q}+C_{m_{\dot{\alpha}}}$	k
M = 0.85		
-00.4	69.09	.0334
-00.7	61.52	.0331
-00.9	55.24	.0330
-00.1	55.13	.0332
00.0	58.38	.0328
M = 0.90		
-00.4	69.67	.0321
-00.6	73.80	.0324
-00.9	68.38	.0322
-00.1	67.97	.0321
00.0	68.18	.0319
00.5	51.29	.0307
M = 1.00		
Flow separated		
-00.6	35.08	.0291
-00.8	33.78	.0293
-01.0	29.60	.0290
-00.4	28.00	.0288
-00.1	14.40	.0281
M = 1.10		
Flow separated		
-00.2	38.96	.0274
00.0	30.07	.0271
-00.7	22.04	.0270

$\delta = \pm 2^\circ$

α	$C_{m_q}+C_{m_{\dot{\alpha}}}$	k
M = 0.65		
-00.3	17.35	.0355
-00.7	16.90	.0354
-01.0	14.59	.0351
-01.7	08.99	.0345
-00.0	17.93	.0353
00.3	16.48	.0350
01.1	10.43	.0341
02.7	-06.12	.0319
04.6	-13.54	.0306
07.6	-11.94	.0300
M = 0.70		
-00.3	19.61	.0336
-00.6	15.99	.0336
-00.9	16.58	.0334
00.0	17.57	.0336
00.3	18.09	.0333
M = 0.75		
-00.3	22.63	.0329
-00.6	20.05	.0327
-00.9	20.36	.0326
-00.0	21.06	.0327
00.3	20.66	.0324
M = 0.80		
-00.3	32.71	.0329
-00.6	34.56	.0330
-00.9	28.65	.0327
-00.0	29.80	.0326
00.1	26.18	.0324
00.7	21.86	.0315
01.4	05.86	.0300
M = 0.85		
-00.4	40.16	.0323
-00.7	40.32	.0322
-00.9	36.54	.0319
-00.1	35.26	.0320
00.0	36.53	.0318
M = 0.90		
-00.4	48.50	.0314
-00.6	48.71	.0315
-00.9	45.51	.0313
-00.1	48.48	.0312
00.0	45.31	.0311
00.5	33.50	.0302
M = 1.00		
Flow attached		
-00.4	-08.17	.0205
-00.9	-08.72	.0204
-01.3	-08.68	.0204
-02.1	-08.23	.0204
00.1	-08.80	.0204
00.4	-07.92	.0204
01.4	-08.92	.0263
Flow separated		
-00.1	09.38	.0276
-00.4	15.63	.0279
-00.6	13.82	.0280
-00.9	13.08	.0282
-01.0	05.79	.0279

α	$C_{m_q}+C_{m_{\dot{\alpha}}}$	k
M = 1.10		
Flow attached		
-00.4	-01.30	.0192
-00.8	-04.02	.0191
-01.4	-01.14	.0192
-02.1	02.57	.0195
00.1	-01.10	.0193
00.4	-03.41	.0192
01.4	06.04	.0195
Flow separated		
-00.4	10.77	.0263
-00.6	09.31	.0262
-00.2	07.78	.0261
00.0	00.83	.0257
-00.7	-02.89	.0258
M = 1.20		
-00.3	-05.27	.0177
-00.7	-05.09	.0177
-01.2	-05.44	.0177
00.1	-05.52	.0176
00.5	-06.87	.0175
M = 1.30		
-00.3	-06.57	.0164
-00.7	-06.63	.0164
-01.3	-07.16	.0164
-02.2	-09.26	.0163
00.1	-06.65	.0164
00.5	-06.84	.0164
01.5	-08.48	.0163
03.5	-11.53	.0160
05.6	-12.41	.0159
08.6	-13.39	.0159
M = 1.60		
-00.3	-09.13	.0140
-00.8	-08.37	.0140
-01.4	-09.24	.0140
00.1	-07.60	.0140
00.5	-08.80	.0140
05.5	-12.81	.0140
11.2	-08.77	.0147
14.0	-05.31	.0150
M = 2.20		
-00.2	-08.00	.0119
-00.7	-07.06	.0118
-01.2	-07.46	.0118
-02.1	-07.49	.0118
00.3	-06.41	.0118
00.7	-07.56	.0118
01.7	-09.27	.0118
03.5	-09.13	.0118
05.5	-08.48	.0119
11.2	-09.25	.0122
16.5	-03.94	.0124

[redacted]

TABLE IV.- DAMPING IN PITCH DATA - Continued
(c) Model 411 - Center of moments at 0.439l

$\delta = \pm 1^{\circ}$

α	$C_{m_q}+C_{m_{\dot{\alpha}}}$	k
M = 0.65		
-00.3	45.94	.0380
-00.6	41.29	.0376
-01.0	28.26	.0370
-01.7	11.91	.0356
-00.0	45.36	.0378
00.2	38.83	.0374
00.9	20.96	.0359
02.5	-13.02	.0326
04.3	-21.96	.0306
07.3	-13.84	.0300
05.4	-17.16	.0304
03.4	-21.38	.0313
02.5	-14.27	.0325
M = 0.80		
-00.4	80.89	.0358
-00.6	72.77	.0358
-00.8	64.15	.0350
-01.3	46.85	.0340
-00.1	78.51	.0355
00.1	76.55	.0354
00.6	59.99	.0340
01.8	08.26	.0302
03.3	-31.72	.0263
06.3	-20.73	.0254
M = 0.90		
-00.4	84.85	.0337
-00.7	86.32	.0335
-01.0	80.86	.0332
-01.4	66.42	.0323
-00.1	82.66	.0333
-00.0	78.76	.0329
02.5	34.14	.0297

α	$C_{m_q}+C_{m_{\dot{\alpha}}}$	k
M = 1.00		
Flow separated		
-00.5	29.93	.0305
-00.7	30.70	.0303
-00.9	27.52	.0303
-01.4	17.94	.0291
-00.3	27.41	.0302
-00.1	25.35	.0297
00.3	08.83	.0282
M = 1.10		
Flow separated		
-01.3	31.94	.0281
-00.9	29.40	.0279
-01.2	16.98	.0265
-00.3	30.10	.0282
-00.2	31.78	.0285
-00.0	32.54	.0284
00.5	23.96	.0273

$\delta = \pm 2^{\circ}$

α	$C_{m_q}+C_{m_{\dot{\alpha}}}$	k
M = 0.65		
-00.3	25.57	.0372
-00.6	22.94	.0369
-01.0	18.62	.0365
-01.7	06.75	.0354
-00.0	26.59	.0370
00.2	23.76	.0369
00.9	14.51	.0356
02.5	-11.56	.0330
04.3	-19.58	.0310
07.3	-15.46	.0303
05.4	-17.74	.0305
03.4	-17.15	.0317
02.5	-11.33	.0329
M = 0.80		
00.5	50.96	.0345
-00.4	51.29	.0345
-00.6	52.06	.0343
-00.8	46.89	.0342
-00.1	51.25	.0345
00.1	50.28	.0343
00.6	41.02	.0337
M = 0.90		
-00.4	63.15	.0328
-00.7	61.15	.0326
-01.0	60.40	.0322
-00.1	62.43	.0325
-00.0	62.25	.0322
M = 1.00		
Flow attached		
-00.4	-05.11	.0212
-00.8	-05.34	.0212
00.0	-04.67	.0211
00.4	-04.67	.0211
01.3	-02.62	.0213
Flow separated		
-00.5	15.03	.0291
-00.8	17.35	.0293
-01.0	15.26	.0291
-01.4	05.13	.0282
-00.3	14.17	.0289
-00.1	09.53	.0285
00.3	-00.71	.0275

α	$C_{m_q}+C_{m_{\dot{\alpha}}}$	k
M = 1.10		
Flow separated		
-00.5	22.80	.0273
-01.3	19.33	.0272
-00.9	18.22	.0271
-01.2	04.92	.0261
-00.2	21.59	.0274
-00.0	18.87	.0273
00.5	09.75	.0263
M = 1.20		
-00.3	-04.00	.0180
-00.8	-04.52	.0180
-01.2	-04.36	.0180
00.0	-03.99	.0180
00.4	-04.00	.0179
M = 1.30		
-00.4	-04.66	.0167
-00.9	-05.04	.0167
-01.3	-05.43	.0167
-02.2	-06.62	.0166
00.0	-04.83	.0167
00.5	-04.86	.0167
01.5	-06.10	.0166
03.4	-09.62	.0162
05.3	-10.36	.0161
08.3	-09.27	.0162
M = 1.60		
-00.4	-11.17	.0143
-00.9	-10.93	.0143
-01.4	-11.76	.0142
00.1	-10.64	.0143
00.5	-10.12	.0142
05.4	-12.62	.0142
11.0	-04.77	.0149
15.9	-02.00	.0156
13.5	08.75	.0154
12.7	07.85	.0153
11.9	01.63	.0151
10.9	-04.74	.0149
14.0	07.53	.0155
16.0	-02.01	.0156
M = 2.20		
-00.2	-08.27	.0120
-00.8	-08.71	.0120
-01.3	-07.68	.0120
-02.2	-08.81	.0120
00.1	-08.35	.0119
00.6	-07.83	.0119
01.6	-09.83	.0119
03.5	-10.92	.0119
05.4	-08.28	.0120
11.1	-07.56	.0123
16.2	-05.73	.0125

[redacted]

TABLE IV.- DAMPING IN PITCH DATA - Continued
(d) Model 321 - Center of moments at 0.391l

$\delta = \pm 1^{\circ}$

α	$C_{m_q}+C_{m_{\dot{\alpha}}}$	k
M = 0.65		
00.0	025.0	.0346
-00.3	021.8	.0339
-00.6	017.2	.0333
-01.4	001.3	.0320
-02.1	-015.0	.0308
00.4	027.2	.0343
00.7	028.9	.0341
01.4	017.1	.0332
02.2	001.2	.0318
03.2	-011.4	.0304
04.9	-013.2	.0295
07.7	-015.8	.0287
M = 0.70		
00.0	030.6	.0327
-00.2	023.5	.0322
-00.6	021.3	.0317
-01.3	000.4	.0303
00.4	030.9	.0327
00.6	032.4	.0326
01.4	018.7	.0317
M = 0.75		
-00.3	036.8	.0319
-00.2	027.9	.0315
-00.6	021.7	.0311
-01.2	008.5	.0297
00.3	034.0	.0318
00.6	031.1	.0317
01.2	023.5	.0311
M = 0.80		
00.0	049.4	.0324
-00.2	053.8	.0322
-00.4	047.8	.0318
-01.0	024.8	.0304
00.3	057.2	.0323
00.6	052.7	.0322
01.1	046.6	.0312
01.7	017.7	.0297
02.3	-002.3	.0280
M = 0.85		
-00.0	074.1	.0325
-00.1	069.2	.0320
-00.4	056.3	.0317
-00.9	027.1	.0300
00.2	071.8	.0326
00.5	069.0	.0324
00.9	062.5	.0316
M = 0.90		
-00.0	088.8	.0316
-00.2	089.5	.0315
-00.4	078.4	.0313
-00.9	068.3	.0299
00.1	090.9	.0319
00.4	086.7	.0314
00.8	079.7	.0308
01.3	052.9	.0296
01.8	031.1	.0279

α	$C_{m_q}+C_{m_{\dot{\alpha}}}$	k
M = 1.00		
Flow attached		
-00.1	-010.4	.0195
-00.8	-009.6	.0195
-01.9	-009.9	.0194
00.7	-010.5	.0195
01.6	-009.6	.0195
Flow separated		
-00.1	038.1	.0291
-00.3	038.9	.0291
-00.5	029.6	.0284
-01.3	-001.2	.0270
00.0	036.4	.0289
00.2	027.0	.0287
00.7	-001.2	.0269
M = 1.10		
Flow attached		
-00.1	-006.7	.0184
-01.0	-002.9	.0185
-01.8	-001.2	.0185
00.8	-003.5	.0185
01.6	-003.6	.0185
Flow separated		
00.0	041.4	.0275
M = 1.20		
-00.0	-009.2	.0170
-00.9	-010.3	.0169
-02.7	-013.7	.0165
00.8	-011.7	.0169
02.6	-014.2	.0165
M = 1.30		
-00.0	-011.7	.0156
-01.0	-012.4	.0156
-02.8	-013.3	.0154
00.8	-012.1	.0156
02.7	-014.7	.0154
05.4	-016.1	.0152
08.3	-018.7	.0151
M = 1.60		
-00.1	-013.4	.0133
-01.1	-013.9	.0133
-03.0	-014.6	.0133
00.8	-012.8	.0133
02.7	-015.6	.0132
05.5	-013.9	.0133
08.3	-015.0	.0136
11.0	-011.9	.0140
13.6	-012.0	.0143
15.9	033.7	.0149
M = 2.20		
00.0	-014.1	.0112
-00.9	-011.7	.0112
-02.9	-012.7	.0112
01.0	-009.8	.0112
02.8	-014.0	.0112
05.7	-010.3	.0113
08.4	-009.5	.0115
11.2	-009.7	.0117
13.8	-009.0	.0119
16.3	-007.1	.0120

$\delta = \pm 2^{\circ}$

α	$C_{m_q}+C_{m_{\dot{\alpha}}}$	k
M = 0.65		
00.0	015.1	.0340
-00.3	012.4	.0336
-00.6	009.7	.0333
-01.4	000.0	.0322
00.4	015.8	.0338
00.7	012.8	.0335
01.4	007.4	.0330
02.2	-002.5	.0320
03.2	-009.9	.0310
04.9	-015.1	.0297
M = 0.70		
00.0	016.1	.0322
-00.2	013.1	.0319
-00.6	009.9	.0315
-01.3	-000.2	.0305
00.4	014.2	.0321
00.6	013.5	.0320
01.3	009.8	.0314
M = 0.75		
-00.3	019.4	.0313
-00.2	017.5	.0311
-00.6	013.7	.0306
00.4	019.2	.0314
00.6	018.4	.0312
01.2	012.0	.0306
M = 0.80		
00.0	030.0	.0316
-00.2	029.7	.0312
-00.4	025.5	.0310
00.3	032.4	.0316
00.6	028.4	.0313
01.1	021.5	.0307
01.7	007.0	.0295
M = 0.85		
00.0	046.8	.0315
-00.2	045.0	.0314
-00.4	029.6	.0308
00.3	041.0	.0313
00.5	040.7	.0311
00.9	039.7	.0308
M = 0.90		
-00.0	062.6	.0308
-00.2	057.7	.0307
-00.4	055.6	.0304
00.2	061.8	.0306
00.4	062.4	.0306
00.8	056.0	.0300

α	$C_{m_q}+C_{m_{\dot{\alpha}}}$	k
M = 1.00		
Flow attached		
-00.0	-012.4	.0196
-00.8	-012.1	.0196
-01.9	-011.5	.0196
00.7	-012.1	.0196
01.6	-010.4	.0197
Flow separated		
-00.1	-000.0	.0272
-00.3	-000.6	.0272
-00.5	002.4	.0270
00.0	-005.9	.0270
00.2	000.2	.0272
00.7	-014.7	.0261
M = 1.10		
Flow attached		
-00.1	-007.7	.0185
-01.0	-004.5	.0187
-01.8	-003.9	.0186
00.8	-007.6	.0185
01.6	-004.1	.0185
M = 1.20		
-00.0	-011.8	.0170
-00.9	-012.1	.0169
-02.7	-014.9	.0167
00.8	-012.7	.0169
02.5	-017.4	.0166
M = 1.30		
-00.1	-012.3	.0158
-01.0	-012.5	.0157
-02.8	-015.5	.0156
00.8	-013.1	.0158
02.7	-015.3	.0156
05.4	-015.5	.0154
08.3	-015.8	.0154
M = 1.60		
-00.1	-013.9	.0135
-01.2	-014.3	.0134
-03.0	-015.3	.0134
00.8	-013.1	.0134
02.7	-015.4	.0134
05.5	-015.3	.0135
08.3	-014.1	.0137
11.0	-012.4	.0141
M = 2.20		
00.0	-013.1	.0113
-00.9	-012.9	.0113
-02.9	-012.9	.0113
01.0	-014.2	.0113
02.8	-013.8	.0113
05.6	-011.5	.0114
08.4	-011.7	.0116
11.2	-011.1	.0118
13.8	-010.8	.0119

[redacted]

TABLE IV.- DAMPING IN PITCH DATA - Continued
(e) Model 322 - Center of moments at 0.359l

$\delta = \pm 1^{\circ}$

α	$C_{m_q}+C_{m_{\dot{\alpha}}}$	k
M = 0.65		
-00.0	040.0	.0272
-00.4	029.0	.0269
-00.8	016.4	.0264
-01.5	000.0	.0252
-02.3	-018.4	.0241
00.2	042.7	.0275
00.5	040.4	.0275
01.1	032.2	.0269
01.8	006.2	.0257
04.3	-019.5	.0235
02.6	-007.5	.0246
07.0	-018.6	.0228
M = 0.70		
-00.1	041.3	.0263
-00.4	040.4	.0259
-00.7	026.5	.0254
-01.4	005.4	.0242
00.1	044.1	.0264
00.5	047.7	.0265
01.1	035.3	.0258
M = 0.75		
-00.1	050.3	.0256
-00.3	045.5	.0255
-00.7	030.2	.0248
-01.3	-001.9	.0234
00.1	057.4	.0261
00.4	054.4	.0259
01.0	046.8	.0255
M = 0.80		
-00.1	080.7	.0266
-00.2	071.9	.0261
-00.5	058.4	.0256
-01.0	005.7	.0240
00.1	079.2	.0268
00.3	082.8	.0268
00.8	050.8	.0260
01.9	-020.8	.0229
M = 0.85		
-00.1	120.7	.0275
-00.2	108.3	.0272
-00.4	090.8	.0265
-00.9	042.9	.0252
00.1	129.4	.0275
00.3	114.5	.0275
00.7	109.7	.0272
M = 0.90		
-00.4	148.7	.0273
-00.4	136.9	.0269
-00.5	123.1	.0264
00.0	151.1	.0272
00.2	136.8	.0274
00.6	135.3	.0268
01.0	102.8	.0257
M = 1.00		
Flow separated		
-00.2	076.2	.0250
-00.0	081.5	.0249
00.1	069.7	.0249
00.4	051.5	.0242
-00.7	074.0	.0247
-00.6	060.3	.0242
-01.0	004.8	.0226
M = 1.10		
Flow separated		
-00.1	075.6	.0234
-00.2	070.7	.0229
-00.3	058.8	.0225
00.0	086.2	.0235
00.4	086.8	.0237
00.5	081.5	.0233
M = 1.30		
04.6	-025.6	.0124
07.3	-025.9	.0123
M = 1.60		
07.5	-024.8	.0109
10.0	-023.4	.0112
M = 2.20		
09.2	-012.0	.0092
12.8	-010.1	.0094

$\delta = \pm 2^{\circ}$

α	$C_{m_q}+C_{m_{\dot{\alpha}}}$	k
M = 0.65		
-00.0	014.3	.0265
-00.4	015.0	.0264
-00.8	009.6	.0261
-01.5	000.7	.0252
00.2	017.5	.0267
00.5	018.4	.0266
01.1	008.5	.0263
01.8	-001.4	.0256
02.6	-011.0	.0249
M = 0.70		
-00.1	019.3	.0256
-00.4	017.8	.0253
-00.7	012.3	.0250
-01.4	006.5	.0243
00.1	018.4	.0256
00.4	018.4	.0255
01.1	013.5	.0251
M = 0.75		
-00.1	020.7	.0248
-00.3	016.4	.0247
-00.7	013.7	.0242
00.1	023.3	.0251
00.4	020.9	.0252
01.0	016.7	.0247
M = 0.80		
-00.0	028.3	.0253
-00.2	024.0	.0249
-00.5	017.4	.0245
00.3	026.0	.0253
00.1	026.2	.0252
00.8	019.0	.0250
M = 0.85		
-00.1	053.1	.0257
-00.3	050.5	.0257
-00.4	041.8	.0252
00.0	055.9	.0260
00.3	053.7	.0258
00.7	043.1	.0256
M = 0.90		
-00.4	080.5	.0258
-00.4	080.8	.0256
00.0	082.8	.0259
00.2	082.5	.0258
M = 1.00		
Flow attached		
-00.4	-019.8	.0159
Flow separated		
-00.3	011.7	.0230
-00.0	010.7	.0233
00.1	009.9	.0231
-00.7	012.9	.0230
-00.6	006.2	.0226
M = 1.10		
Flow attached		
-00.4	-005.6	.0151
Flow separated		
-00.1	024.7	.0218
-00.2	017.3	.0215
00.0	037.7	.0223
00.4	038.6	.0223
M = 1.20		
-00.3	-021.7	.0137
-01.2	-022.5	.0136
-02.8	-026.1	.0134
00.4	-023.2	.0136
02.0	-025.7	.0135
M = 1.30		
-00.5	-024.4	.0127
-01.2	-025.5	.0126
-02.9	-028.3	.0125
00.4	-026.3	.0127
02.0	-026.9	.0126
M = 1.60		
-00.4	-025.1	.0107
-01.4	-027.7	.0108
-03.2	-026.4	.0108
00.4	-027.3	.0108
02.1	-027.4	.0108
04.8	-032.5	.0108
M = 2.20		
-00.3	-019.7	.0089
-01.3	-016.0	.0089
-03.1	-018.8	.0089
00.5	-018.1	.0088
02.4	-019.8	.0089
05.1	-021.3	.0089
07.8	-022.7	.0091

[redacted]

TABLE IV.- DAMPING IN PITCH DATA - Continued
(f) Model 323 - Center of moments at 0.332l

$\delta = \pm 1^{\circ}$

α	$C_{m_q}+C_{m_{\dot{\alpha}}}$	k
M = 0.65		
-00.4	023.6	.0209
-00.7	008.2	.0203
-01.0	-013.7	.0199
-01.8	-027.6	.0189
-02.6	-032.0	.0184
-00.1	031.9	.0213
00.1	039.9	.0215
00.7	040.8	.0214
M = 0.70		
-00.4	026.9	.0201
-00.6	010.4	.0197
-01.0	-002.4	.0193
-01.6	-031.0	.0182
-00.0	043.4	.0206
00.1	044.1	.0207
00.7	041.7	.0207
M = 0.75		
-00.4	040.5	.0200
-00.6	021.8	.0196
-01.3	007.0	.0191
-01.5	-028.4	.0179
-00.0	051.8	.0205
00.1	062.5	.0206
00.6	052.7	.0205
M = 0.80		
-00.2	080.3	.0210
-00.4	062.6	.0206
-00.7	020.5	.0199
-01.1	-015.5	.0187
-00.0	097.8	.0216
00.1	086.6	.0217
00.5	079.0	.0214
M = 0.85		
-00.2	119.8	.0218
-00.5	098.7	.0215
-00.6	090.1	.0210
-00.9	040.7	.0197
-00.0	138.3	.0221
00.0	136.8	.0222
00.4	150.5	.0223

α	$C_{m_q}+C_{m_{\dot{\alpha}}}$	k
M = 0.90		
-00.3	166.3	.0219
-00.5	159.6	.0217
-00.6	137.3	.0214
-00.9	098.4	.0204
-00.0	168.6	.0221
00.0	179.8	.0222
00.3	160.3	.0222
M = 1.00		
Flow separated		
-00.4	107.8	.0204
-00.5	106.8	.0202
-00.6	099.7	.0199
-01.0	067.0	.0190
-00.2	100.6	.0207
-00.1	113.7	.0204
00.1	104.3	.0206
M = 1.10		
Flow separated		
-00.2	094.3	.0190
-00.3	091.8	.0187
-00.5	072.3	.0180
-00.7	049.9	.0174
-00.1	113.2	.0191
-00.0	108.5	.0192
00.2	116.1	.0194
M = 1.20		
01.4	-047.5	.0107
M = 1.30		
01.4	-051.0	.0100
03.8	-047.0	.0099
M = 1.60		
01.5	-039.7	.0084
04.2	-040.5	.0084
M = 2.20		
04.3	-029.9	.0069
06.8	-033.7	.0070

$\delta = \pm 2^{\circ}$

α	$C_{m_q}+C_{m_{\dot{\alpha}}}$	k
M = 0.65		
-00.4	003.8	.0204
-00.7	-002.9	.0202
-01.0	-011.7	.0199
-01.8	-024.7	.0192
-02.6	-030.1	.0186
-00.1	011.2	.0207
00.1	009.8	.0208
00.7	008.5	.0207
M = 0.70		
-00.4	005.6	.0196
-00.6	001.1	.0194
-01.0	-001.8	.0192
-01.6	-018.7	.0184
-00.0	007.2	.0199
00.1	011.6	.0200
00.7	005.6	.0199
M = 0.75		
-00.4	011.6	.0194
-00.6	-000.4	.0191
-01.2	-003.3	.0188
-01.5	-017.5	.0180
-00.0	015.4	.0196
00.1	016.7	.0197
00.6	015.8	.0197
M = 0.80		
-00.2	022.4	.0200
-00.4	016.6	.0196
-00.7	009.8	.0194
-00.0	028.7	.0202
00.1	035.4	.0204
M = 0.85		
-00.2	060.7	.0207
-00.5	052.2	.0204
-00.5	040.6	.0199
-00.0	058.6	.0207
00.0	071.3	.0208
M = 0.90		
-00.2	101.7	.0209
-00.5	092.9	.0208
-00.6	086.9	.0205
-00.0	103.1	.0210
00.0	108.3	.0210

α	$C_{m_q}+C_{m_{\dot{\alpha}}}$	k
M = 1.00		
Flow separated		
-00.3	051.6	.0191
-00.5	052.2	.0192
-00.6	045.8	.0186
-00.2	051.4	.0193
-00.1	051.3	.0193
M = 1.10		
Flow separated		
-00.2	044.3	.0176
-00.3	033.9	.0175
-00.5	028.9	.0173
-00.1	065.3	.0180
00.0	061.2	.0181
M = 1.20		
-00.7	-031.0	.0109
-01.4	-031.6	.0108
-02.9	-032.9	.0107
-00.0	-031.5	.0109
M = 1.30		
-00.8	-031.7	.0101
-01.7	-035.4	.0100
-03.1	-034.1	.0099
-00.0	-032.4	.0101
M = 1.60		
-00.9	-032.8	.0085
-01.8	-031.2	.0085
-03.4	-032.5	.0085
-00.1	-030.1	.0085
M = 2.20		
-00.8	-021.8	.0069
-01.8	-022.4	.0069
-03.5	-024.8	.0069
-00.0	-027.1	.0069
01.6	-026.9	.0069

[redacted]

TABLE IV.- DAMPING IN PITCH DATA - Continued
(g) Model 511 - Center of moments at 0.396l

$\delta = \pm 1^{\circ}$

α	$C_{m_q}+C_{m_{\dot{\alpha}}}$	k
M = 0.65		
-00.3	22.81	.0328
-00.7	19.64	.0325
-01.1	15.52	.0322
-01.8	07.52	.0314
00.0	21.17	.0328
00.4	18.24	.0324
01.2	08.25	.0316
02.9	-00.14	.0304
04.7	-06.66	.0293
07.6	-13.41	.0285
M = 0.70		
-00.3	20.64	.0305
-00.7	19.10	.0303
-01.1	16.07	.0302
00.0	21.52	.0305
00.4	19.16	.0305
M = 0.75		
-00.3	18.63	.0292
-00.7	15.09	.0291
-01.1	17.64	.0290
00.0	18.12	.0292
00.4	18.09	.0292
M = 0.80		
-00.3	23.56	.0293
-00.6	23.56	.0293
-00.9	21.61	.0292
-01.6	07.04	.0281
00.0	22.45	.0297
00.3	24.42	.0294
00.9	13.66	.0287
02.4	-12.41	.0262
04.1	-12.18	.0251
06.8	-11.14	.0244

α	$C_{m_q}+C_{m_{\dot{\alpha}}}$	k
M = 0.85		
-00.3	35.14	.0307
-00.5	16.40	.0303
-00.8	-09.19	.0293
-00.0	35.23	.0313
00.1	36.24	.0311
M = 0.88		
-00.3	42.57	.0302
-00.1	44.30	.0307
00.1	33.81	.0303
-00.6	33.06	.0304
-00.8	08.29	.0291
-01.3	-23.70	.0278
00.6	06.63	.0288
M = 0.90		
-00.2	56.82	.0310
-01.2	-04.96	.0278
-00.8	33.79	.0298
00.0	45.47	.0301
00.5	08.83	.0281
M = 0.94		
-00.1	55.44	.0302
-00.6	53.61	.0301
-00.8	49.77	.0296
-01.2	25.55	.0279
-00.0	55.46	.0302
00.1	51.59	.0298
00.5	00.22	.0277
M = 0.96		
-00.4	-16.53	.0206
-00.4	-09.96	.0206
M = 1.00		
-00.4	-10.14	.0199
-00.8	-10.03	.0199
-01.3	-10.12	.0198
00.0	-10.00	.0198
00.5	-10.08	.0198

$\delta = \pm 2^{\circ}$

α	$C_{m_q}+C_{m_{\dot{\alpha}}}$	k
M = 0.65		
-00.5	01.65	.0318
-01.2	04.49	.0315
-02.0	-04.93	.0310
-02.9	-07.43	.0303
-00.4	02.02	.0318
00.2	05.59	.0317
01.0	05.96	.0313
01.9	02.19	.0308
02.8	-00.34	.0300
03.7	-05.99	.0294
04.6	-08.41	.0290
07.5	-12.71	.0285
M = 0.70		
-00.3	12.17	.0304
-00.7	10.71	.0302
-01.1	10.14	.0301
00.0	12.63	.0302
00.4	11.66	.0302
M = 0.75		
-00.3	12.75	.0291
-00.7	11.66	.0291
-01.1	10.51	.0289
00.0	12.60	.0290
00.4	12.00	.0290
M = 0.80		
-00.2	15.61	.0290
-00.6	14.55	.0288
-00.9	10.74	.0288
-01.6	03.46	.0281
00.0	11.57	.0290
00.3	13.00	.0290
00.9	06.27	.0283
M = 0.85		
-00.3	-15.61	.0291
-00.5	-15.67	.0287
-00.8	-20.55	.0284
-00.0	-10.82	.0293
00.1	-12.60	.0287
M = 0.88		
-00.3	-09.66	.0291
-00.1	-01.57	.0288
00.1	-02.52	.0286
-00.6	-06.39	.0289
-00.8	-12.11	.0284
M = 0.90		
-00.5	13.27	.0291
-00.9	08.21	.0286
-00.1	03.88	.0283
00.4	-08.08	.0271
-00.6	03.77	.0284
-01.0	-01.47	.0282

α	$C_{m_q}+C_{m_{\dot{\alpha}}}$	k
M = 0.94		
-00.1	07.07	.0283
-00.6	16.52	.0284
-00.8	16.22	.0280
-00.1	05.12	.0282
00.0	01.47	.0281
M = 0.96		
-00.4	-12.70	.0208
-00.4	-12.63	.0207
M = 1.00		
-00.5	-14.10	.0194
-01.4	-14.17	.0194
00.3	-14.43	.0193
01.2	-13.79	.0193
M = 1.10		
-00.3	-12.40	.0181
-01.2	-07.29	.0183
00.6	-08.94	.0182
01.2	-10.05	.0181
M = 1.20		
-00.3	-09.66	.0170
-00.9	-10.37	.0169
-01.3	-10.98	.0169
00.0	-09.01	.0169
00.5	-08.88	.0169
M = 1.30		
-00.4	-09.08	.0160
-00.9	-09.73	.0160
-01.3	-10.29	.0160
-02.2	-12.88	.0159
00.1	-09.27	.0160
00.5	-09.30	.0159
01.4	-10.41	.0159
03.3	-15.49	.0156
05.2	-15.67	.0156
08.1	-14.41	.0157
M = 1.60		
-00.5	-12.10	.0135
-01.5	-12.45	.0135
-03.4	-15.02	.0134
00.3	-11.72	.0135
02.3	-14.76	.0134
05.2	-16.54	.0134
08.1	-13.21	.0138
M = 2.20		
-00.3	-12.39	.0113
-01.3	-11.51	.0113
-03.2	-11.50	.0113
00.5	-11.58	.0112
02.4	-12.08	.0113
05.3	-11.41	.0114
08.1	-10.03	.0115

A-229

[redacted]

TABLE IV.- DAMPING IN PITCH DATA - Continued
(h) Model 511 - Center of moments at 0.465l

α	$C_{m_q}+C_{m_{\dot{\alpha}}}$	k
$\delta = \pm 1^\circ$		
M = 0.65		
-00.1	009.5	.0336
-00.5	010.1	.0335
-01.0	006.5	.0331
-01.8	003.0	.0325
00.2	007.3	.0336
00.6	004.0	.0334
01.4	-006.0	.0321
M = 0.70		
-00.5	012.8	.0312
-00.1	014.9	.0314
-01.0	006.8	.0308
-01.8	002.9	.0303
00.2	011.4	.0315
00.6	007.3	.0312
01.5	-001.4	.0303
M = 0.75		
-00.1	011.0	.0300
-00.6	007.2	.0297
-01.0	004.1	.0294
-01.7	-002.1	.0288
00.2	012.5	.0301
00.6	009.3	.0299
01.4	-002.7	.0291
M = 0.80		
-00.1	017.4	.0293
-00.5	016.0	.0291
-01.0	002.6	.0285
-01.7	-000.9	.0279
00.1	023.7	.0297
00.5	018.4	.0292
01.3	-009.6	.0278
M = 0.85		
-00.1	033.2	.0302
-00.5	026.3	.0299
-00.8	005.5	.0291
-01.5	-017.4	.0272
00.1	027.5	.0300
00.4	013.3	.0286
01.1	-006.5	.0267
M = 0.90		
-00.2	027.6	.0304
-00.5	020.0	.0305
-00.8	010.8	.0299
-01.4	-030.8	.0278
00.0	019.3	.0300
00.3	003.4	.0285
00.9	-021.9	.0268
$\delta = \pm 2^\circ$		
M = 0.65		
-00.3	06.75	.0332
-01.1	07.36	.0330
-01.9	01.47	.0323
-02.8	-06.22	.0314
00.4	05.13	.0330
01.3	03.33	.0324
02.2	00.51	.0316
03.1	-05.69	.0309
05.0	-13.67	.0298
08.1	-13.12	.0293
M = 0.70		
-00.3	04.77	.0311
-00.3	06.17	.0311
M = 0.75		
-00.3	03.72	.0297
-00.1	04.88	.0297
M = 0.80		
-00.3	-01.34	.0294
-00.3	00.04	.0294
M = 0.85		
-00.4	-04.76	.0298
-00.4	-05.33	.0298
M = 0.90		
-00.4	13.65	.0296
-01.0	06.86	.0295
-00.0	07.07	.0289
00.5	-01.31	.0282
M = 1.00		
-00.3	-10.56	.0199
-01.3	-10.79	.0200
00.5	-10.30	.0199
01.6	-10.40	.0200
M = 1.10		
-00.3	-04.97	.0187
-01.3	-05.88	.0186
00.5	-05.18	.0186
01.5	-04.22	.0187
M = 1.20		
-00.3	-05.68	.0174
-00.3	-06.20	.0174
M = 1.30		
-00.3	-06.21	.0162
-00.3	-06.91	.0162
M = 1.60		
-00.4	-09.43	.0140
-01.3	-10.29	.0140
-03.4	-13.41	.0139
00.6	-09.49	.0139
02.6	-12.70	.0138
05.7	-13.20	.0140
08.6	-10.25	.0143
M = 2.20		
-00.1	-09.00	.0118
-01.1	-08.51	.0118
-03.2	-07.96	.0118
00.7	-06.93	.0118
02.7	-08.54	.0118
05.6	-07.96	.0119
08.6	-07.71	.0121

[redacted]

TABLE IV.- DAMPING IN PITCH DATA - Continued
(i) Model 514 - Center of moments at 0.358l

$\delta = \pm 1^\circ$

α	$C_{m_q}+C_{m_{\dot{\alpha}}}$	k
M = 0.65		
-00.4	19.61	.0282
-00.8	19.41	.0280
-01.2	15.21	.0278
-02.0	04.25	.0271
00.0	22.11	.0282
00.3	20.62	.0281
01.1	15.67	.0278
02.8	-00.19	.0268
04.7	-09.42	.0258
07.5	-16.94	.0250
10.5	-15.49	.0251
M = 0.70		
-00.4	16.04	.0263
-00.8	15.55	.0261
-01.2	12.99	.0259
-00.0	17.20	.0261
00.3	17.39	.0261
M = 0.75		
-00.4	14.60	.0251
-00.8	14.01	.0250
-01.2	11.47	.0249
-02.0	01.19	.0245
-00.0	14.64	.0251
00.3	14.75	.0251
01.0	13.68	.0250
M = 0.80		
-00.5	11.78	.0251
-00.8	10.85	.0251
-01.2	04.31	.0247
-01.8	-09.39	.0235
-01.2	04.30	.0247
-00.1	15.65	.0251
00.1	14.58	.0251
00.6	-07.62	.0240
01.5	-17.48	.0230
M = 0.85		
-00.6	15.32	.0256
-00.8	17.57	.0256
-01.1	-00.58	.0245
-00.1	20.49	.0259
-00.0	10.38	.0254
00.5	-24.81	.0236
M = 0.90		
-00.6	26.36	.0261
-00.8	21.55	.0257
-01.1	06.87	.0251
-00.3	31.21	.0259
-00.1	21.50	.0256
00.4	-05.13	.0236

$\delta = \pm 2^\circ$

α	$C_{m_q}+C_{m_{\dot{\alpha}}}$	k
M = 0.65		
-00.4	09.58	.0278
-00.8	08.42	.0277
-01.2	05.81	.0276
-02.0	01.58	.0272
00.0	10.03	.0279
00.3	10.00	.0278
01.1	08.06	.0277
02.8	-01.54	.0267
M = 0.70		
-00.4	07.20	.0262
-00.8	06.71	.0259
-01.2	05.93	.0259
-00.0	08.56	.0260
00.3	08.22	.0259
M = 0.75		
-00.4	05.66	.0250
-00.8	04.89	.0249
-01.2	03.32	.0248
-02.0	-01.29	.0244
-00.0	06.25	.0250
00.3	07.21	.0250
01.0	06.05	.0248
M = 0.80		
-00.5	-06.00	.0246
-00.8	-05.52	.0245
-01.2	-06.68	.0243
-01.8	-07.49	.0239
-01.2	-06.26	.0243
-00.1	-06.99	.0246
00.1	-05.35	.0246
00.6	-06.79	.0242
01.5	-12.01	.0234
M = 0.85		
-00.6	-15.27	.0247
-00.8	-12.39	.0245
-01.1	-13.78	.0243
-00.1	-17.73	.0246
-00.0	-12.39	.0245
00.5	-18.26	.0238
M = 0.90		
-00.6	-15.28	.0247
-00.6	-14.27	.0247
-00.8	-09.75	.0246
-01.1	-09.46	.0243
-00.3	-05.62	.0248
-00.1	-05.24	.0245
00.4	-08.06	.0239
M = 1.00		
-00.7	-22.02	.0167
-01.0	-22.27	.0168
-01.5	-21.50	.0167
-02.4	-21.03	.0169
-00.1	-21.40	.0168
00.2	-22.46	.0167
01.1	-22.68	.0167
M = 1.10		
-00.6	-20.06	.0155
-01.2	-19.97	.0155
-01.6	-19.94	.0155
-02.5	-20.55	.0154
00.1	-19.48	.0155
00.1	-20.07	.0154
01.2	-19.13	.0155
03.4	-20.78	.0154
M = 1.20		
-00.5	-22.32	.0143
-01.0	-22.79	.0142
-01.5	-22.56	.0142
-00.2	-21.57	.0142
00.2	-21.51	.0142
M = 1.30		
-00.6	-23.22	.0133
-01.2	-22.43	.0134
-01.6	-23.66	.0133
-02.4	-24.31	.0133
-00.2	-23.60	.0133
00.2	-22.81	.0133
01.2	-22.76	.0133
03.1	-23.41	.0132
05.1	-23.84	.0133
08.0	-20.71	.0135
M = 1.60		
-00.6	-20.86	.0117
-01.2	-20.55	.0116
-01.7	-20.30	.0116
-00.2	-19.90	.0117
00.2	-20.29	.0117
04.9	-20.47	.0117
10.5	-19.07	.0124
M = 2.20		
-00.5	-06.14	.0098
-01.1	-06.78	.0098
-01.4	-11.40	.0098
-02.3	-10.71	.0098
-00.0	-10.66	.0098
00.3	-12.53	.0098
01.3	-07.99	.0098
03.2	-08.45	.0099
05.1	-06.40	.0099
10.5	-13.78	.0103

[redacted]

TABLE IV.- DAMPING IN PITCH DATA - Continued
(j) Model 531 - Center of moments at 0.358l

$\delta = \pm 1^\circ$

α	$C_{m_q}+C_{m_{\dot{\alpha}}}$	k
M = 0.65		
-00.4	27.42	.0290
-00.8	25.94	.0287
-01.2	19.93	.0284
-02.0	09.75	.0277
-00.0	27.63	.0289
00.3	20.66	.0287
01.1	06.27	.0280
01.9	-00.36	.0275
02.8	-08.53	.0268
04.6	-07.21	.0261
07.4	-10.80	.0253
M = 0.80		
-00.3	52.71	.0260
-00.7	54.11	.0257
-00.7	51.32	.0260
-01.0	23.56	.0252
-01.7	-05.30	.0239
-00.0	33.73	.0260
00.3	34.61	.0256
00.9	18.43	.0249
01.6	-16.24	.0236
02.5	-18.17	.0228
04.1	-14.29	.0225
06.7	-18.90	.0217

α	$C_{m_q}+C_{m_{\dot{\alpha}}}$	k
M = 0.90		
-00.4	25.82	.0265
-00.6	18.27	.0261
-00.9	12.36	.0258
-00.1	30.04	.0264
00.0	05.11	.0256
00.6	-34.84	.0239
01.3	-49.40	.0224
02.0	-43.16	.0219
02.7	-36.74	.0212

$\delta = \pm 2^\circ$

α	$C_{m_q}+C_{m_{\dot{\alpha}}}$	k
M = 0.65		
-00.4	10.14	.0285
-00.8	10.31	.0284
-01.2	09.32	.0283
-00.0	08.87	.0283
00.3	07.80	.0284
01.1	02.91	.0279
01.9	-04.35	.0274
02.8	-09.72	.0270
04.6	-12.47	.0262
07.4	-16.64	.0254
M = 0.80		
-00.3	02.84	.0252
00.0	04.92	.0251
00.2	08.04	.0249
00.9	00.61	.0246
01.6	-04.20	.0241
M = 0.90		
-00.4	-11.30	.0249
-00.6	-10.19	.0250
-00.1	-11.82	.0248
00.0	-11.95	.0247
00.6	-16.34	.0241
M = 1.00		
-00.5	-25.56	.0172
-00.9	-26.50	.0171
-01.4	-26.77	.0172
-02.3	-27.44	.0170
-00.0	-28.03	.0170
00.3	-26.70	.0170
01.3	-27.03	.0170
M = 1.10		
-00.6	-19.92	.0158
-01.0	-20.06	.0158
-01.4	-20.86	.0157
-02.4	-21.18	.0158
-00.1	-19.58	.0158
00.2	-18.96	.0158
01.1	-18.75	.0157

α	$C_{m_q}+C_{m_{\dot{\alpha}}}$	k
M = 1.20		
-00.4	-20.24	.0146
-00.9	-20.91	.0146
-01.3	-21.70	.0146
-00.0	-21.57	.0146
00.3	-22.33	.0146
M = 1.30		
-00.5	-22.56	.0137
-01.0	-22.39	.0137
-01.4	-22.65	.0136
-02.2	-24.02	.0136
-00.0	-21.63	.0137
00.3	-20.43	.0137
01.2	-19.43	.0136
03.0	-23.78	.0135
04.9	-23.28	.0134
07.8	-17.38	.0135
M = 1.60		
-00.6	-20.63	.0117
-01.1	-22.21	.0117
-01.5	-23.08	.0117
-00.1	-20.97	.0117
00.3	-20.78	.0117
05.0	-21.64	.0117
10.4	-13.33	.0124
M = 2.20		
-00.3	-18.71	.0098
-00.9	-17.82	.0098
-01.4	-16.99	.0098
-02.3	-18.49	.0098
00.0	-18.33	.0098
00.5	-17.15	.0098
01.4	-17.81	.0098
03.3	-17.39	.0098
05.1	-18.34	.0099
07.9	-14.12	.0101
10.5	-12.54	.0103

[redacted]

TABLE IV.- DAMPING IN PITCH DATA - Continued
(k) Model 515 - Center of moments at 0.335l

$\delta = \pm 1^{\circ}$

α	$C_{m_q}+C_{m_{\dot{\alpha}}}$	k
M = 0.65		
-00.5	011.7	.0207
-00.8	013.0	.0207
-01.2	011.6	.0204
-02.0	-004.0	.0199
-02.8	-010.1	.0195
-00.0	016.6	.0209
00.3	016.1	.0211
01.0	013.9	.0210
01.8	005.5	.0206
02.5	-001.0	.0202
M = 0.70		
-00.4	014.6	.0195
-00.7	013.1	.0195
-01.2	009.5	.0192
-01.9	003.1	.0189
-00.3	015.4	.0197
00.2	016.1	.0197
01.0	015.4	.0196
M = 0.75		
-00.4	010.6	.0188
-00.8	008.8	.0186
-01.1	007.5	.0185
-01.9	001.4	.0182
-00.0	011.6	.0189
00.2	017.4	.0189
00.9	009.5	.0189
M = 0.80		
-00.3	013.1	.0188
-00.6	005.9	.0185
-01.0	-008.8	.0180
-01.7	-018.6	.0174
-02.4	-012.3	.0170
-00.0	021.3	.0191
00.2	021.8	.0192
00.8	017.1	.0190
01.5	-009.3	.0182
02.2	-031.0	.0174
M = 0.85		
-00.2	-010.0	.0189
-00.5	-024.6	.0183
-00.8	-046.8	.0178
-01.5	-051.1	.0166
00.0	021.3	.0194
00.2	010.3	.0195
00.7	000.3	.0189
M = 0.90		
-00.2	009.2	.0196
-00.4	-014.2	.0189
-00.7	-038.8	.0183
-01.2	-063.7	.0168
-00.0	029.6	.0198
00.1	028.2	.0198
00.6	-002.3	.0192
M = 1.00		
-00.7	-032.2	.0128
-01.5	-026.6	.0128
00.0	-038.9	.0127
M = 1.10		
-00.8	-033.5	.0117
-01.6	-032.7	.0117
-03.3	-025.4	.0116
-00.0	-035.4	.0117
01.5	-038.8	.0116
M = 1.20		
-00.7	-042.0	.0108
-01.5	-036.8	.0107
-03.2	-032.9	.0107
00.1	-037.6	.0108
01.8	-041.1	.0107
M = 1.30		
-00.9	-039.3	.0101
-01.7	-036.4	.0100
-03.4	-036.7	.0101
00.0	-036.3	.0101
01.7	-052.3	.0100
04.4	-042.7	.0101
06.7	-038.3	.0101
M = 1.60		
-00.9	-033.5	.0087
-01.8	-032.8	.0087
-03.5	-037.1	.0087
00.2	-029.9	.0087
01.7	-038.1	.0086
04.4	-041.5	.0087
07.1	-032.1	.0088
M = 2.20		
-00.6	-017.5	.0072
-01.7	-018.9	.0072
-03.1	-014.2	.0072
00.0	-014.3	.0072
02.0	-020.7	.0072
04.6	-029.7	.0072
07.2	-029.1	.0073

$\delta = \pm 2^{\circ}$

α	$C_{m_q}+C_{m_{\dot{\alpha}}}$	k
M = 0.65		
-00.5	008.4	.0207
-00.8	007.1	.0206
-01.2	002.8	.0204
-02.0	-002.2	.0199
-02.8	-009.1	.0196
-00.0	006.8	.0207
00.3	005.6	.0208
01.0	004.5	.0207
01.8	-001.7	.0206
M = 0.70		
-00.4	007.5	.0195
-00.7	004.9	.0194
-01.2	005.2	.0192
-01.9	-003.6	.0189
-00.3	008.4	.0195
00.2	008.1	.0196
01.0	004.6	.0195
M = 0.75		
-00.4	004.6	.0187
-00.8	005.2	.0186
-01.1	006.2	.0185
-01.9	002.4	.0182
-00.0	007.5	.0188
00.2	008.1	.0188
00.9	005.1	.0188
M = 0.80		
-00.3	001.0	.0185
-00.7	-004.2	.0184
-01.0	-004.7	.0181
-01.7	-013.1	.0175
-02.4	-018.9	.0171
-00.0	001.4	.0186
00.2	001.6	.0186
00.8	-003.8	.0185
M = 0.85		
-00.2	-022.0	.0181
-00.5	-023.8	.0180
-00.8	-024.4	.0178
-01.5	-034.5	.0172
00.0	-012.3	.0185
00.2	-018.6	.0186
M = 0.90		
-00.2	-024.8	.0183
-00.4	-031.9	.0181
-00.7	-026.8	.0178
-00.0	-028.0	.0185
00.1	-022.2	.0185
M = 1.00		
-00.7	-028.7	.0128
-01.5	-030.0	.0127
00.0	-030.0	.0128
M = 1.10		
-00.9	-025.1	.0119
-01.6	-026.5	.0117
-03.3	-025.0	.0118
-00.0	-025.5	.0117
M = 1.20		
-00.7	-031.3	.0108
-01.5	-034.3	.0108
-03.1	-032.7	.0108
00.1	-038.9	.0108
01.8	-034.3	.0108
M = 1.30		
-00.9	-032.1	.0101
-01.7	-033.1	.0101
-03.4	-032.2	.0101
00.0	-037.9	.0102
01.7	-033.4	.0101
M = 1.60		
-00.9	-029.0	.0088
-01.8	-031.5	.0087
-03.5	-030.9	.0088
00.2	-033.9	.0087
01.7	-029.2	.0087
M = 2.20		
-00.6	-022.8	.0072
-01.7	-023.2	.0072
-03.1	-024.0	.0073
00.1	-021.0	.0072
01.9	-023.3	.0072
04.6	-023.6	.0073

[redacted]

TABLE IV.- DAMPING IN PITCH DATA - Continued
(1) Model 516 - Center of moments at 0.335l

$\delta = \pm 1^{\circ}$

α	$C_{m_q}+C_{m_{\dot{\alpha}}}$	k
M = 0.65		
-00.3	-007.9	.0228
-00.6	000.8	.0227
-01.1	-009.3	.0225
-01.8	-014.8	.0221
-02.7	-023.4	.0217
00.1	-008.4	.0229
00.5	-008.7	.0229
01.2	-014.2	.0227
02.0	-012.6	.0224
02.8	-017.4	.0221
04.4	-022.0	.0217
07.1	-027.1	.0213
M = 0.70		
-00.3	-008.6	.0215
-00.7	-009.5	.0214
-01.0	-010.1	.0214
-01.8	-012.1	.0210
00.1	000.0	.0216
00.4	004.7	.0216
01.2	-007.7	.0214
M = 0.75		
-00.3	-008.0	.0207
-00.6	003.0	.0207
-01.0	-009.2	.0205
-01.7	-015.9	.0201
00.0	-004.9	.0207
00.3	-000.0	.0207
01.1	-007.5	.0206
M = 0.80		
-00.2	-004.9	.0205
-00.5	-016.3	.0202
-00.9	-019.1	.0198
-01.6	-031.3	.0192
-02.2	-031.7	.0187
00.1	-012.3	.0205
00.4	-008.7	.0206
01.0	-015.0	.0202
01.7	-037.4	.0195
02.4	-021.7	.0192

α	$C_{m_q}+C_{m_{\dot{\alpha}}}$	k
M = 0.85		
-00.2	-009.8	.0209
-00.4	-013.3	.0206
-00.8	-043.4	.0198
-01.7	-056.9	.0186
00.1	-003.3	.0210
00.3	-004.4	.0210
00.9	-034.8	.0200
M = 0.90		
-00.2	005.7	.0216
-00.4	-003.5	.0212
-00.6	-014.0	.0206
-01.1	-057.4	.0189
-01.9	-064.3	.0176
00.0	015.1	.0218
00.2	-004.7	.0214
00.7	-033.4	.0203
01.3	-065.3	.0191
M = 1.00		
04.6	-025.3	.0147
M = 1.10		
04.5	-027.7	.0137
M = 1.30		
04.5	-022.8	.0119
07.1	-034.9	.0118
M = 1.60		
04.6	-028.6	.0102
07.2	-033.2	.0102
09.7	-035.1	.0104
M = 2.20		
07.5	-022.3	.0085
10.0	-018.2	.0086

$\delta = \pm 2^{\circ}$

α	$C_{m_q}+C_{m_{\dot{\alpha}}}$	k
M = 0.65		
-00.3	-010.1	.0227
-00.6	-009.3	.0227
-01.1	-012.8	.0225
-01.8	-015.0	.0222
-02.7	-020.8	.0218
00.1	-013.0	.0227
00.5	-014.6	.0227
01.2	-012.5	.0226
02.0	-012.1	.0224
02.8	-016.2	.0221
M = 0.70		
-00.3	-010.2	.0214
-00.7	-011.4	.0213
-01.0	-013.0	.0212
-01.8	-010.7	.0210
00.1	-008.6	.0214
00.4	-009.5	.0214
01.2	-011.2	.0213
M = 0.75		
-00.3	-008.8	.0204
-00.6	-007.6	.0205
-01.0	-012.7	.0204
-01.7	-013.6	.0201
00.0	-009.3	.0205
00.4	-009.4	.0205
01.1	-010.7	.0204
M = 0.80		
-00.2	-015.3	.0201
-00.5	-014.2	.0200
-00.9	-019.6	.0198
-01.6	-021.3	.0195
00.0	-019.7	.0202
00.4	-016.3	.0202
01.0	-023.3	.0200
M = 0.85		
-00.1	-026.0	.0201
-00.5	-028.6	.0200
-00.7	-030.9	.0197
-01.7	-039.9	.0191
00.1	-027.1	.0201
00.3	-023.9	.0202
00.9	-030.0	.0199

α	$C_{m_q}+C_{m_{\dot{\alpha}}}$	k
M = 0.90		
-00.1	-028.0	.0203
-00.4	-025.0	.0202
-00.6	-029.7	.0199
-01.1	-034.3	.0192
00.0	-025.0	.0204
00.2	-027.8	.0203
M = 1.00		
-00.4	-027.1	.0149
-01.3	-028.2	.0149
-03.0	-027.9	.0148
00.2	-026.9	.0149
01.9	-028.5	.0148
M = 1.10		
-00.5	-026.9	.0137
-01.5	-027.0	.0137
-03.1	-026.0	.0137
00.2	-028.3	.0135
02.0	-026.7	.0137
M = 1.20		
-00.4	-029.9	.0126
-01.2	-030.6	.0127
-02.9	-031.6	.0127
00.4	-030.5	.0127
02.0	-032.5	.0126
M = 1.30		
-00.6	-030.9	.0118
-01.4	-031.5	.0118
-03.0	-033.5	.0118
00.2	-031.5	.0117
02.0	-032.8	.0117
M = 1.60		
-00.6	-029.0	.0101
-01.5	-029.9	.0101
-03.2	-032.5	.0101
00.3	-033.2	.0101
01.9	-028.4	.0101
M = 2.20		
-00.5	-021.4	.0083
-01.5	-022.1	.0083
-03.3	-020.0	.0084
00.3	-022.9	.0083
02.2	-020.8	.0083
04.8	-022.1	.0084

[redacted]

TABLE IV.- DAMPING IN PITCH DATA - Continued
(m) Model 641 - Center of moments at 0.402l

$\delta = \pm 2^{\circ}$

α	$C_{m_q}+C_{m_{\dot{\alpha}}}$	k
M = 0.65		
-00.4	-05.43	.0280
-00.9	-06.04	.0280
-01.4	-05.62	.0280
-02.3	-05.43	.0280
00.0	-05.49	.0280
00.5	-05.63	.0280
01.4	-05.19	.0279
03.4	-05.99	.0279
05.3	-00.66	.0281
08.1	04.20	.0283
M = 0.70		
-00.4	-03.56	.0265
-00.9	-01.89	.0265
-01.3	-02.31	.0265
00.0	-02.34	.0265
00.4	-02.94	.0265
M = 0.75		
-00.4	02.79	.0256
-00.8	05.84	.0256
-01.3	04.70	.0256
-00.0	02.43	.0257
00.4	05.27	.0257

α	$C_{m_q}+C_{m_{\dot{\alpha}}}$	k
M = 0.80		
-00.4	04.39	.0252
-00.8	04.76	.0252
-01.2	04.96	.0252
-02.0	03.87	.0248
-00.0	05.86	.0252
00.3	04.77	.0252
01.1	00.41	.0249
02.8	-06.25	.0241
04.6	-03.19	.0237
07.4	-02.57	.0233
M = 0.85		
-00.4	04.48	.0249
-00.7	02.43	.0248
-01.1	00.54	.0247
-00.0	04.82	.0249
00.1	04.65	.0248
M = 0.90		
-00.5	25.40	.0261
-00.7	26.37	.0260
-01.0	21.30	.0260
-01.5	13.25	.0251
-00.1	30.86	.0260
00.0	32.96	.0256
00.6	24.57	.0250
01.4	19.80	.0240

$\delta = \pm 2^{\circ}$

α	$C_{m_q}+C_{m_{\dot{\alpha}}}$	k
M = 1.00		
-00.4	-16.02	.0183
-01.0	-16.86	.0183
-01.4	-15.81	.0182
-02.4	-16.33	.0182
00.0	-15.35	.0182
00.5	-15.67	.0183
01.5	-15.97	.0181
03.5	-15.69	.0181
M = 1.10		
-00.3	-12.79	.0169
-00.9	-13.07	.0169
-01.3	-13.74	.0169
-02.4	-14.05	.0168
00.1	-13.45	.0169
00.4	-13.22	.0169
01.4	-12.48	.0168
03.5	-14.72	.0166
05.4	-15.51	.0165
M = 1.20		
-00.4	-11.23	.0159
-00.8	-11.09	.0159
-01.4	-11.87	.0158
00.0	-11.20	.0158
00.5	-12.17	.0158

α	$C_{m_q}+C_{m_{\dot{\alpha}}}$	k
M = 1.30		
-00.5	-10.05	.0149
-01.0	-10.40	.0149
-01.4	-12.44	.0149
-02.3	-13.88	.0148
00.1	-09.89	.0149
00.5	-10.76	.0149
01.5	-13.10	.0148
03.5	-19.15	.0145
05.5	-18.84	.0145
08.6	-14.02	.0149
M = 1.60		
-00.5	-12.97	.0129
-00.9	-13.50	.0129
-01.4	-13.22	.0129
00.0	-12.54	.0129
00.5	-13.46	.0129
M = 2.20		
-00.2	-11.27	.0109
-00.8	-10.73	.0109
-01.2	-12.02	.0109
-02.3	-12.47	.0109
00.2	-11.91	.0109
00.6	-12.02	.0109
01.5	-11.42	.0109
03.5	-10.82	.0109
05.4	-10.60	.0110
08.3	-08.58	.0111

TABLE IV.- DAMPING IN PITCH DATA - Concluded
(n) Model 5-8 - Center of moments at 0.358l

$\delta = \pm 1^{\circ}$

M = 0.65

α	$C_{m_q}+C_{m_{\dot{\alpha}}}$	k
-00.7	06.31	.0219
-01.3	01.90	.0217
-01.8	-03.83	.0215
-02.8	-10.79	.0211
-00.3	07.41	.0220
00.0	11.19	.0220
01.0	10.11	.0219
02.9	-01.99	.0213
04.9	-10.70	.0210
07.9	-13.83	.0208

M = 0.80

α	$C_{m_q}+C_{m_{\dot{\alpha}}}$	k
-00.8	00.97	.0187
-01.3	-02.57	.0184
-01.6	-05.62	.0182
-02.5	-12.40	.0179
-00.3	06.75	.0187
00.0	09.20	.0188
00.9	05.31	.0187
02.7	-04.59	.0179
04.6	-10.82	.0175
07.7	-18.00	.0170

M = 0.90

α	$C_{m_q}+C_{m_{\dot{\alpha}}}$	k
-00.9	-15.87	.0153
-01.4	-15.99	.0154
-01.6	-11.10	.0166
-02.5	-02.06	.0161
-00.8	-17.04	.0153
-00.4	-17.05	.0153
00.0	-15.83	.0153
01.0	-15.50	.0153
01.6	07.15	.0164
02.4	-00.65	.0161
04.3	-15.12	.0155
07.3	-20.62	.0153

$\delta = \pm 1^{\circ}$

M = 0.65

α	$C_{m_q}+C_{m_{\dot{\alpha}}}$	k
-00.7	01.29	.0219
-01.3	-01.22	.0217
-01.8	-02.64	.0216
-02.8	-07.83	.0214
-00.3	01.58	.0220
00.0	04.88	.0219
00.9	01.55	.0218
02.9	-03.52	.0214
04.9	-08.38	.0212
07.9	-13.77	.0210

M = 0.80

α	$C_{m_q}+C_{m_{\dot{\alpha}}}$	k
-00.8	-02.42	.0186
-01.3	-04.11	.0185
-01.6	-05.86	.0183
-02.5	-09.93	.0180
-00.3	-02.40	.0186
00.0	-01.90	.0187
00.9	-02.15	.0186
02.7	-07.35	.0180
04.6	-12.20	.0176
07.7	-16.22	.0171

M = 0.90

α	$C_{m_q}+C_{m_{\dot{\alpha}}}$	k
-00.9	-16.19	.0154
-01.4	-05.43	.0170
-01.6	-07.76	.0169
-02.5	-01.93	.0162
-00.8	-16.00	.0154
-00.4	-14.47	.0155
00.0	-15.22	.0154
01.0	-09.64	.0160
01.6	01.76	.0166
02.4	-03.58	.0162

M = 1.00

α	$C_{m_q}+C_{m_{\dot{\alpha}}}$	k
-00.9	-27.27	.0134
-01.6	-30.49	.0134
-02.1	-30.36	.0134
-03.1	-26.56	.0134
-00.4	-33.34	.0134
00.0	-27.38	.0134
01.0	-27.58	.0134
03.1	-25.30	.0134
05.3	-26.15	.0134
08.5	-28.21	.0134

M = 1.10

α	$C_{m_q}+C_{m_{\dot{\alpha}}}$	k
-01.4	-27.42	.0123
-02.4	-24.26	.0123
-04.6	-24.52	.0123
-00.4	-26.66	.0121
02.1	-27.26	.0122
05.1	-30.45	.0122

M = 1.20

α	$C_{m_q}+C_{m_{\dot{\alpha}}}$	k
-01.0	-30.08	.0114
-02.1	-28.90	.0115
-04.2	-31.38	.0115
00.0	-29.44	.0114
02.2	-31.18	.0115
05.4	-27.55	.0116
08.4	-26.20	.0119

M = 1.30

α	$C_{m_q}+C_{m_{\dot{\alpha}}}$	k
-01.1	-26.42	.0109
-02.2	-26.75	.0110
-04.2	-28.30	.0110
-00.1	-26.94	.0108
02.0	-27.04	.0108
05.1	-24.41	.0111
08.0	-22.90	.0114

M = 1.60

α	$C_{m_q}+C_{m_{\dot{\alpha}}}$	k
-01.1	-19.95	.0099
-02.0	-20.18	.0099
-04.0	-20.12	.0100
-00.1	-20.35	.0099
01.8	-21.05	.0099
04.6	-19.28	.0099
07.4	-17.74	.0102
-01.0	-19.92	.0098

M = 2.20

α	$C_{m_q}+C_{m_{\dot{\alpha}}}$	k
-00.9	-13.21	.0084
-01.8	-11.80	.0084
-03.7	-12.54	.0084
00.0	-10.22	.0083
01.9	-11.66	.0084
04.7	-09.90	.0084
07.5	-11.18	.0085

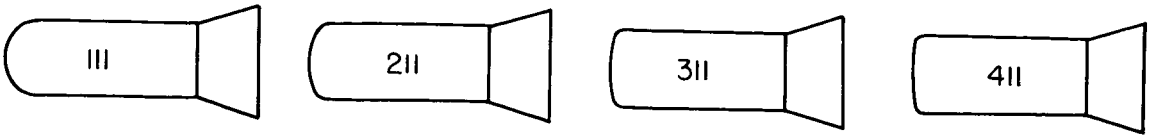

Group 1— Variation of nose shape

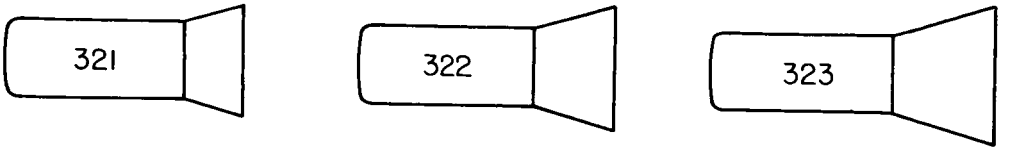

Group 2— Variation of flare base area

Group 3— Variation of flare angle

Group 4 — Variation of cylinder length

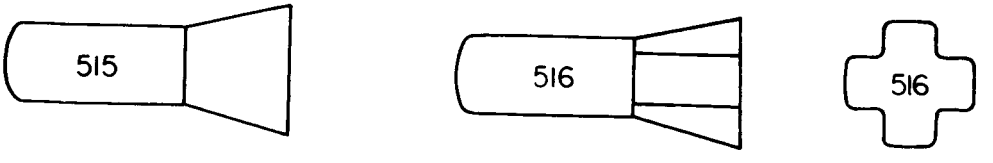

Group 5— Flare relief

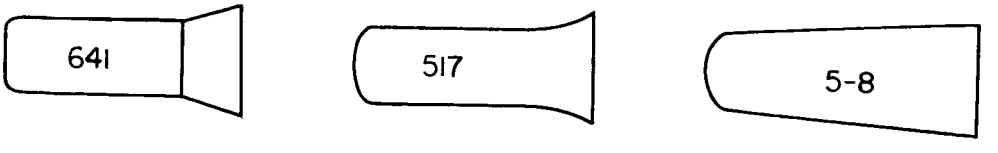

Group 6— Other models

Figure 1.- Sketch of models.

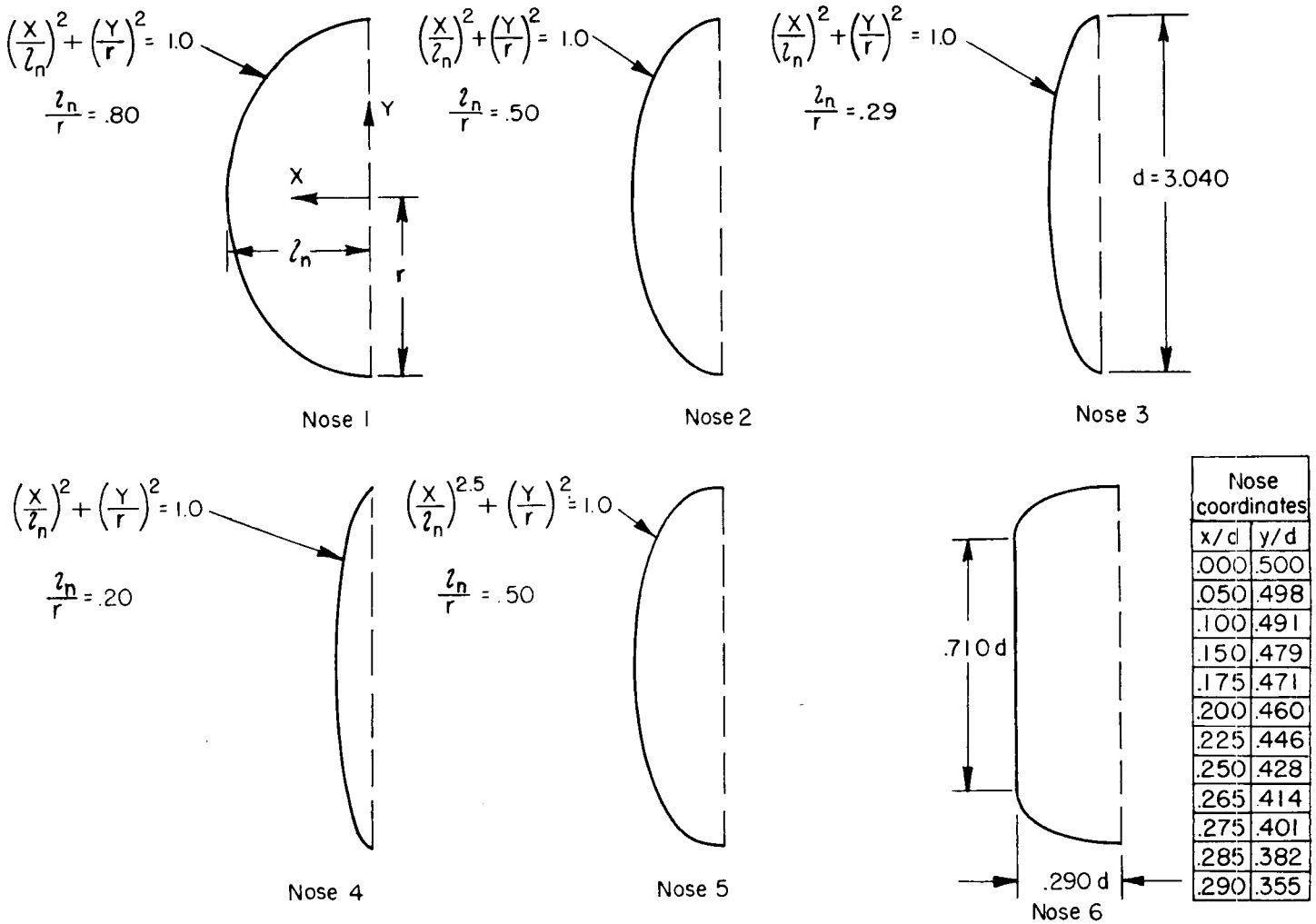

Nose coordinates	
x/d	y/d
.000	.500
.050	.498
.100	.491
.150	.479
.175	.471
.200	.460
.225	.446
.250	.428
.265	.414
.275	.401
.285	.382
.290	.355

(a) Nose shapes.

Figure 2.- Model dimensions.

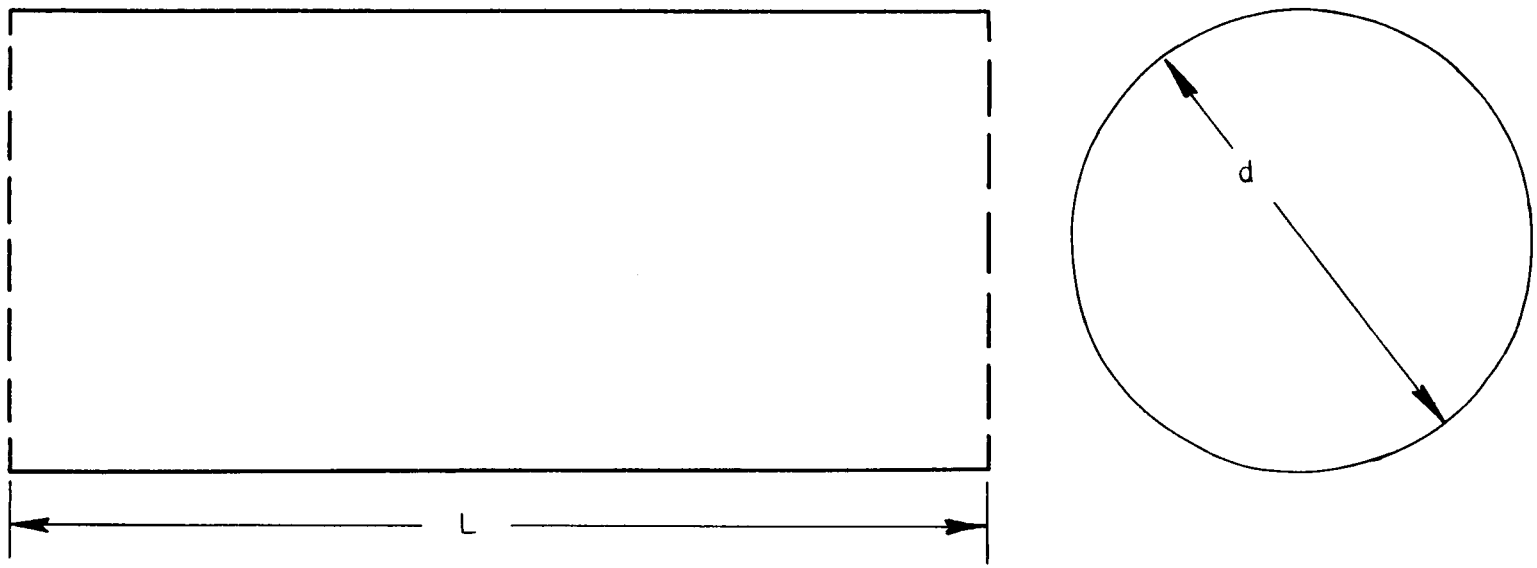

Body	L
1	2.120 d
2	2.199 d
3	2.451 d
4	2.113 d

(b) Cylindrical bodies.

Figure 2.- Continued.

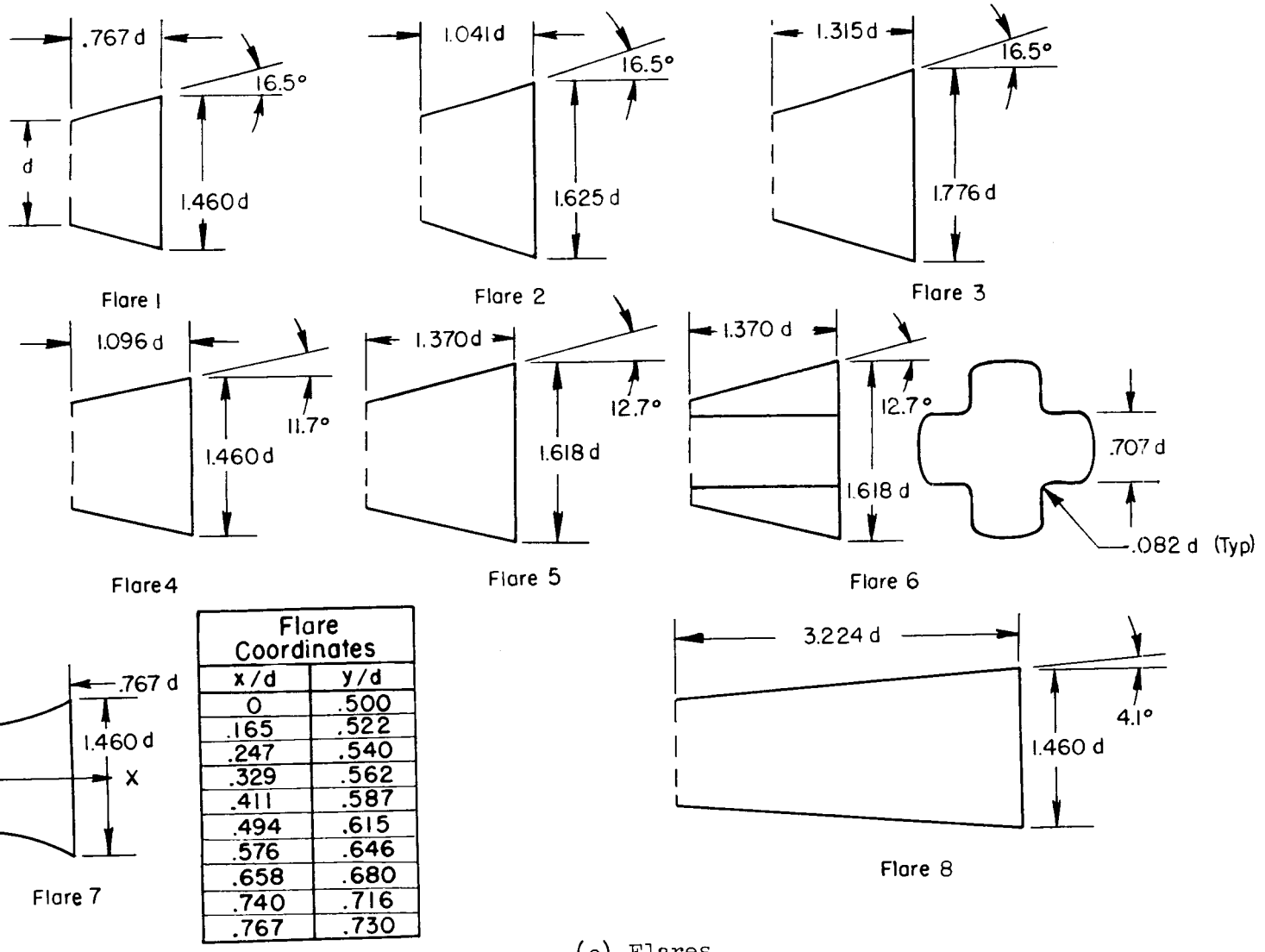

Flare Coordinates	
x/d	y/d
0	.500
.165	.522
.247	.540
.329	.562
.411	.587
.494	.615
.576	.646
.658	.680
.740	.716
.767	.730

(c) Flares.

Figure 2.- Concluded.

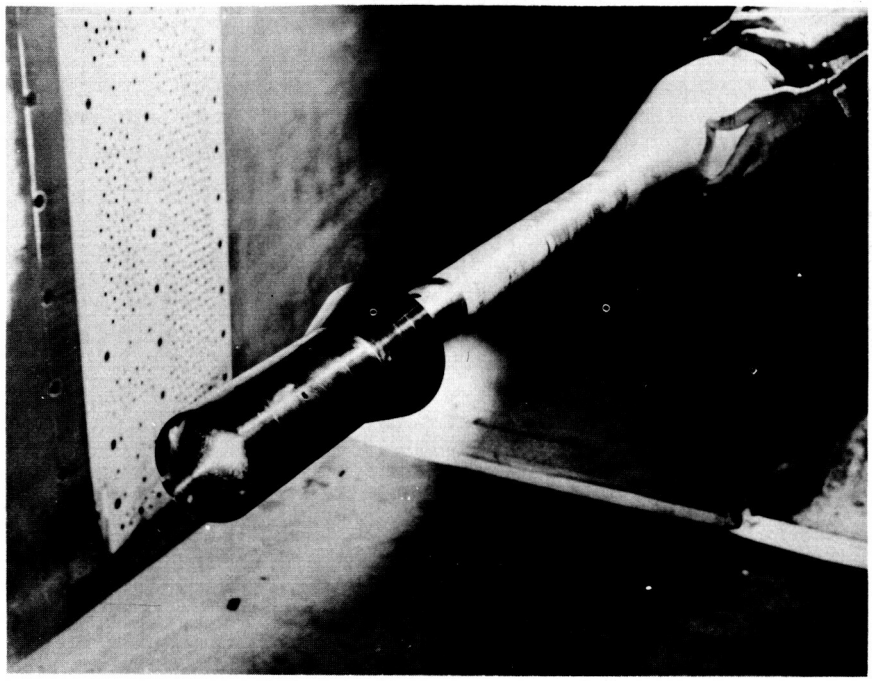

A-24402

Figure 3.- Photograph of model ready for static force tests.

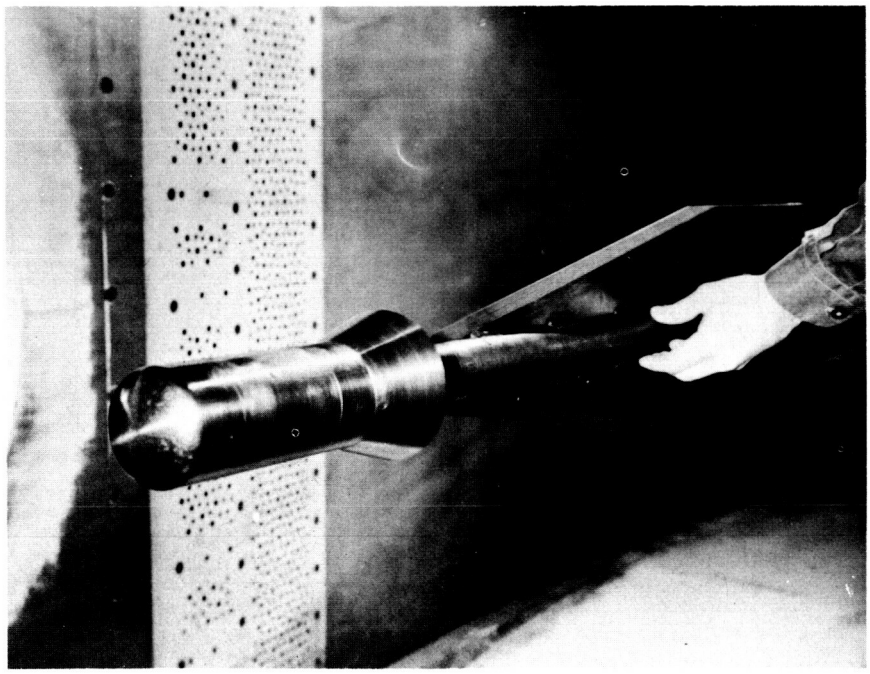

A-24467

Figure 4.- Photograph of model ready for damping-in-pitch tests.

[redacted]

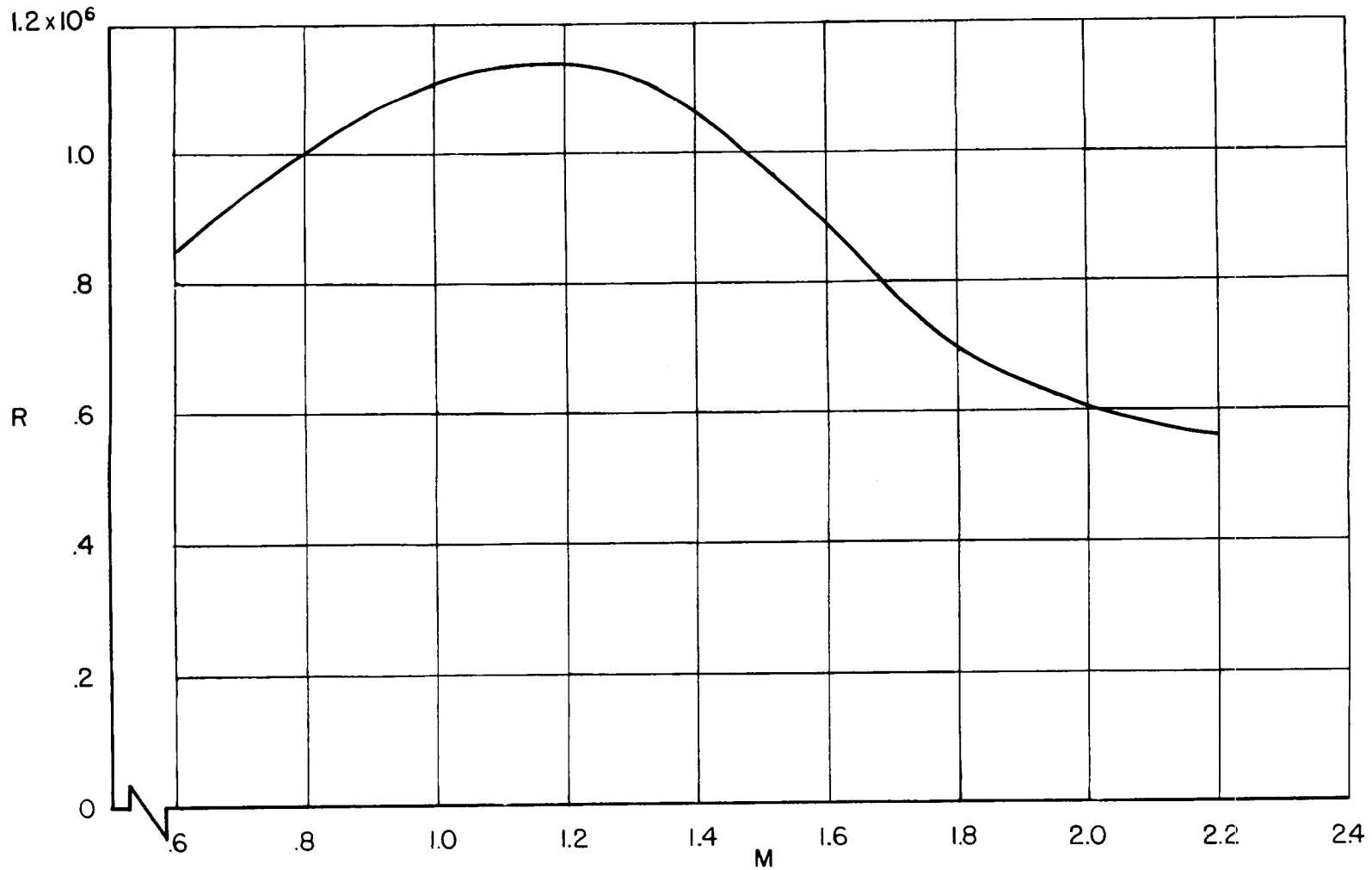

Figure 5.- Variation of Reynolds number with Mach number.

[redacted]

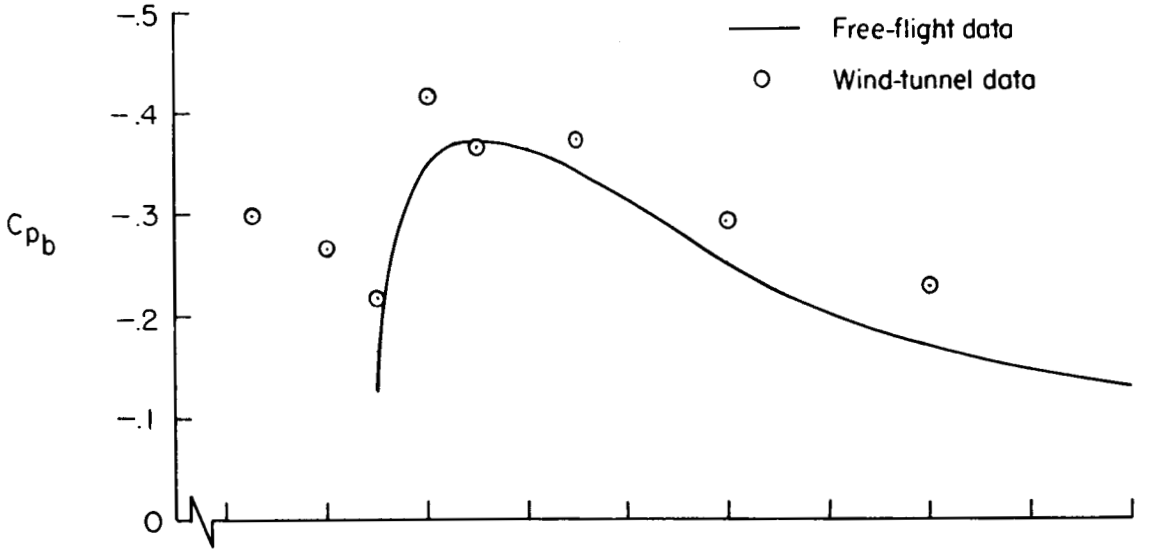

(a) Base-pressure coefficient.

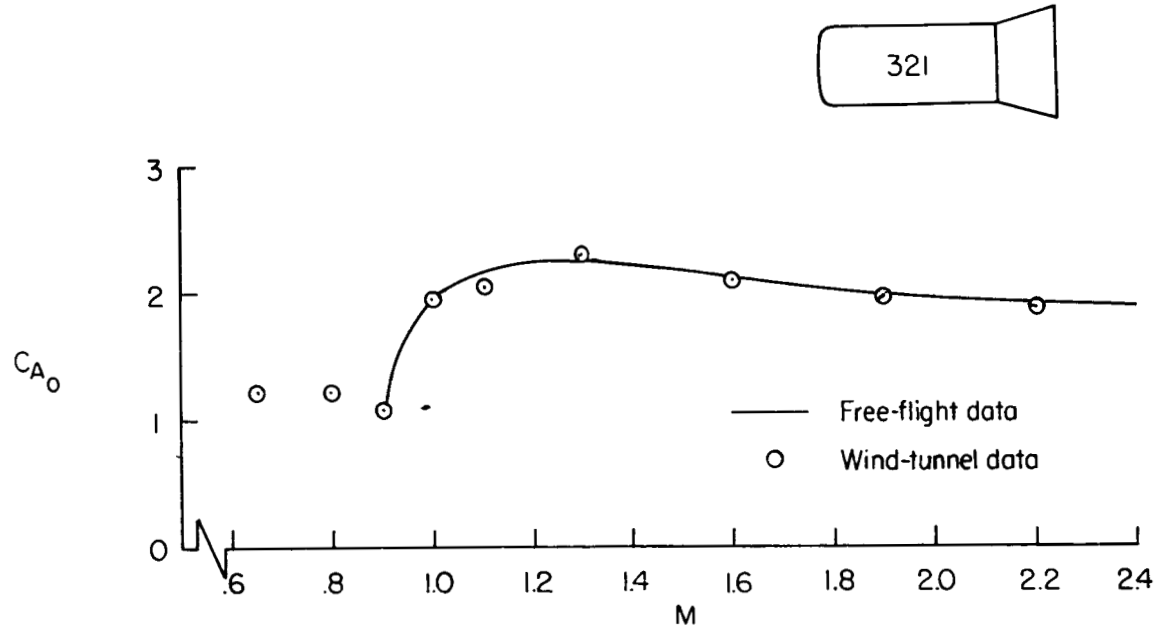

(b) Axial-force coefficient at $\alpha = 0^{\circ}$.

Figure 6.- Comparison of free-flight and wind-tunnel values of base-pressure and axial-force coefficients.

[redacted]

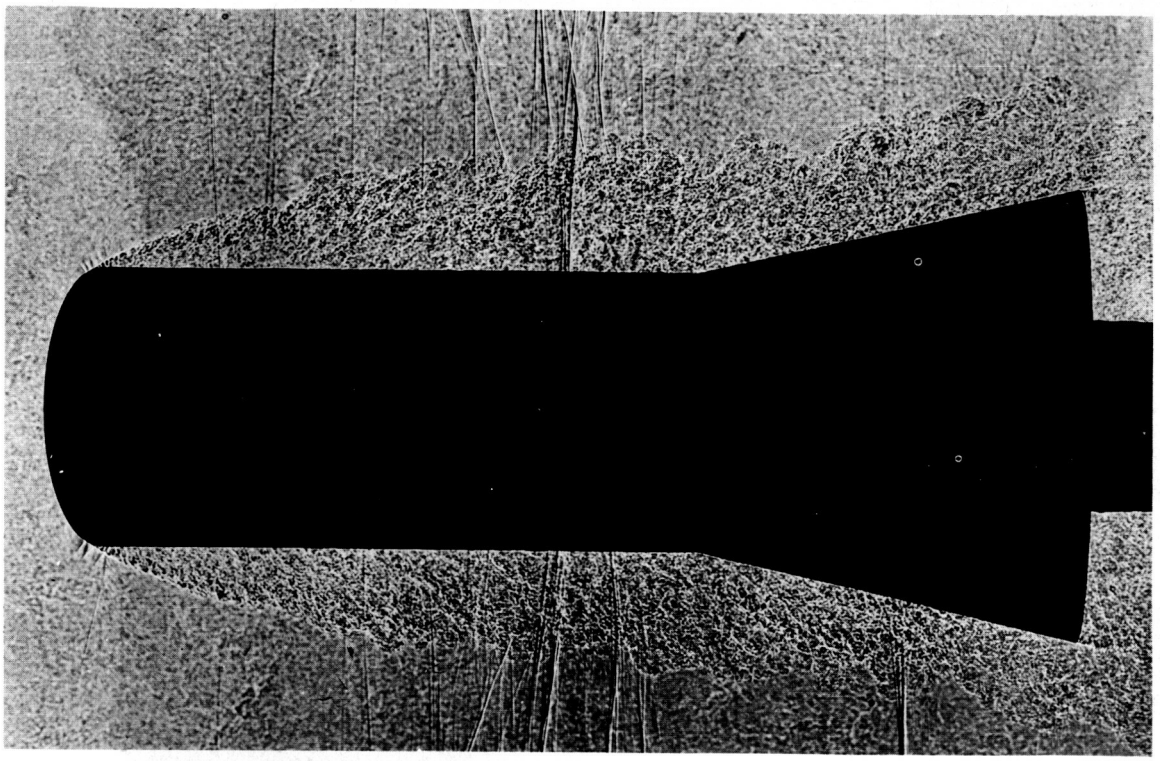

(a) M = 0.90. A-25573

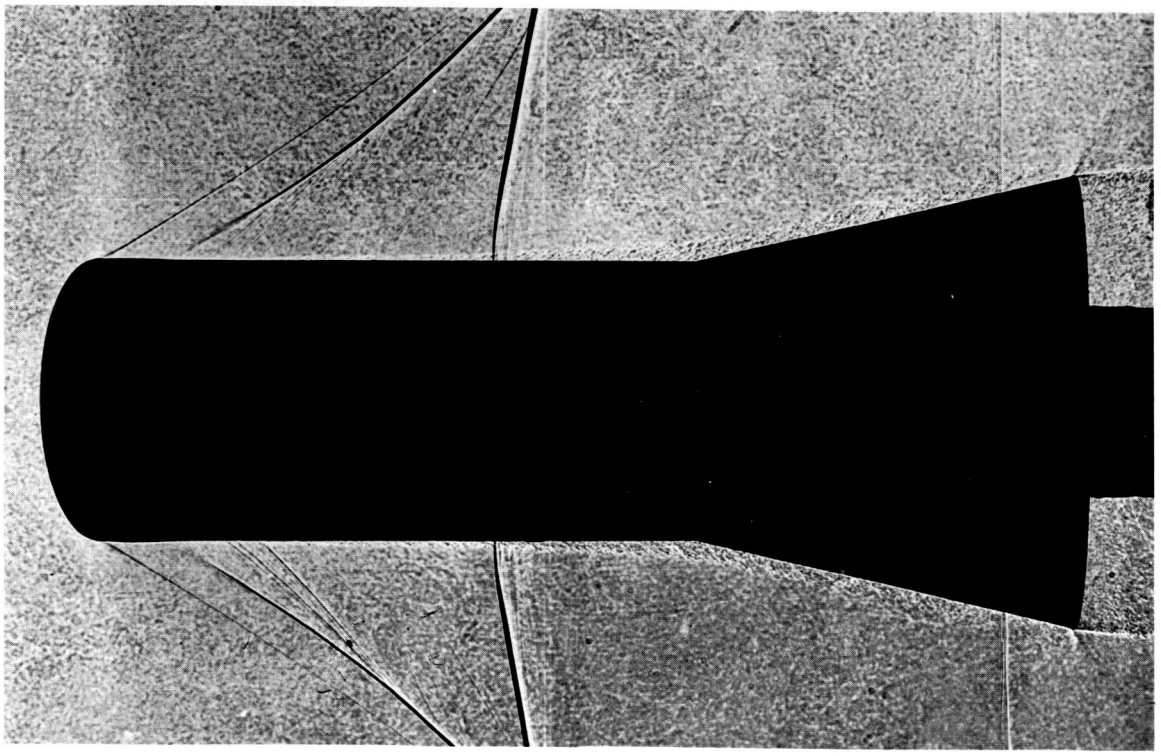

(b) M = 1.00. A-25574

Figure 7.- Photographs of flow around model 515.

[redacted]

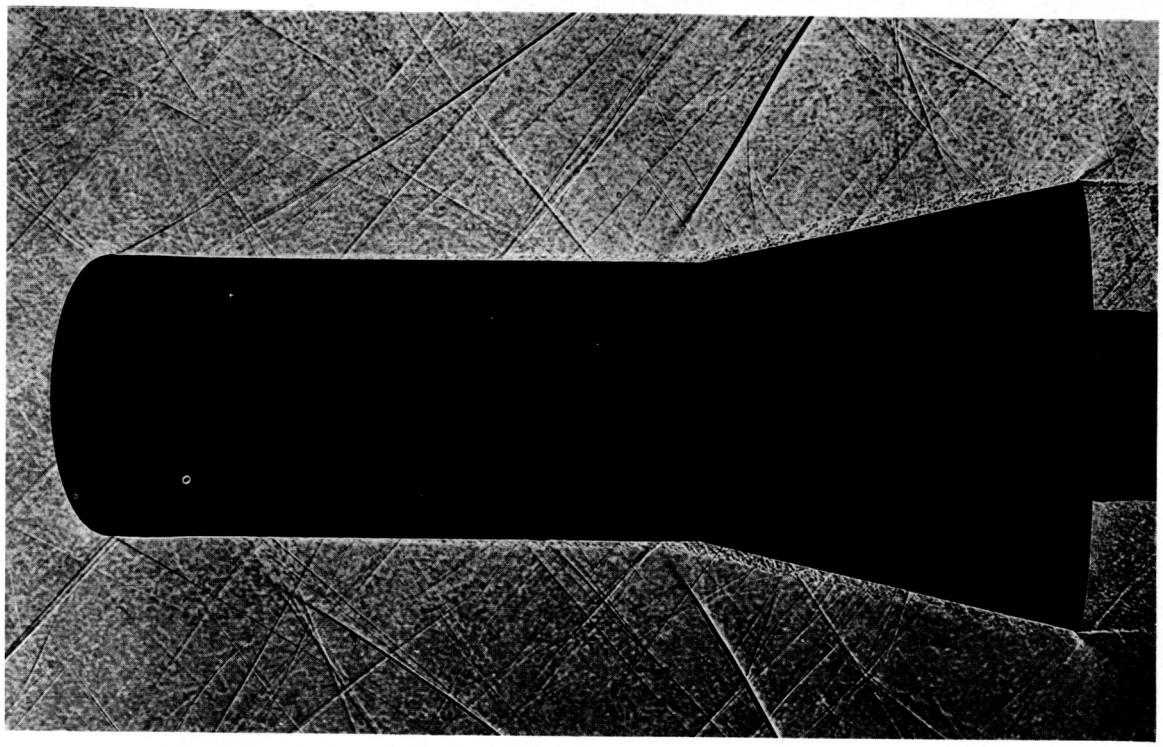

(c) M = 1.30. A-25575

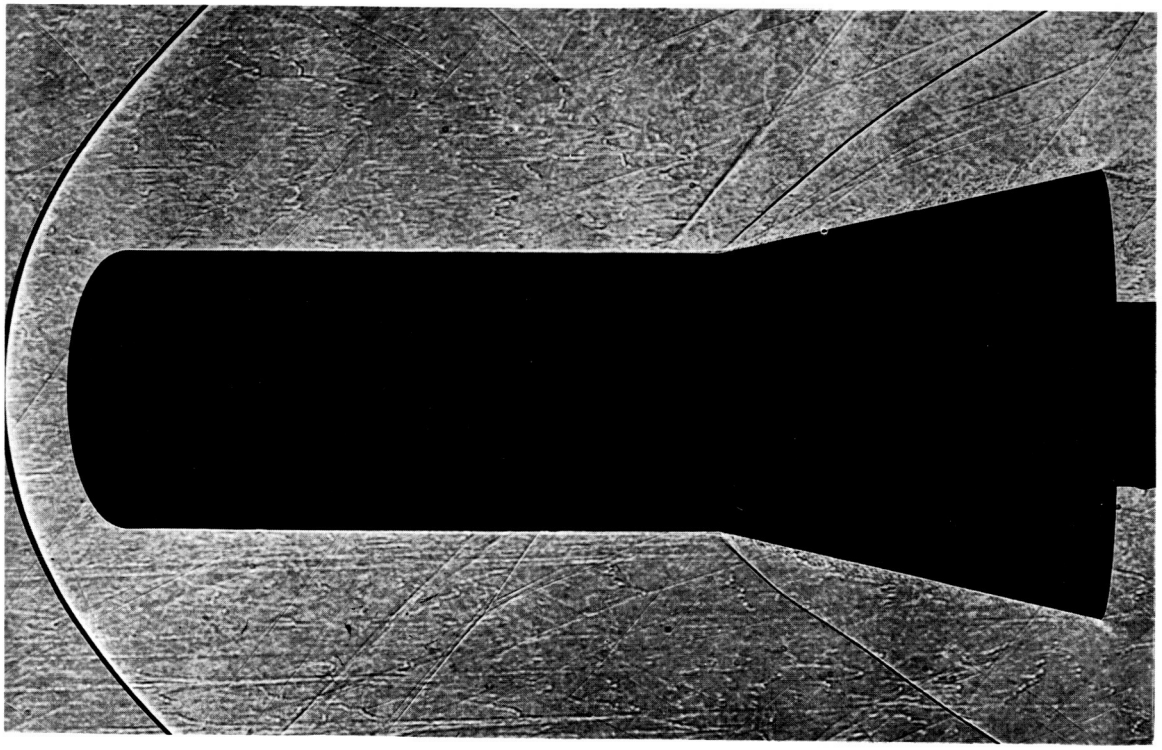

(d) M = 2.20. A-25576

Figure 7.- Concluded.

[redacted]

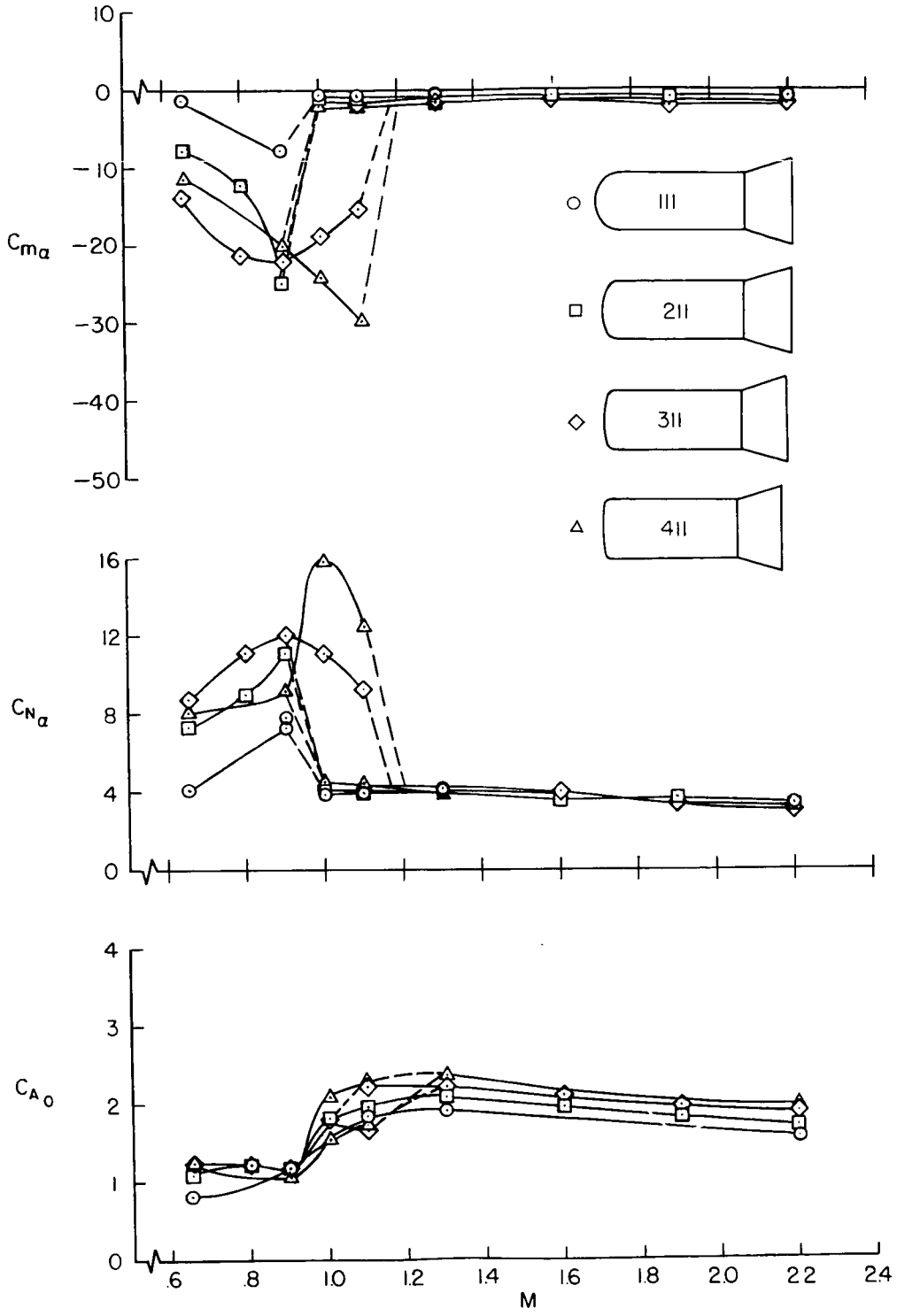

(a) Effect of nose shape.

Figure 8.- Effect of model geometry on the static force characteristics.

[redacted]

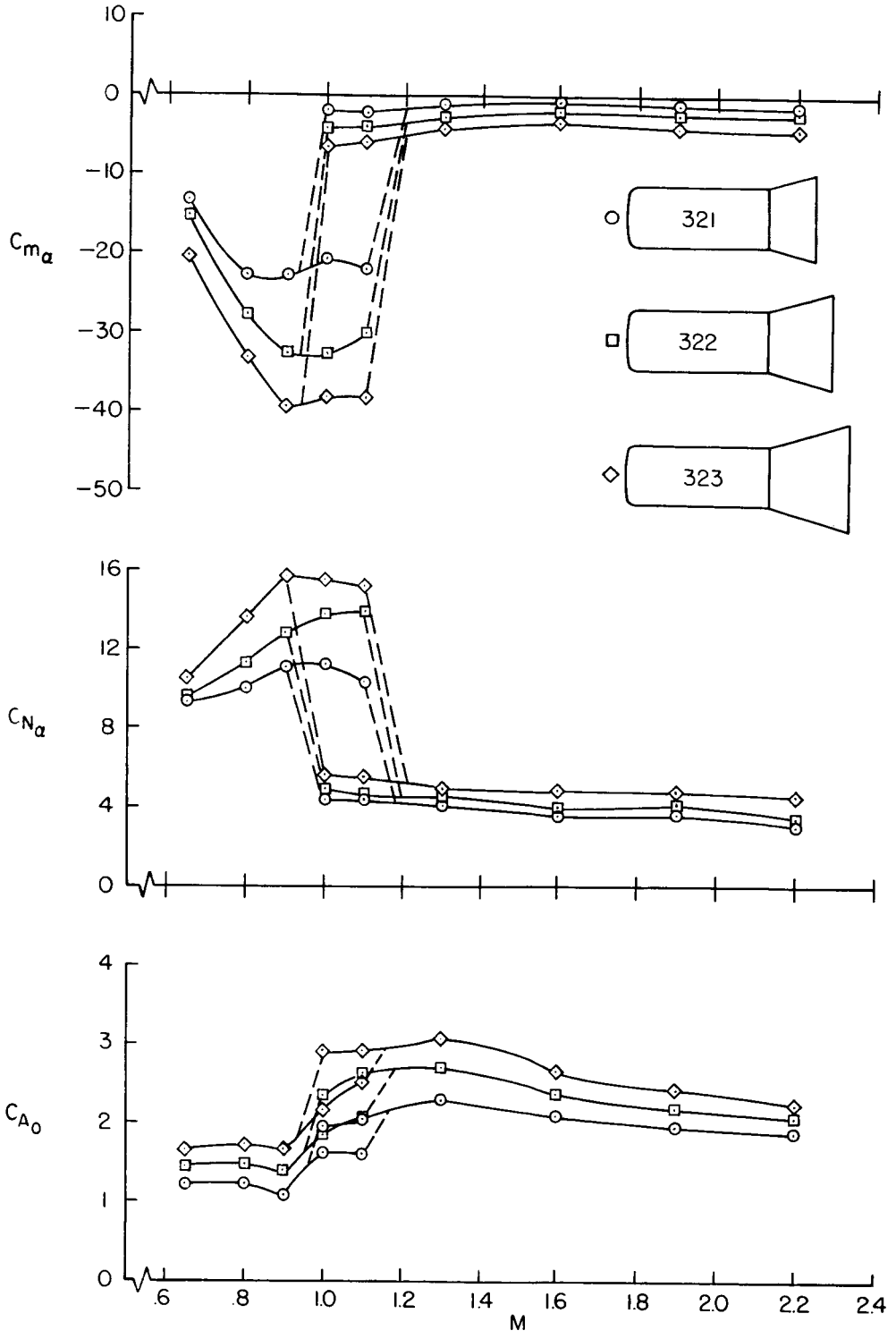

(b) Effect of flare base area.

Figure 8.- Continued.

[redacted]

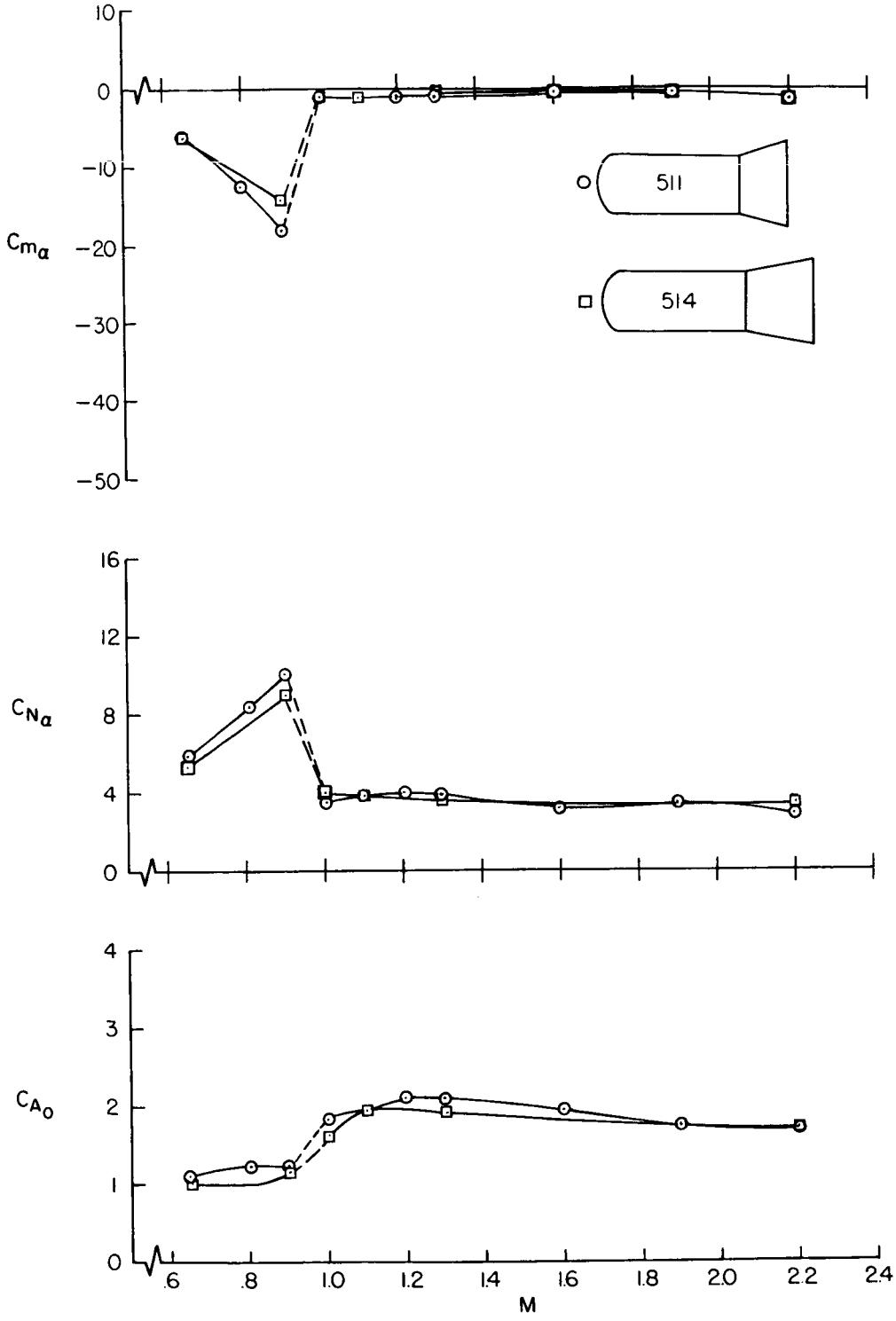

(c) Effect of flare angle.

Figure 8.- Continued.

[redacted]

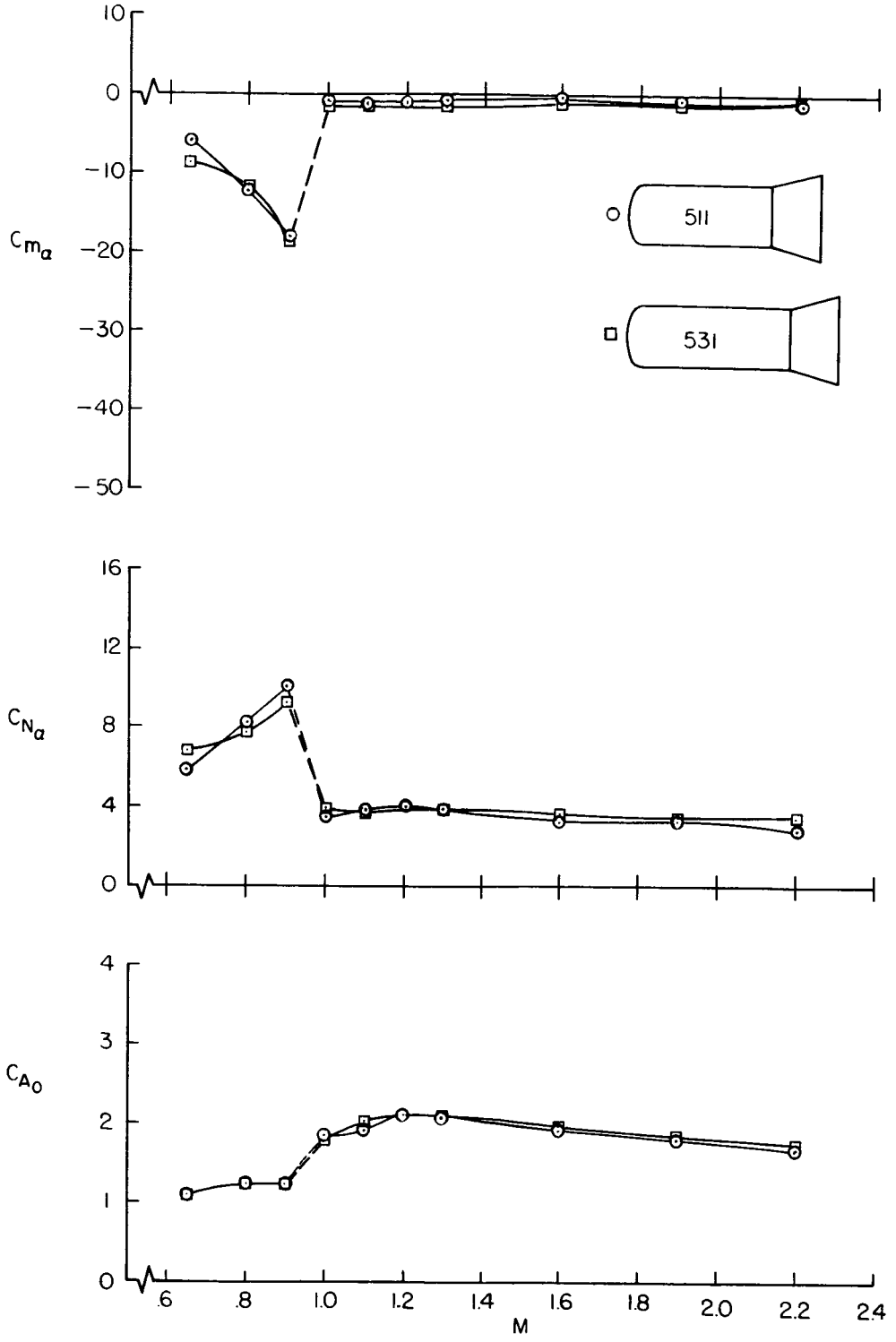

(d) Effect of cylindrical body length.

Figure 8.- Continued.

[redacted]

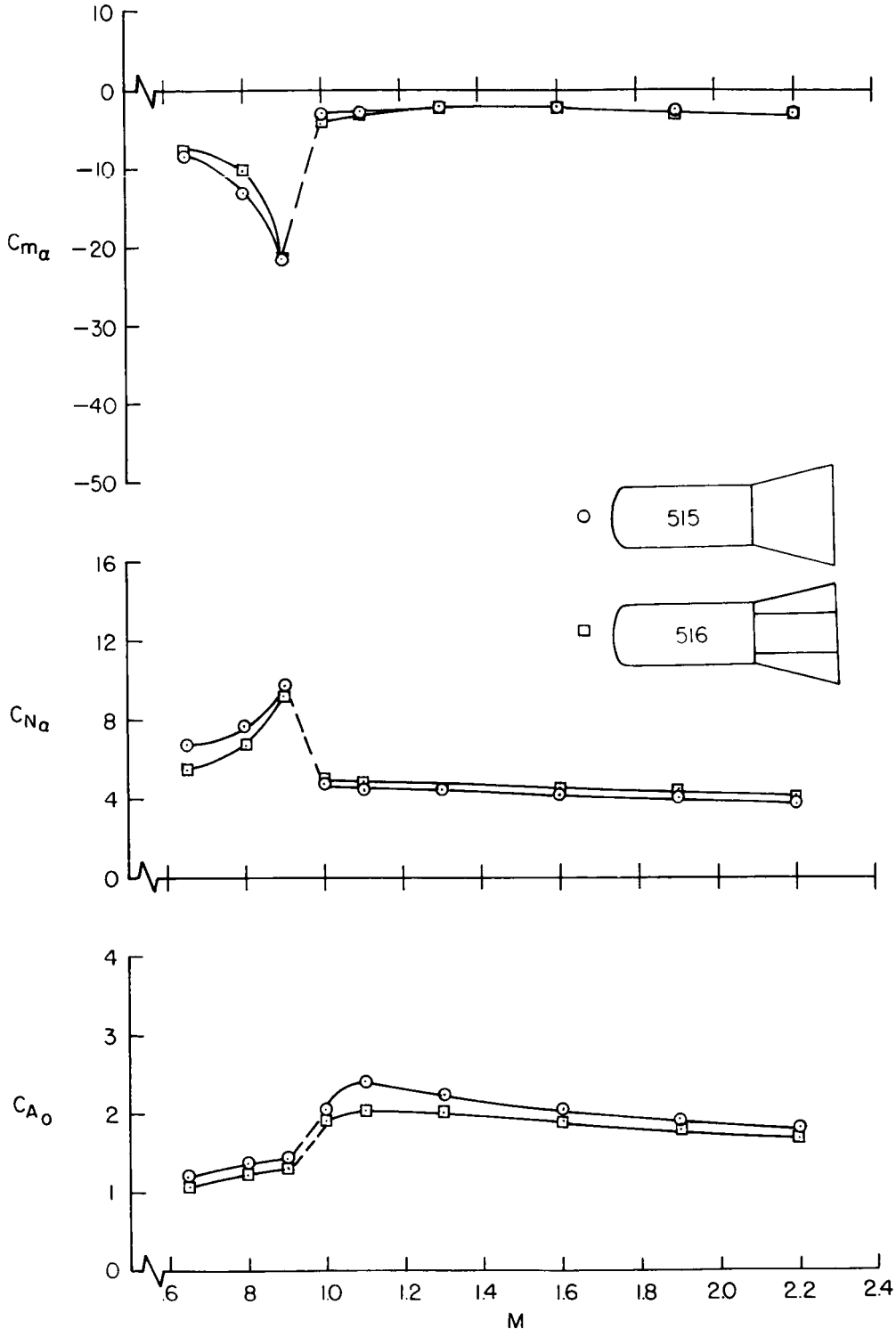

(e) Effect of flare relief.

Figure 8.- Continued.

[redacted]

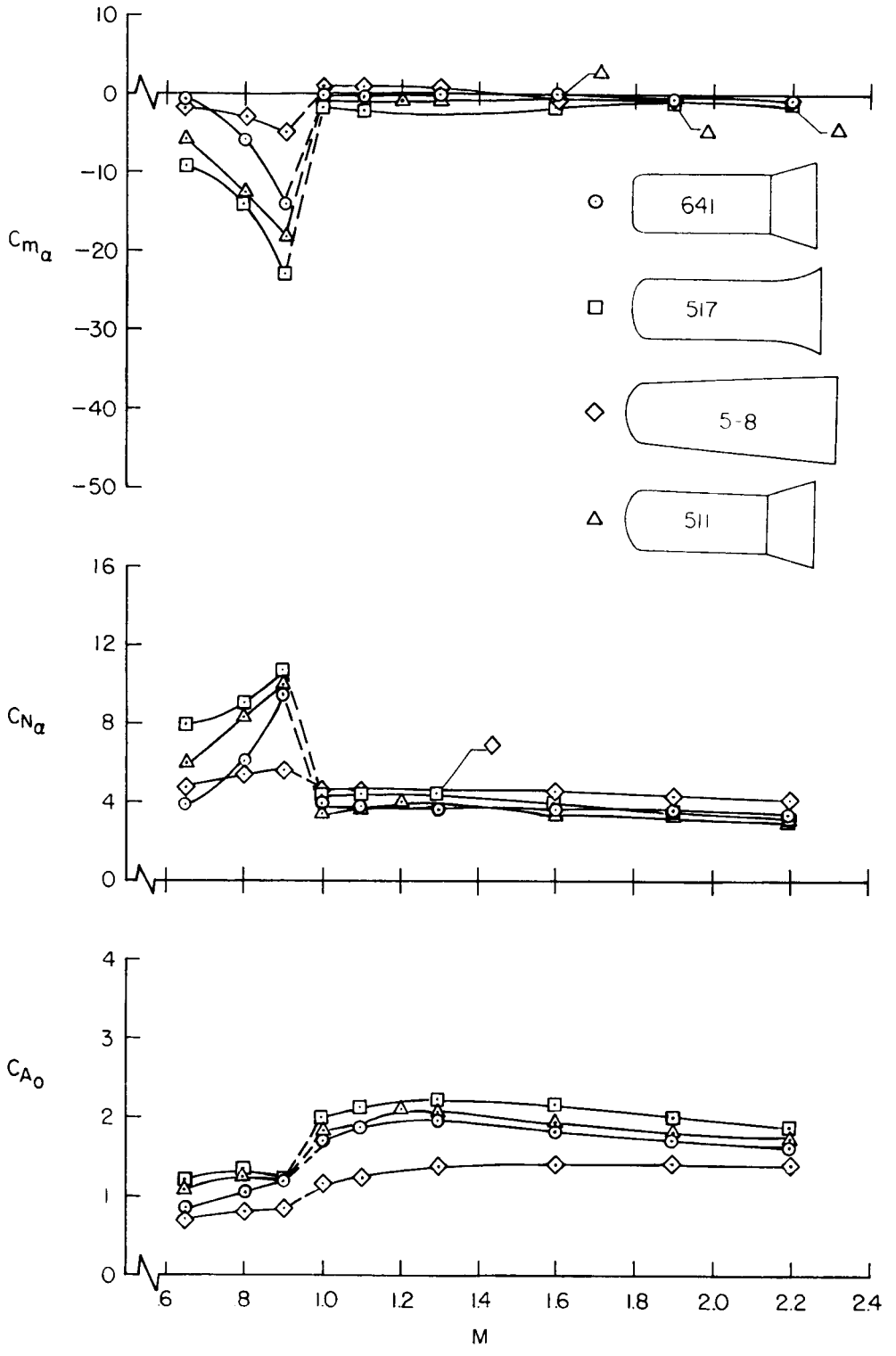

(f) Other models.

Figure 8.- Concluded.

~~CONFIDENTIAL~~

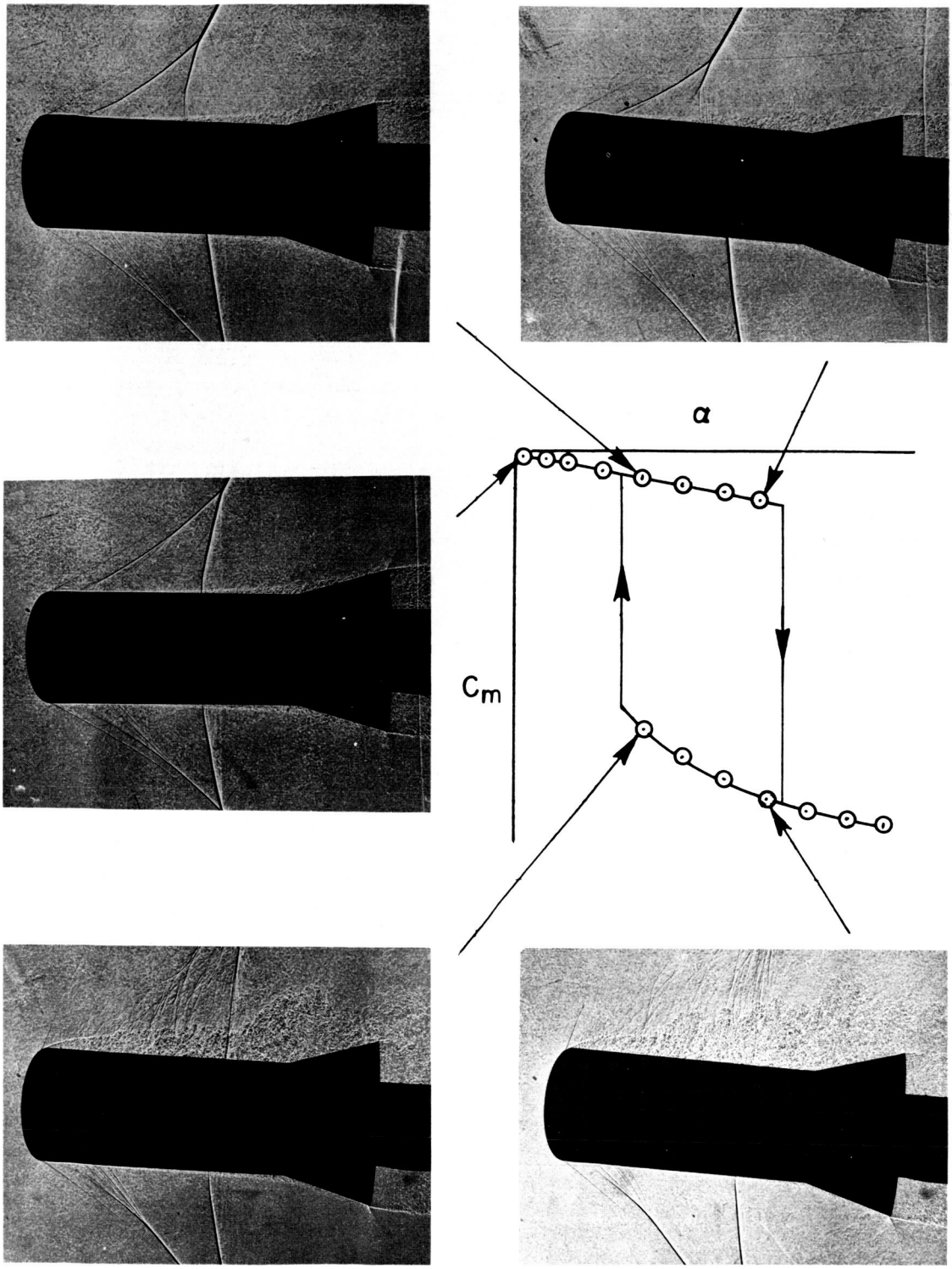

A-24425.2

Figure 9.- Photographs of flow associated with pitching-moment loops for model 511 ; $1.0 \leq M \leq 1.3$.

~~CONFIDENTIAL~~

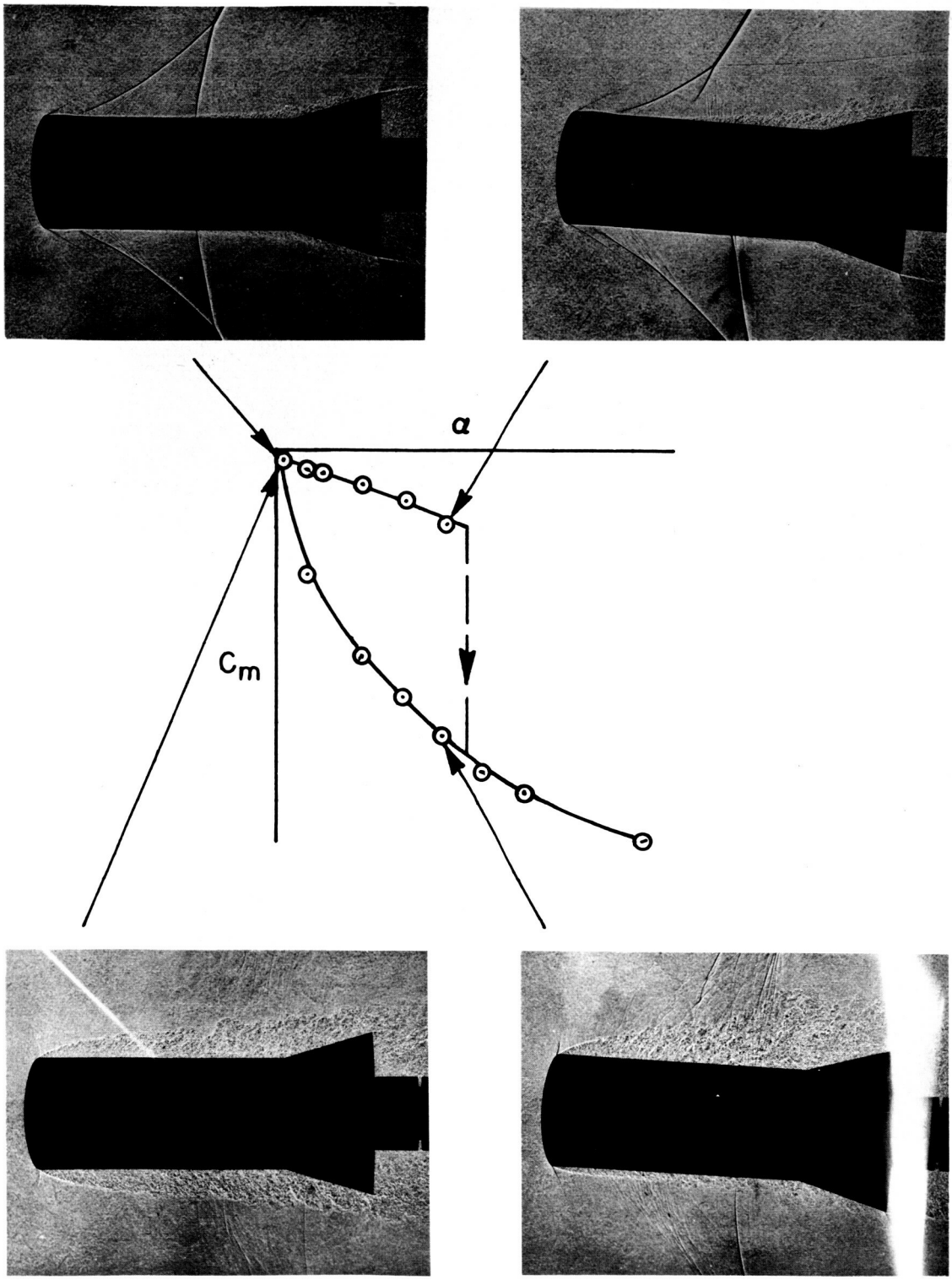

A-24455.1

Figure 10.- Photographs of flow associated with pitching-moment loops for model 321 ; $1.0 \leq M \leq 1.1$.

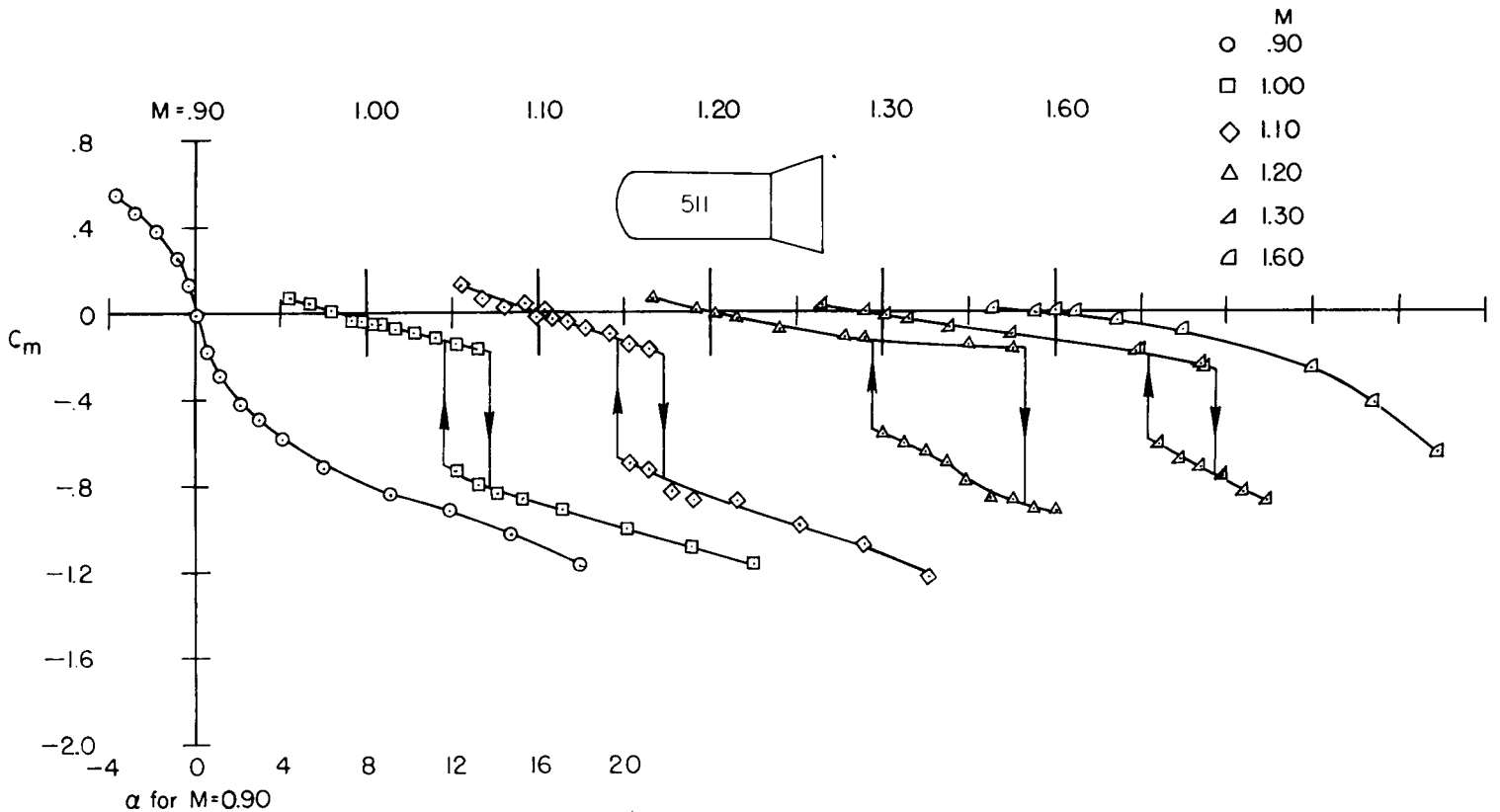

(a) Model 511.

Figure 11.- Typical pitching-moment characteristics.

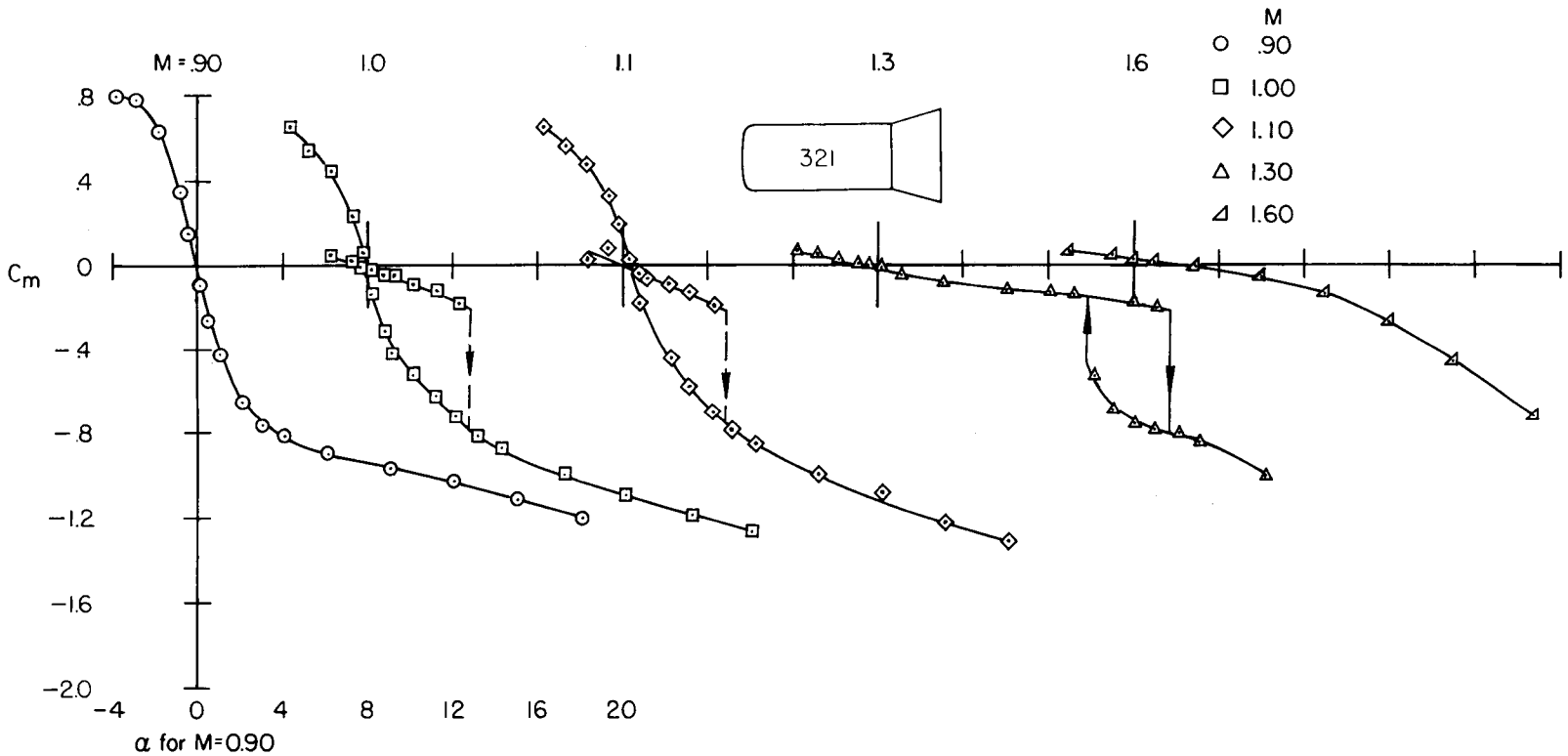

(b) Model 321.

Figure 11.- Concluded.

[redacted]

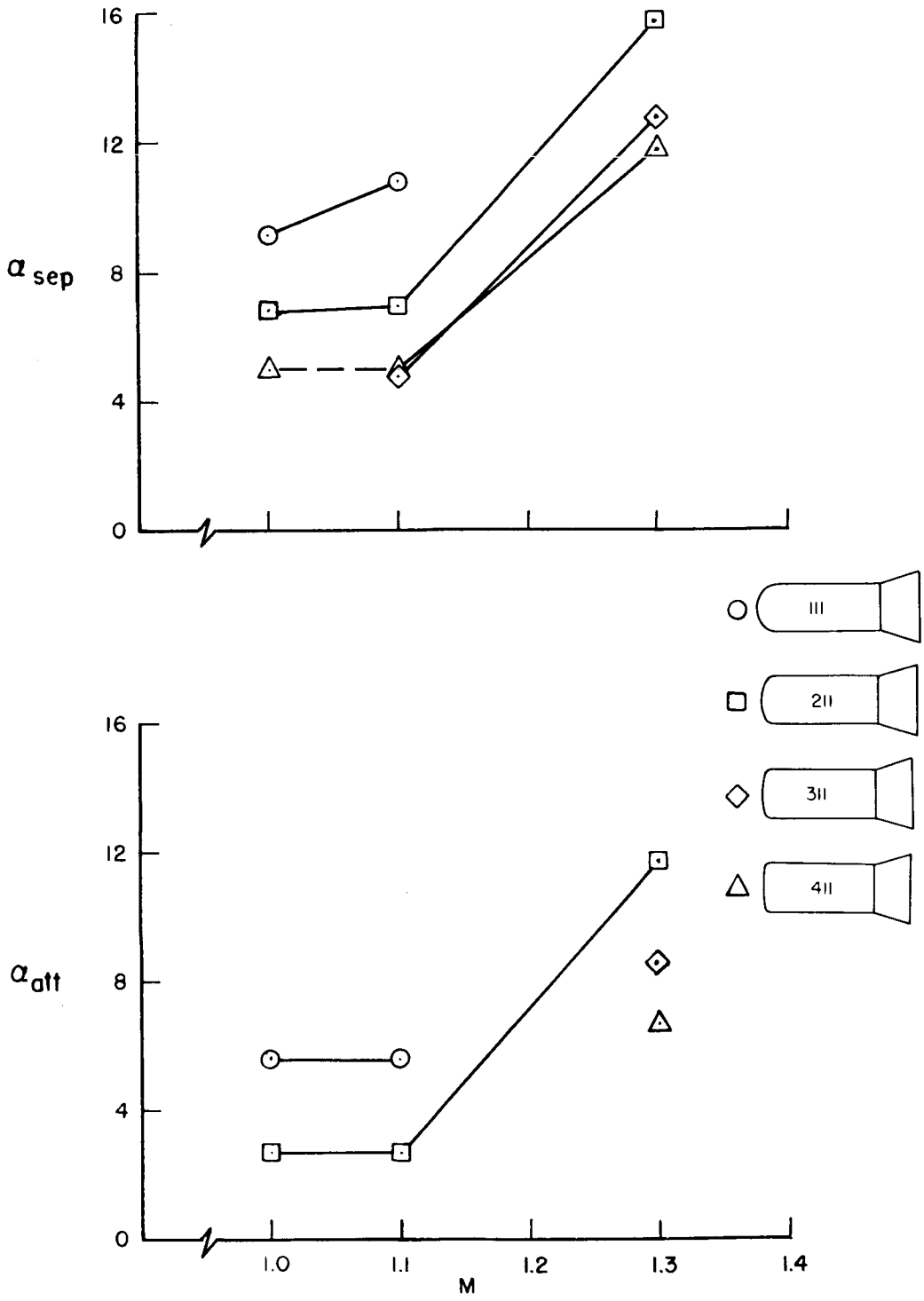

(a) Effect of nose shape.

Figure 12.- The effect of model geometry on angle of attack for flow separation and attachment.

[redacted]

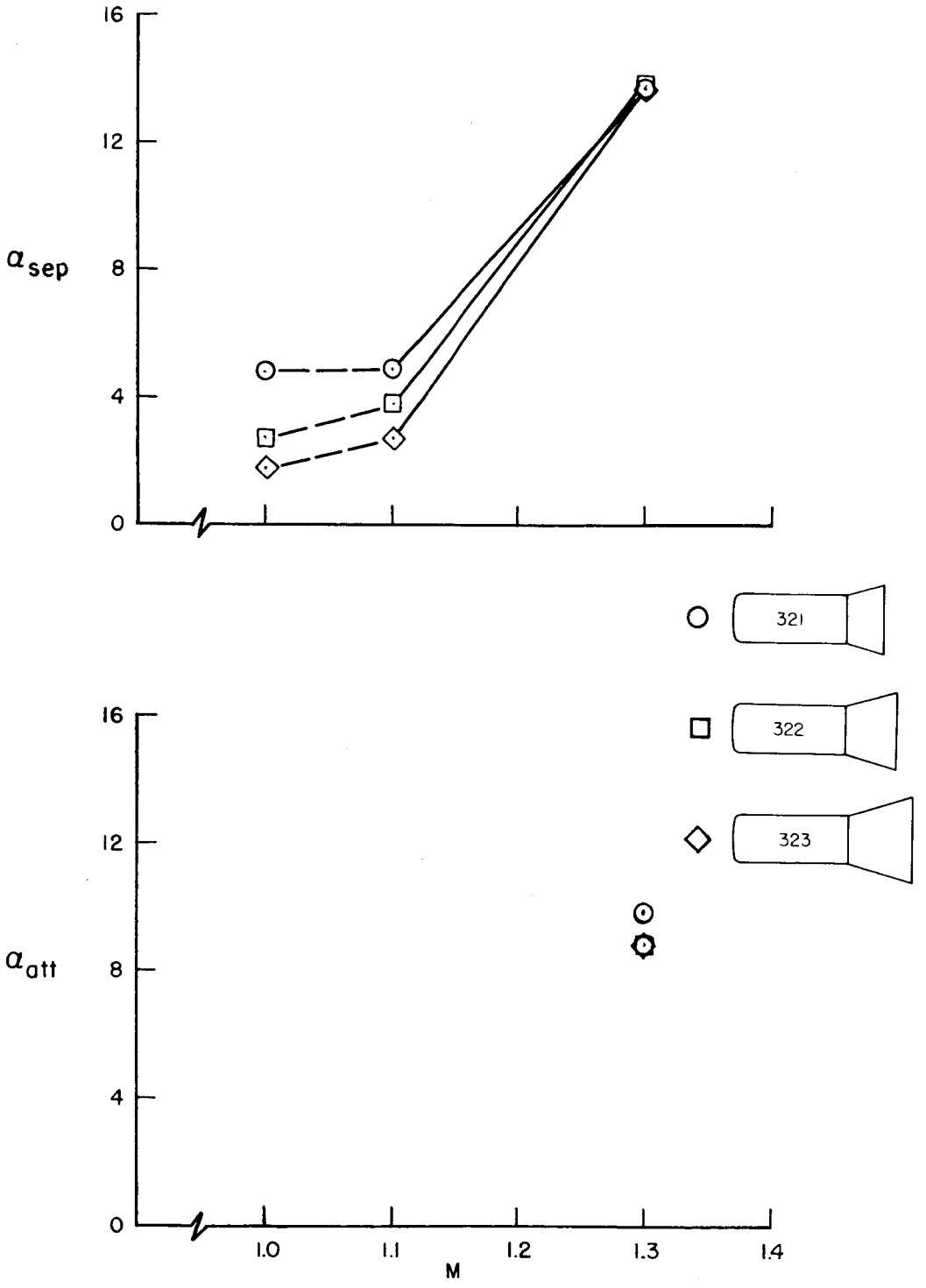

(b) Effect of flare base area.

Figure 12.- Continued.

[redacted]

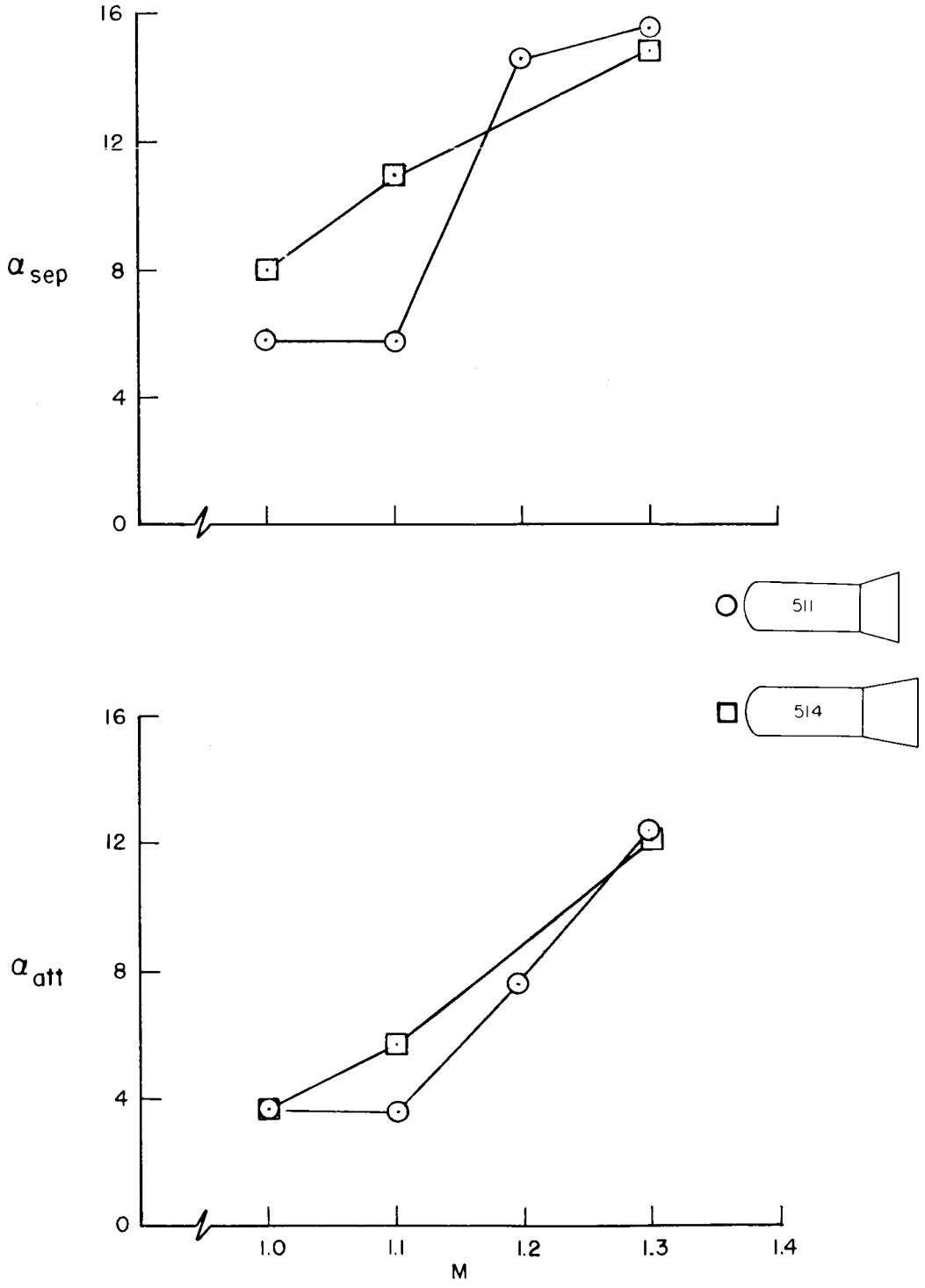

(c) Effect of flare angle.

Figure 12.- Continued.

[redacted]

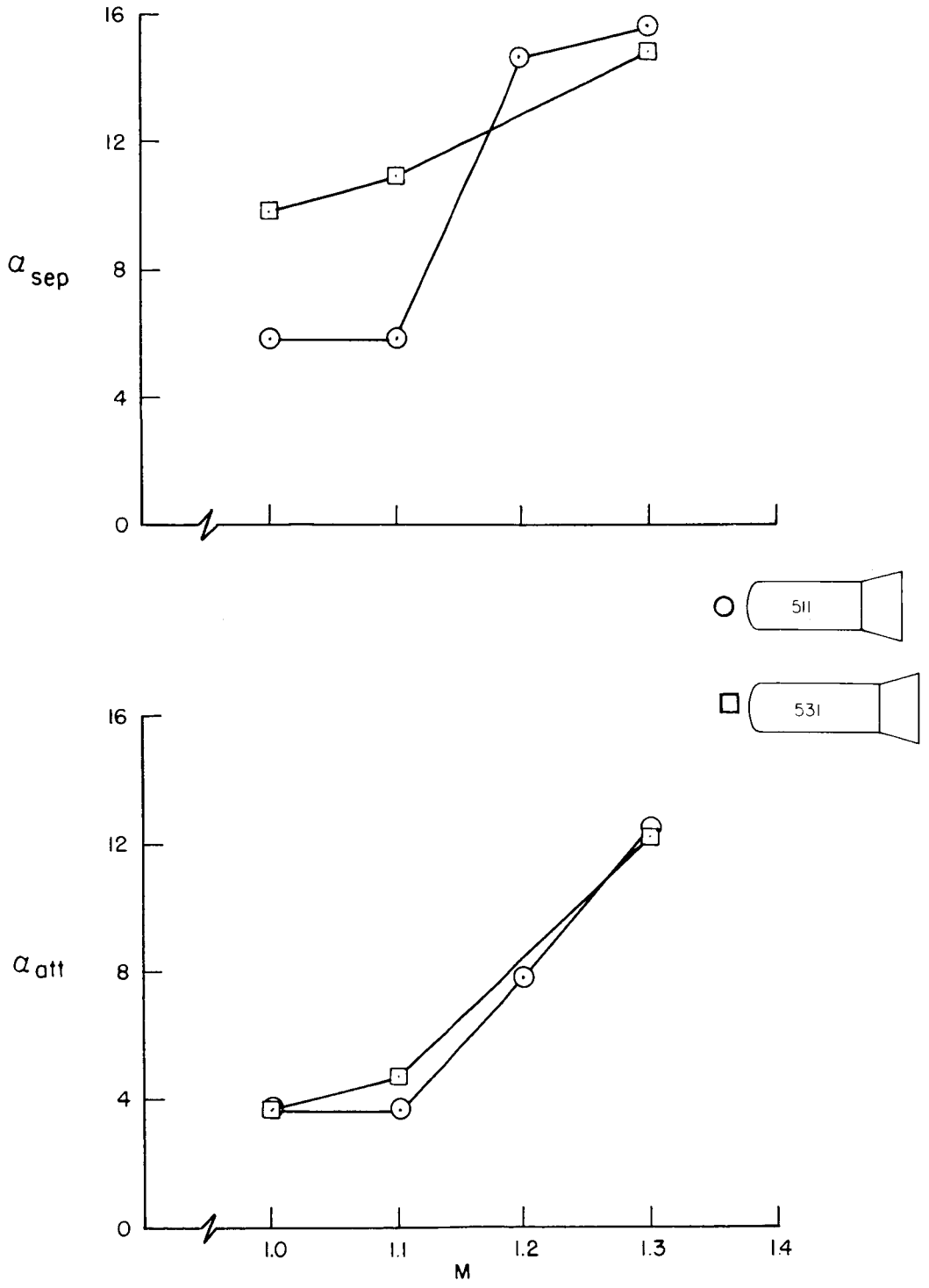

(d) Effect of cylindrical body length.

Figure 12.- Continued.

[redacted]

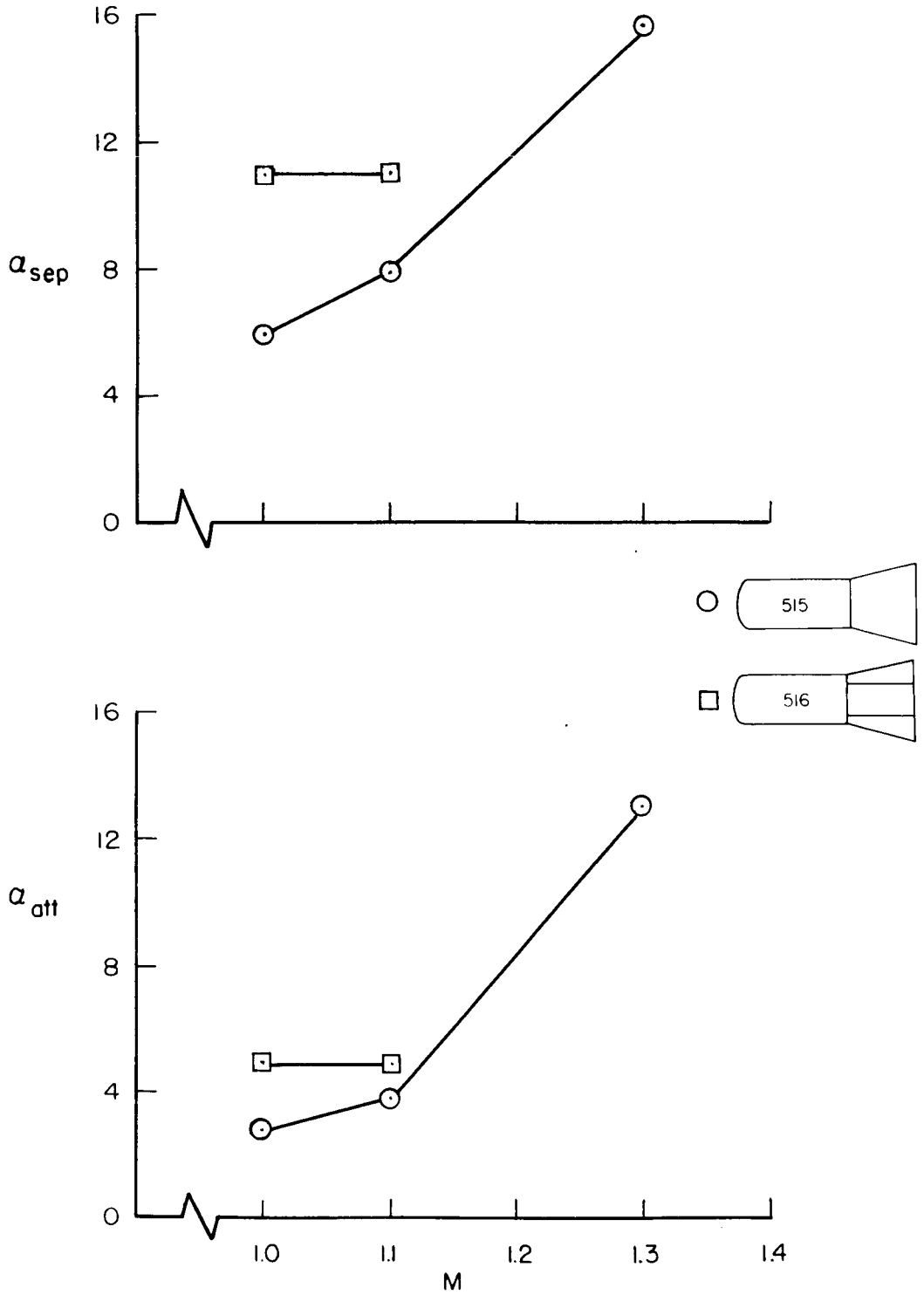

(e) Effect of flare relief.

Figure 12.- Continued.

[redacted]

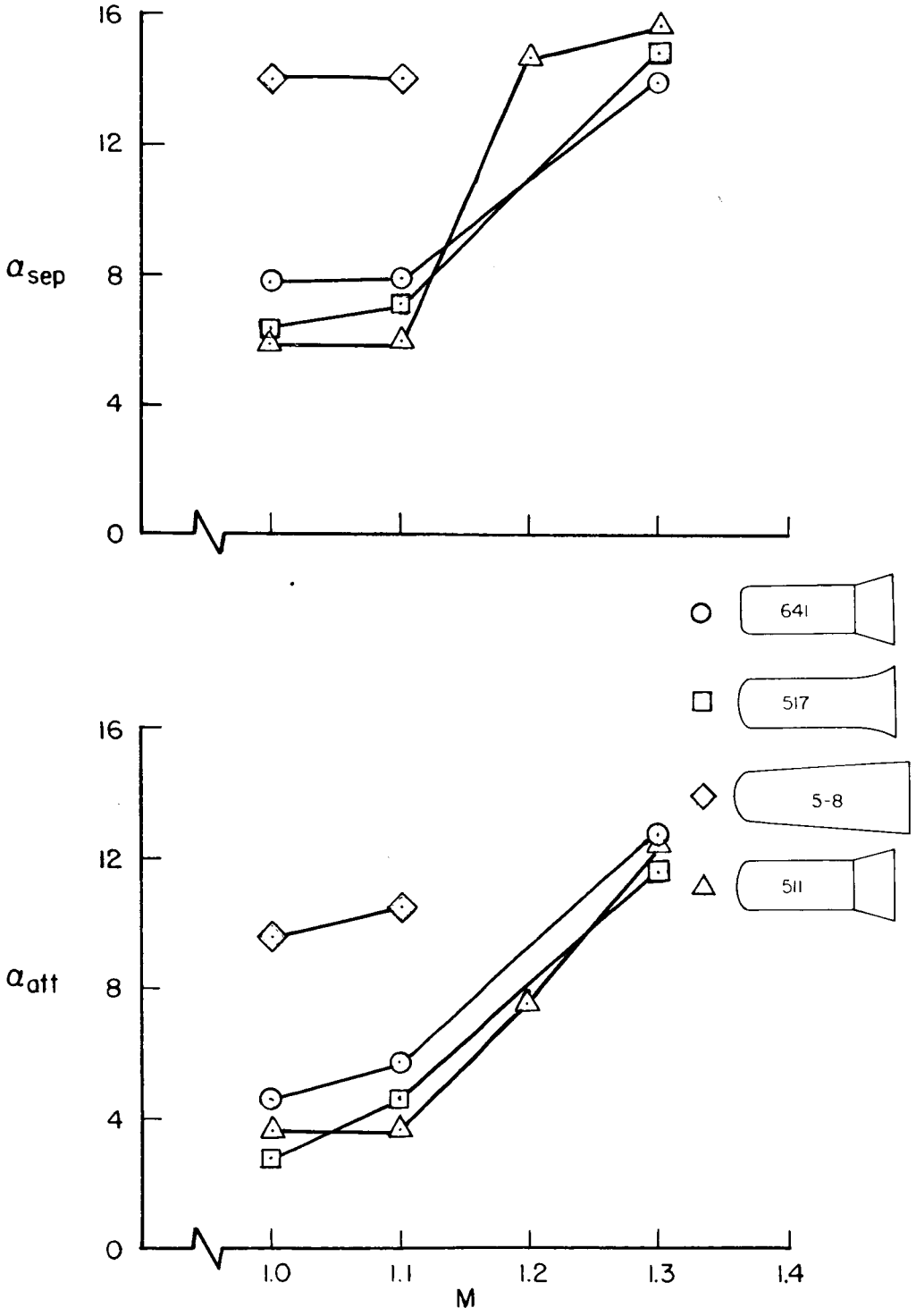

(f) Other models.

Figure 12.- Concluded.

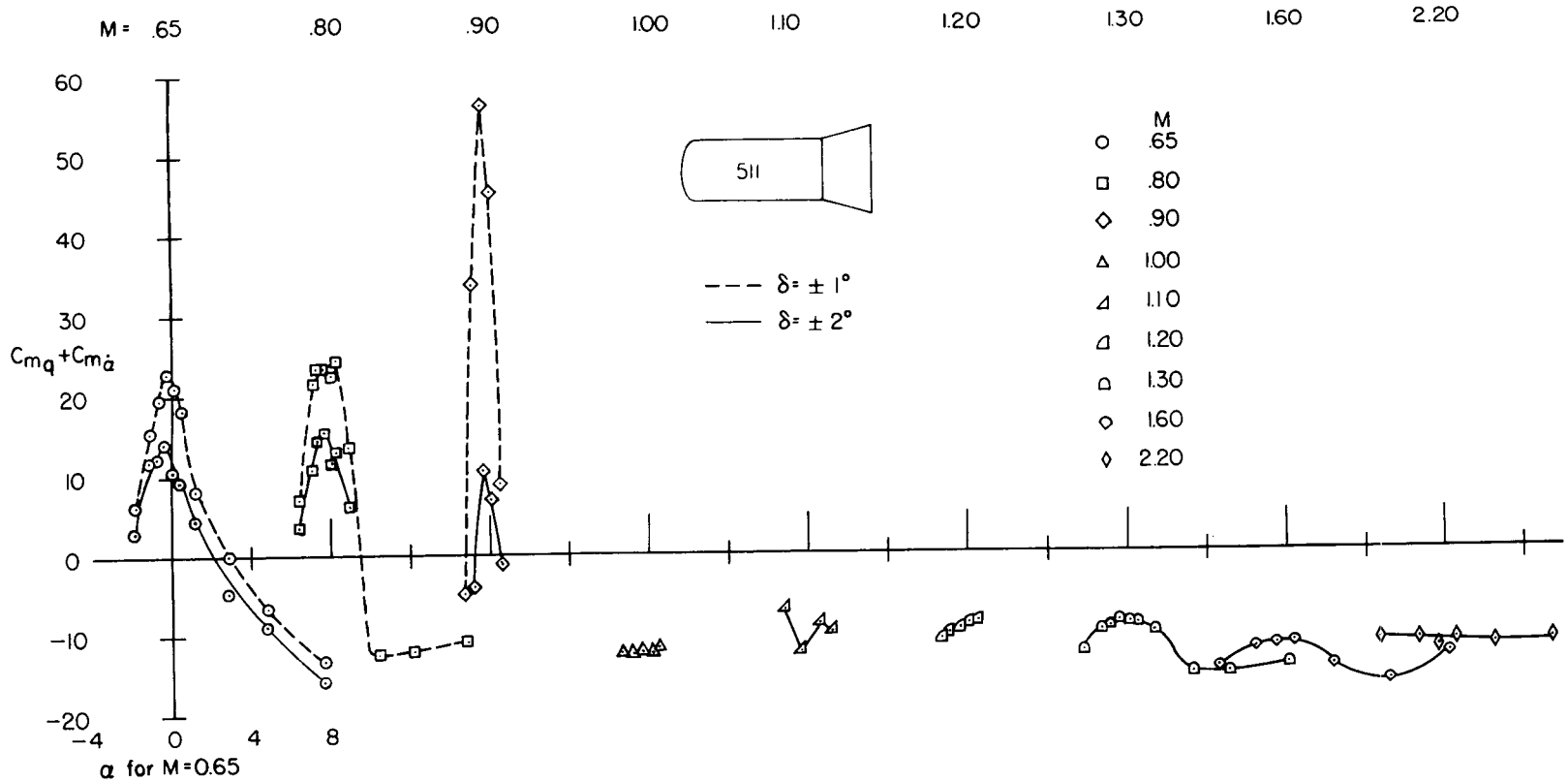

Figure 13.- Typical damping-in-pitch characteristics versus angle of attack.

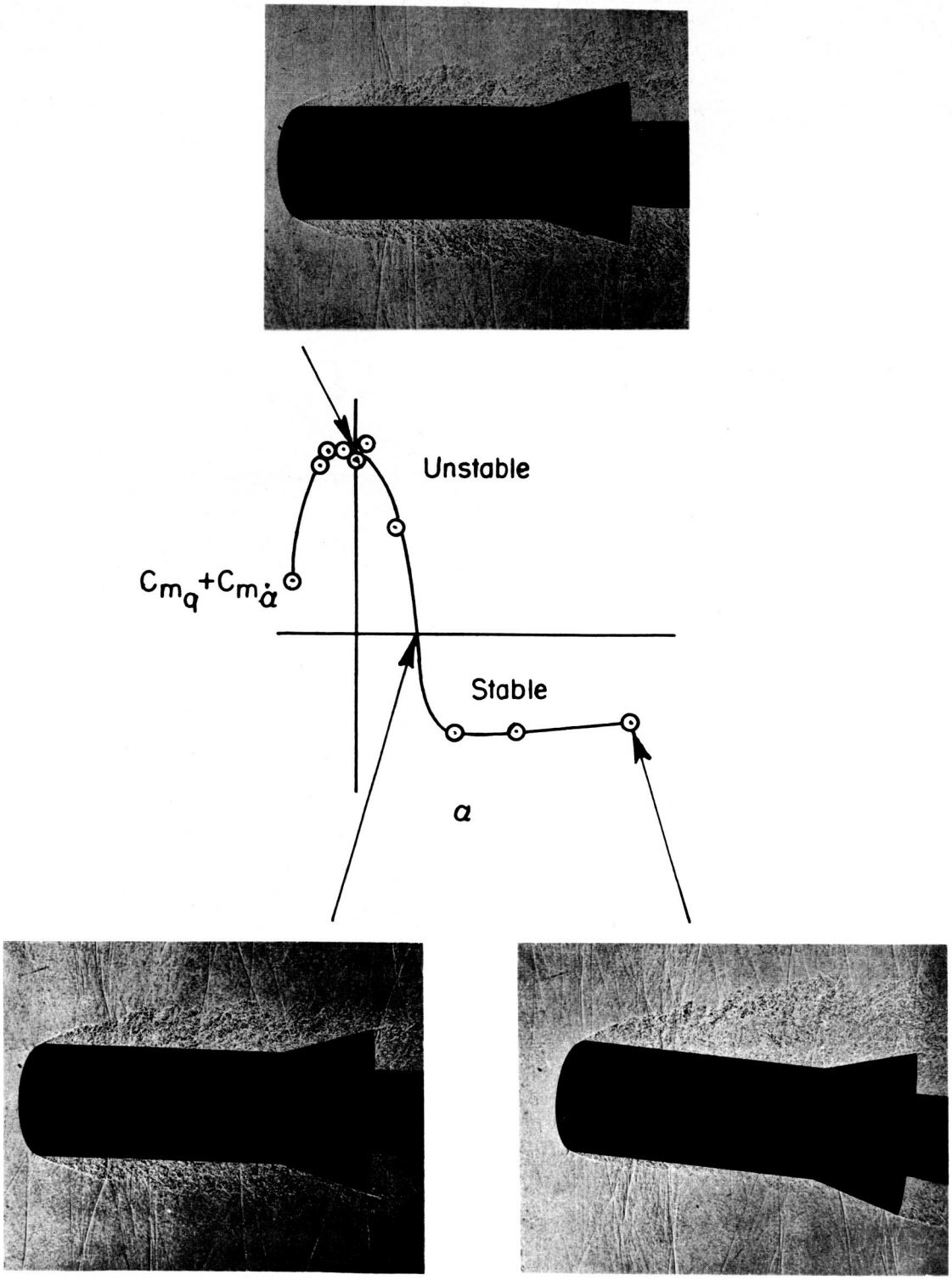

A-24424.1

Figure 14.- Photographs showing the flow associated with the damping-in-pitch variation at subsonic speeds.

[redacted]

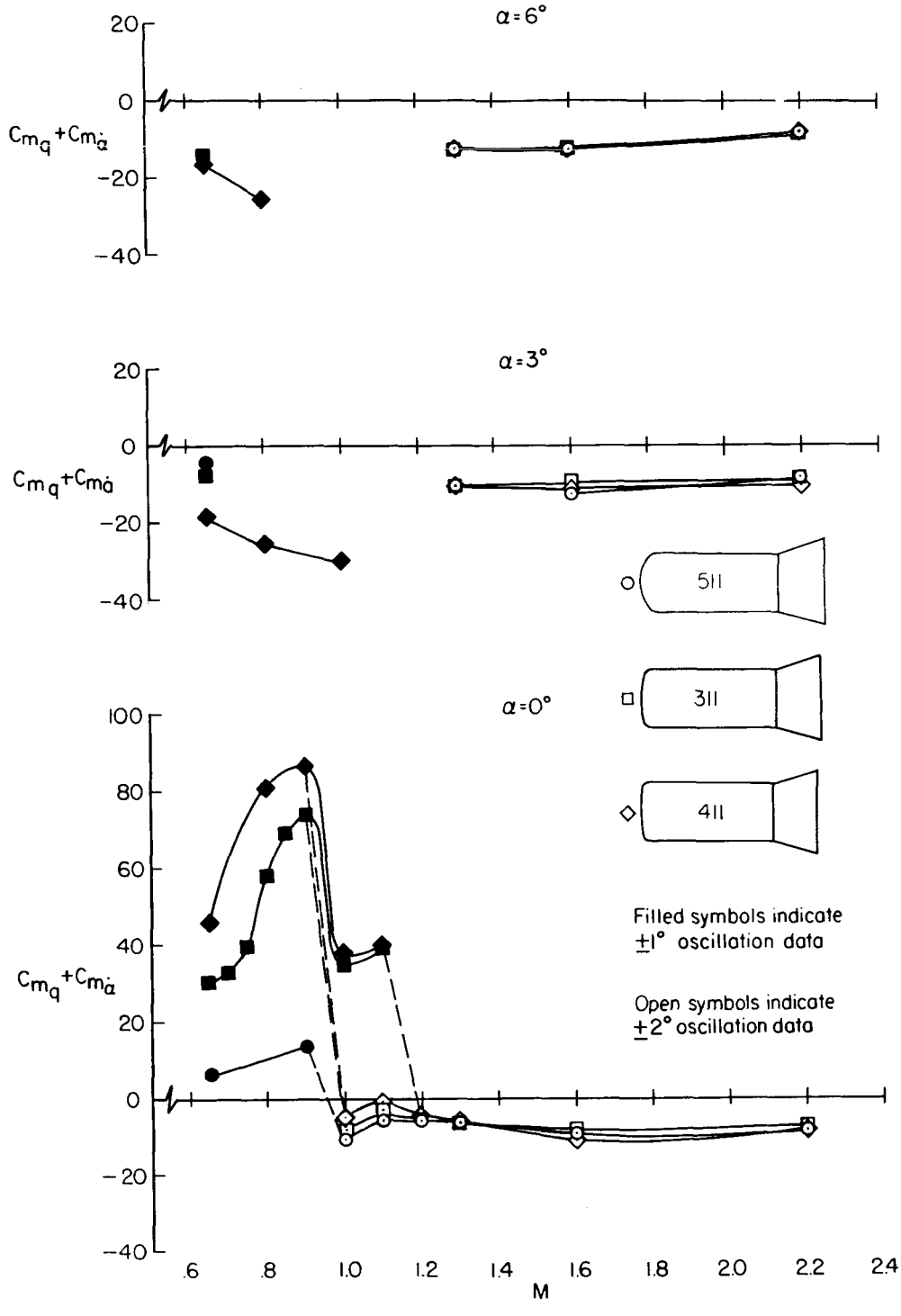

(a) Effect of nose shape.

Figure 15.- The effect of model geometry on the damping-in-pitch characteristics.

[redacted]

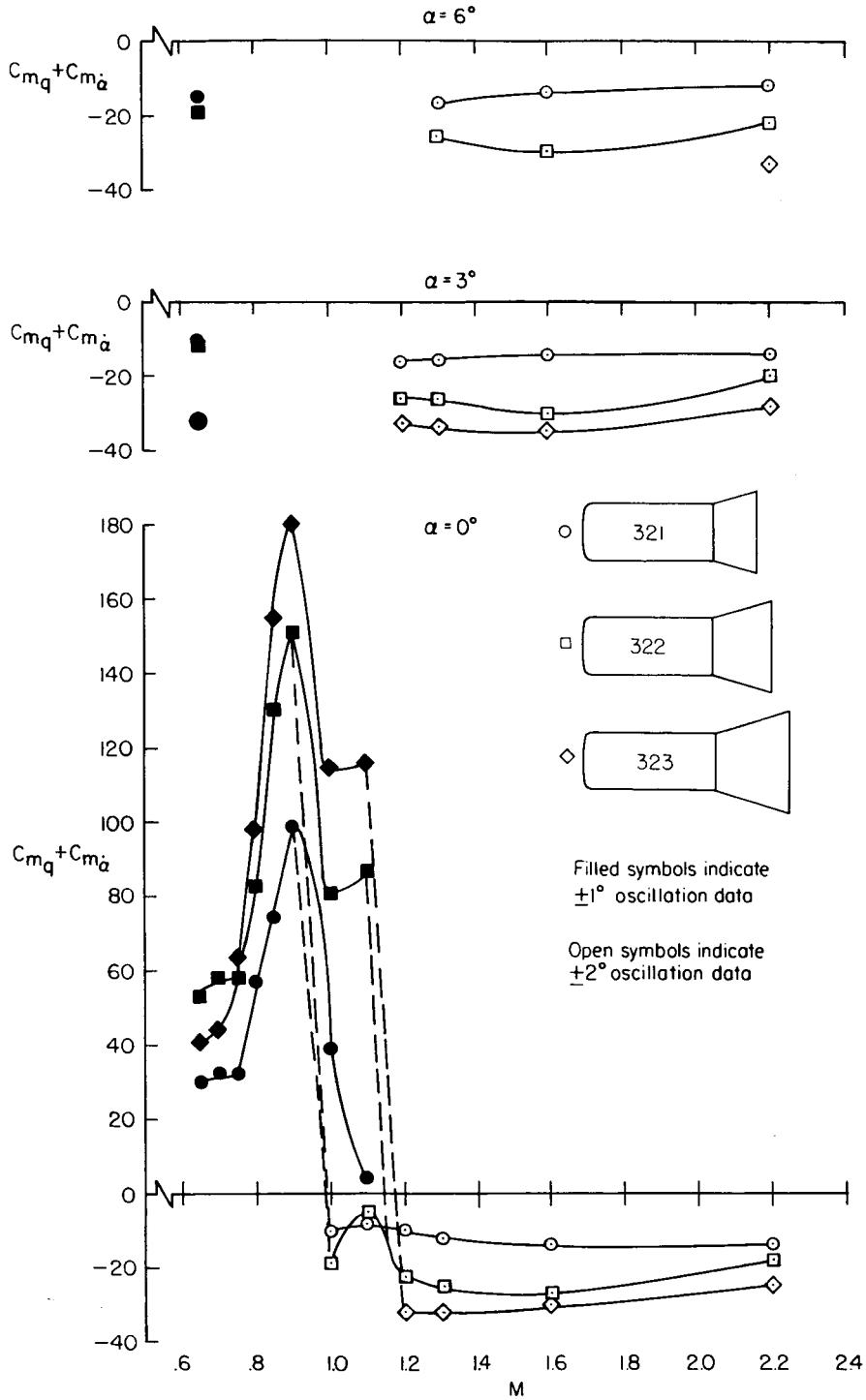

(b) Effect of flare base area.

Figure 15.- Continued.

[redacted]

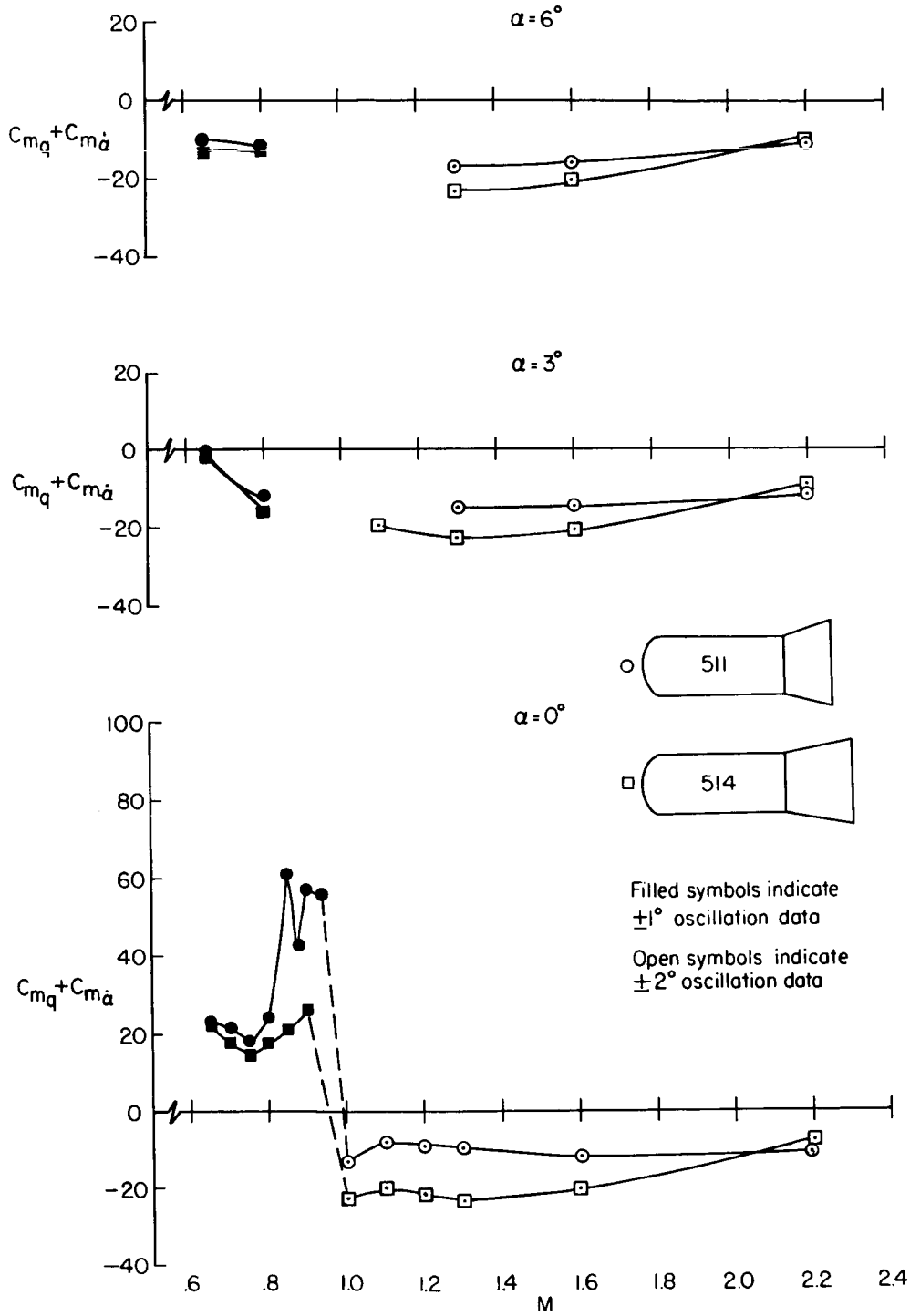

(c) Effect of flare angle.

Figure 15.- Continued.

[redacted]

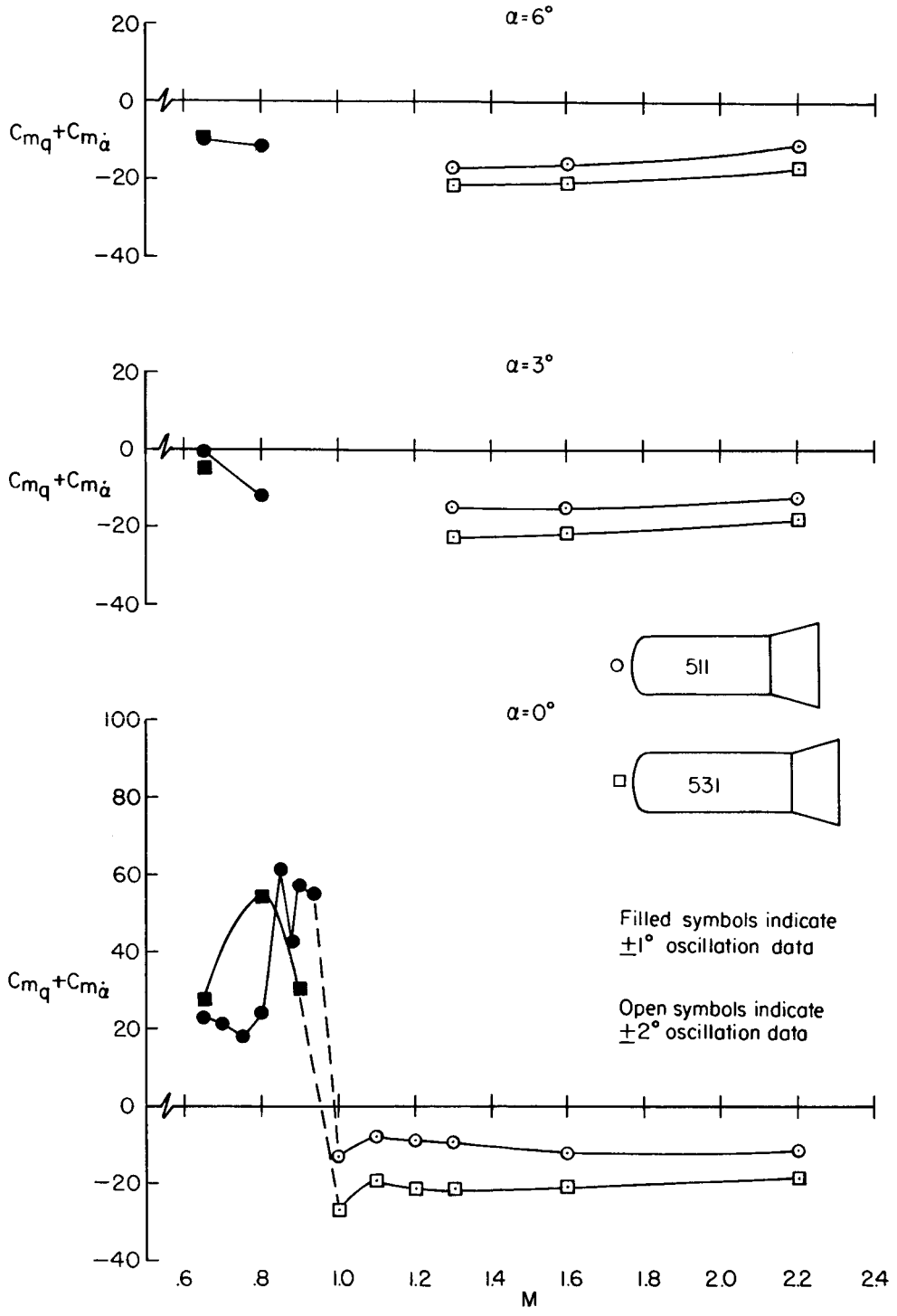

(d) Effect of cylindrical body length.

Figure 15.- Continued.

[redacted]

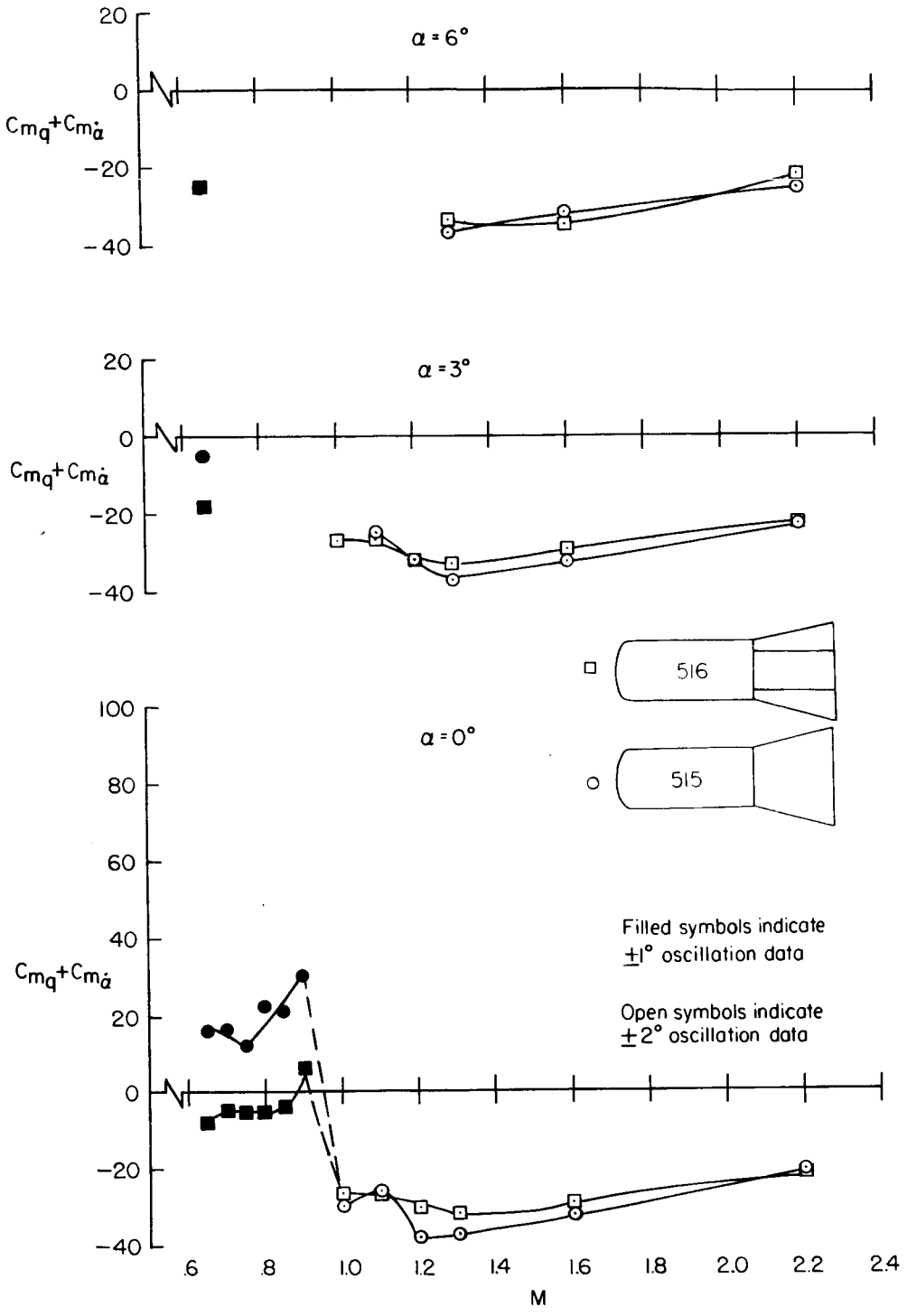

(e) Effect of flare relief.

Figure 15.- Continued.

[redacted]

A-229

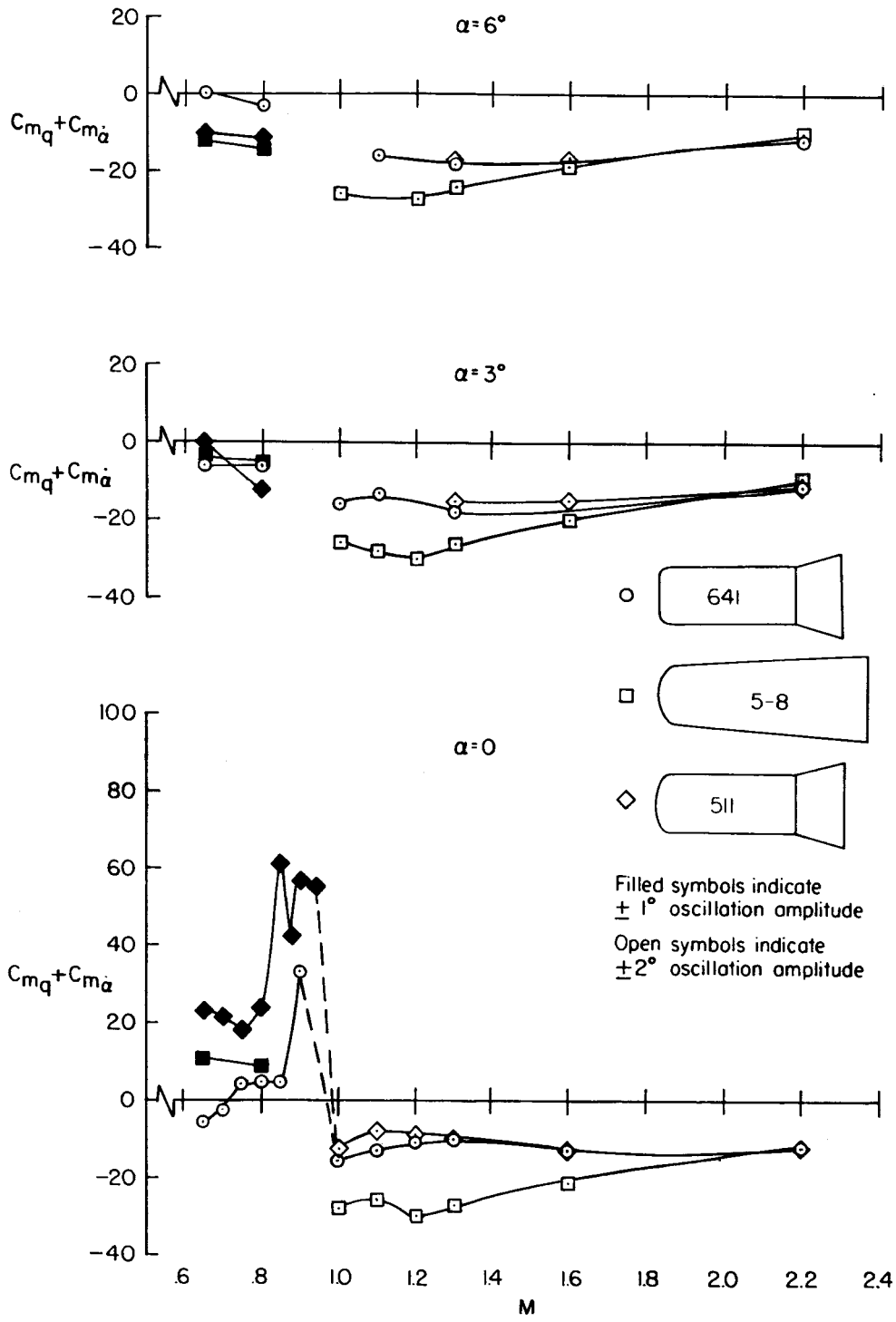

(f) Other models.

Figure 15.- Concluded.

[redacted]

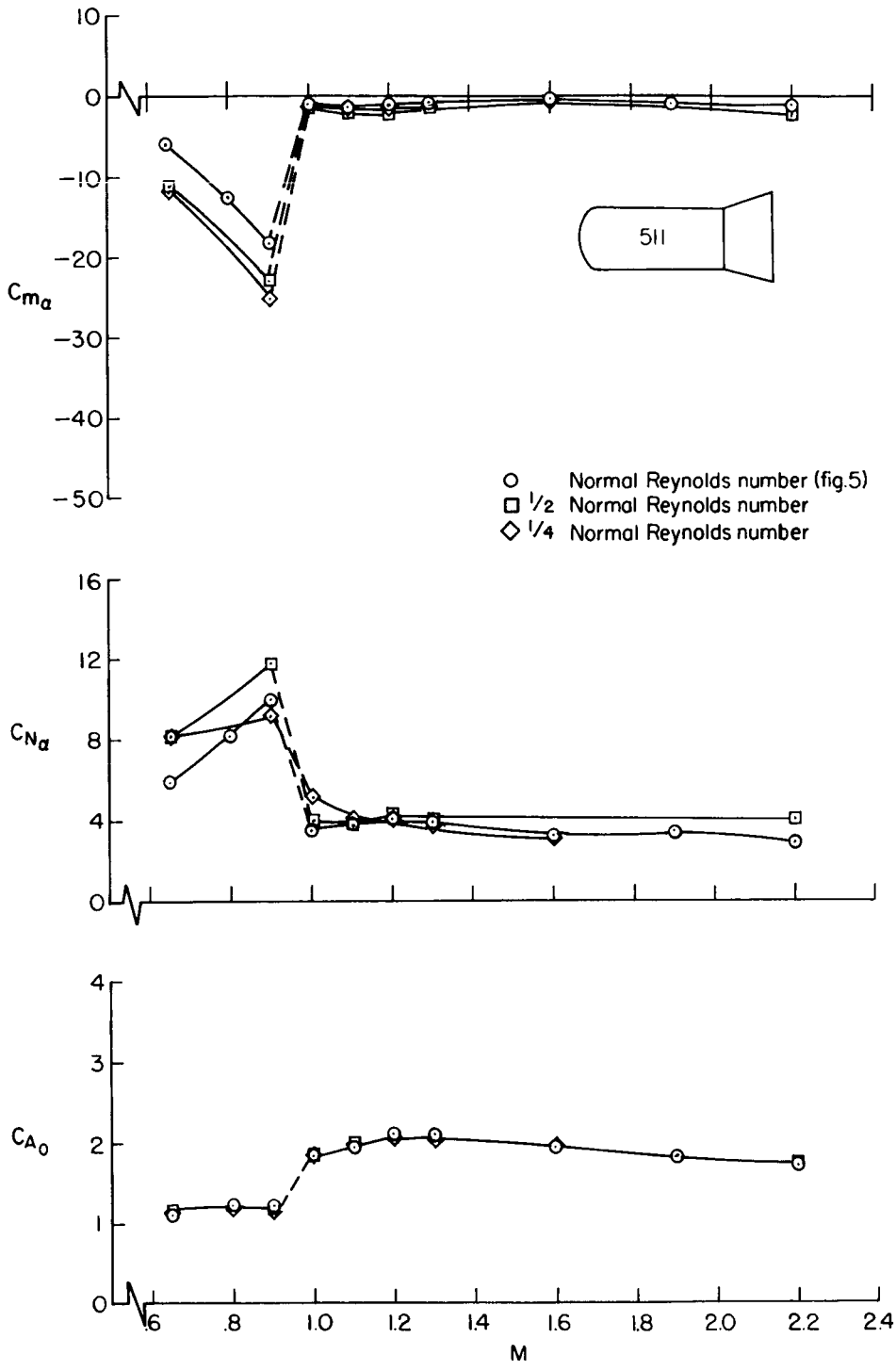

(a) Static force characteristics.

Figure 16.- The effect of Reynolds number on the static force characteristics, separation and attachment angles of attack, and damping in pitch.

[redacted]

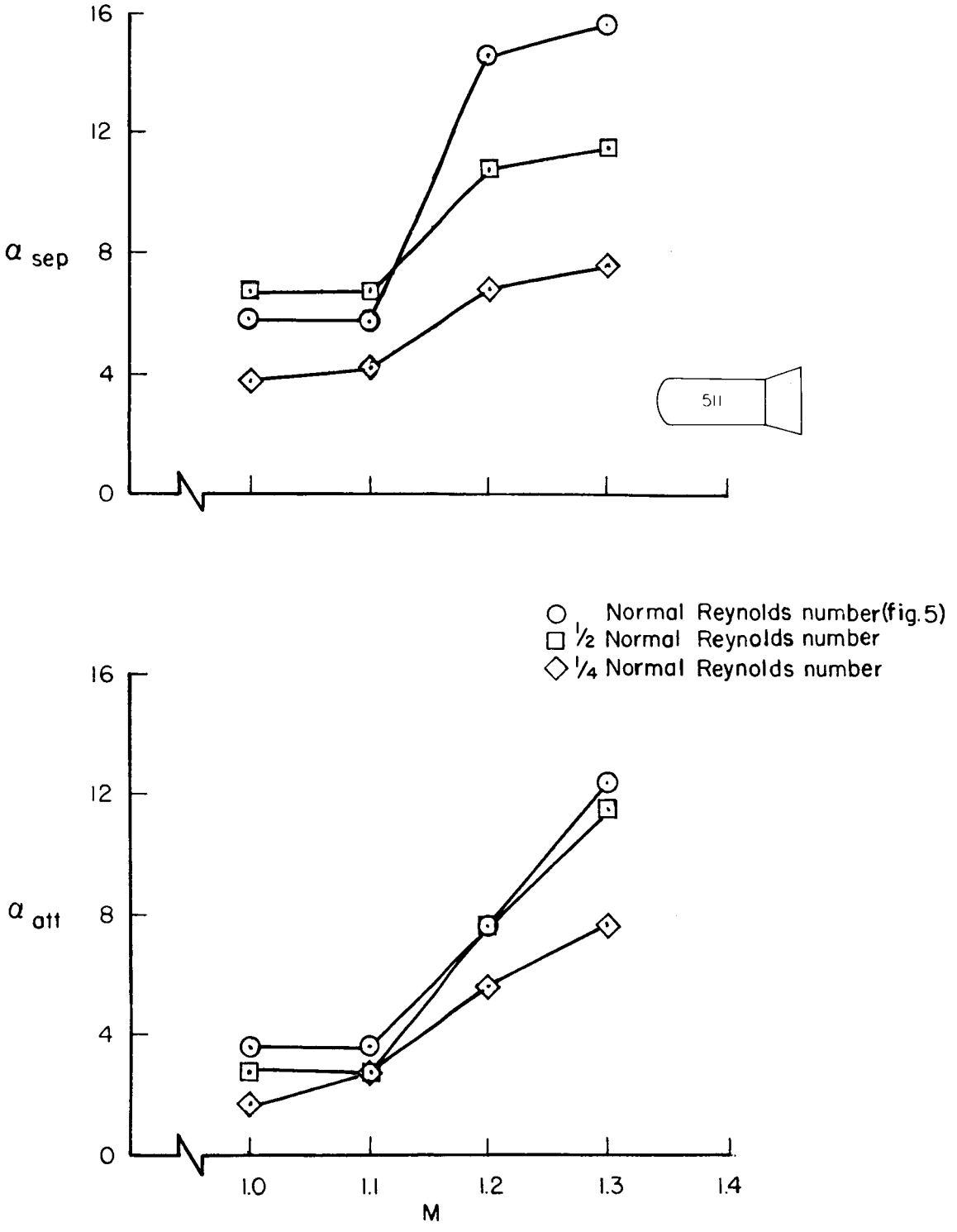

(b) Angles for separation and attachment.

Figure 16.- Continued.

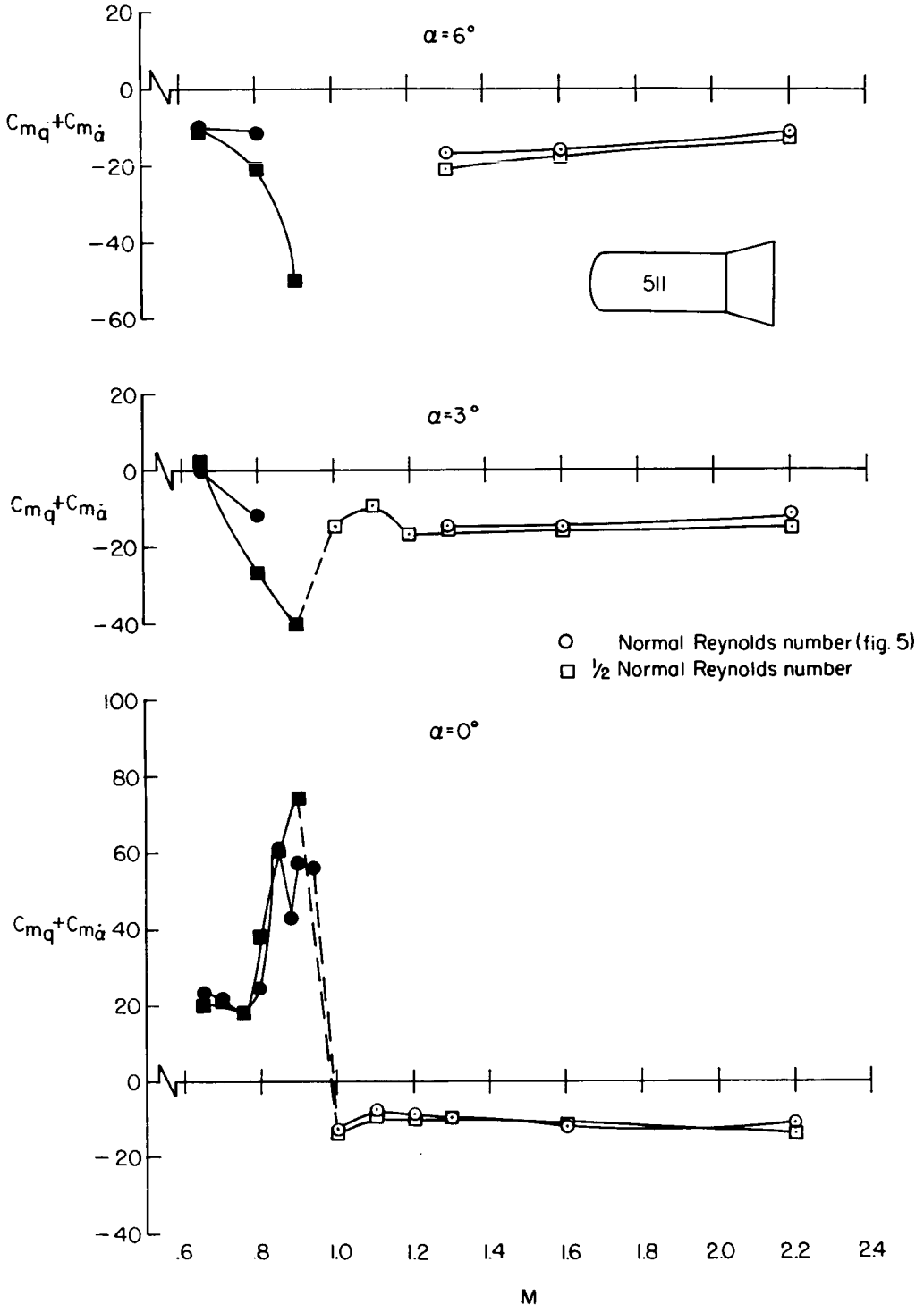

(c) Damping in pitch.

Figure 16.- Concluded.

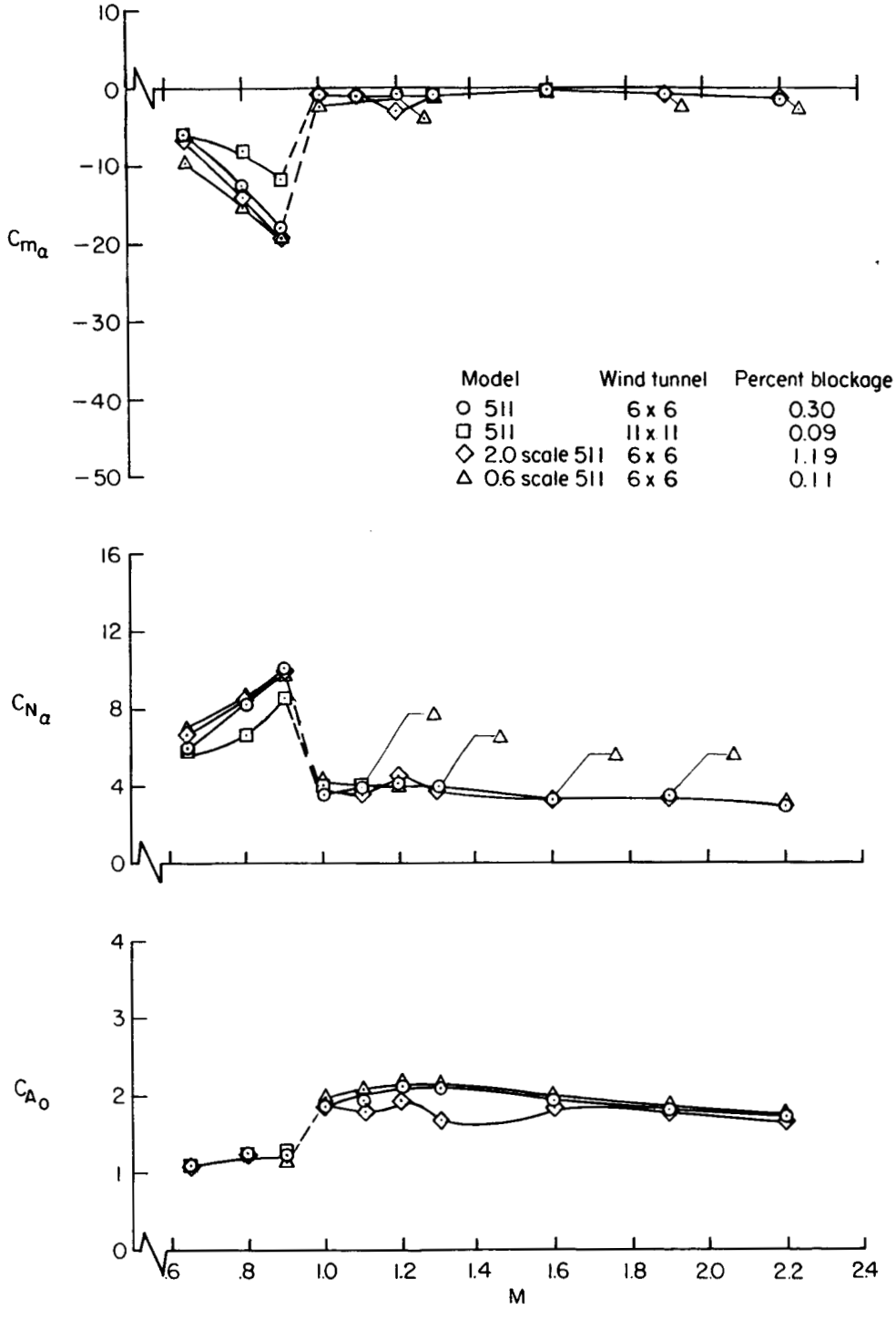

(a) Static force characteristics.

Figure 17.- Effect of wind-tunnel walls on static forces and separation and attachment angles of attack.

[redacted]

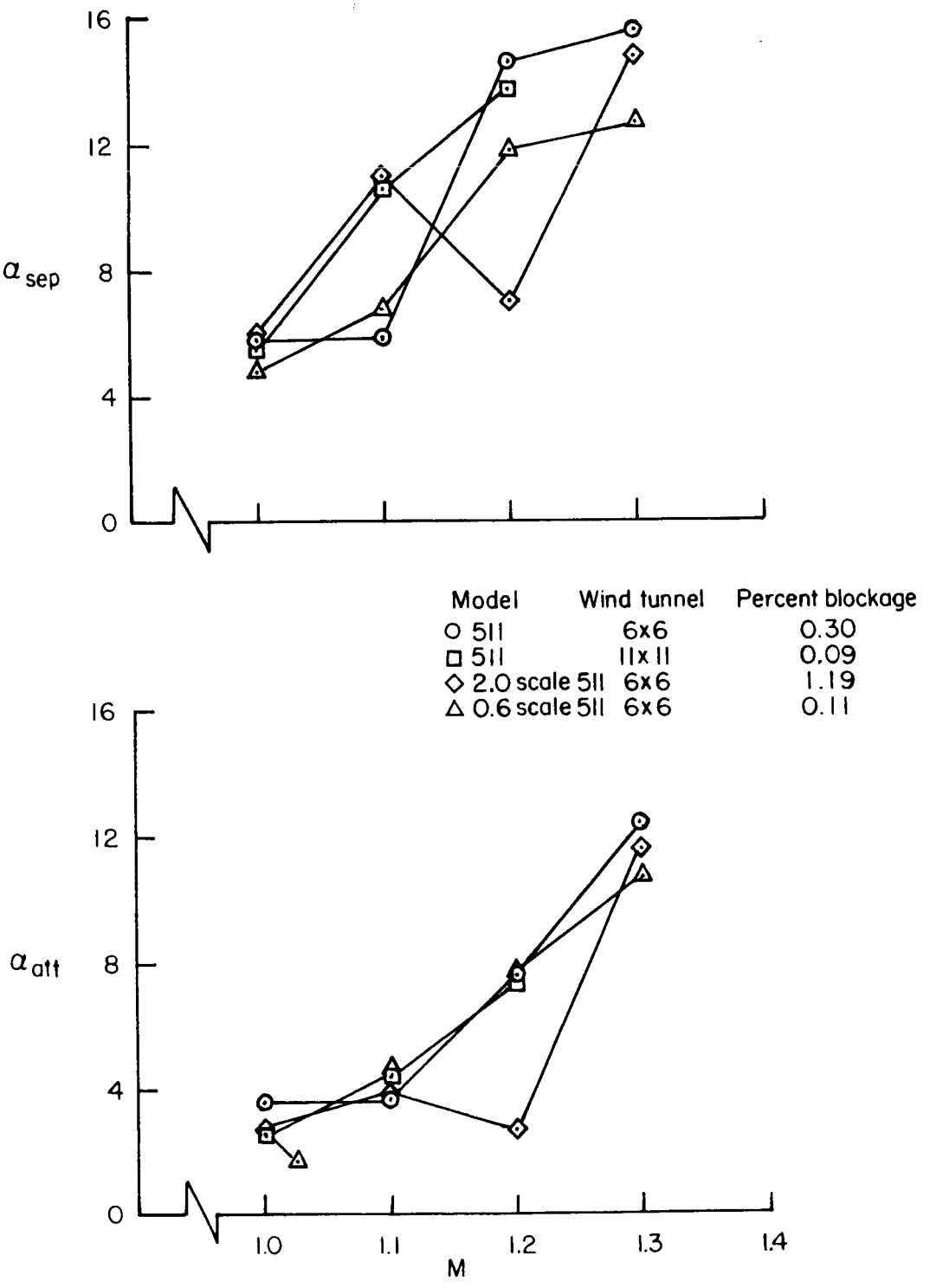

(b) Separation and attachment angles of attack.

Figure 17.- Concluded.

[redacted]